Modeling and Control of Membrane Filtration Systems for Offshore Produced Water Treatment

Jepsen, Kasper Lund

DOI (link to publication from Publisher):
10.54337/aau311246781

Publication date:
2019

Document Version
Publisher's PDF, also known as Version of record

MODELING AND CONTROL OF MEMBRANE FILTRATION SYSTEMS FOR OFFSHORE PRODUCED WATER TREATMENT

BY
KASPER LUND JEPSEN

DISSERTATION SUBMITTED 2019

AALBORG UNIVERSITY
DENMARK

Modeling and Control of Membrane Filtration Systems for Offshore Produced Water Treatment

Ph.D. Dissertation

Kasper Lund Jepsen

Dissertation submitted March 14, 2019

Dissertation submitted: March 14, 2019

PhD supervisor: Associate Prof. Zhenyu Yang
Aalborg University

PhD committee: Professor Henrik C. Pedersen (chairman)
Aalborg Universitet

Dr. Ming Yang
TUV SUD NEL

Associate Professor Johannes Jäschke
Norwegian University of Science and Technology
(NTNU)

PhD Series: Faculty of Engineering and Science, Aalborg University

Department: Department of Energy Technology

ISSN (online): 2446-1636
ISBN (online): 978-87-7210-409-6

Published by:
Aalborg University Press
Langagervej 2
DK – 9220 Aalborg Ø
Phone: +45 99407140
aauf@forlag.aau.dk
forlag.aau.dk

Printed in Denmark by Rosendahls, 2019

Abstract

In the offshore oil and gas sector large quantities of gas, oil, and water are extracted from the underground reservoirs and transported to the topside separation facilities where the three phases are separated. The oil and gas phases are transported onshore, while the treated produced water is discharged into the sea. However, the produced water often contains traces of oil, which potentially affects the surrounding environment. Existing facilities in the Danish North Sea cannot always guarantee that the discharged water complies with the regulations in terms of hydrocarbon concentration. The severity of the compliance issue is further aggravated by political tendencies towards zero-discharge.

In this thesis, membrane filtration technology is investigated as a potential technology for improving the separation of oil and water. However, fouling is a major challenge, which greatly increases the capital and operating expenses compared to the commonly deployed de-oiling hydrocyclones. A crucial factor for increasing the cost-effectiveness of membrane filtration is fouling management. In recent decades most studies addressing fouling management and modeling neglect the potential time-varying dynamic behavior of system. Neglecting the time-varying behavior in the design of the dynamic controllers and fouling management system causes poorly maintained operating conditions and sub-optimal scheduling of cleaning procedures, thus increasing fouling growth. Another method reducing fouling growth is crossflow filtration, but the method complicates the filtration system and increases energy consumption significantly compared to the dead-end configuration. Based on these observations, the objective of the thesis is to reduce the capital and operating expenses by; (1) maintaining the selected operating conditions using advanced control design techniques, (2) optimally controlling the filtration and backwashing durations, and (3) optimizing the energy efficiency of the crossflow pumping system.

By selecting control pairings that minimize the interaction between the control loops, poor control performance caused by interactions can be avoided, consequently keeping permeability high. Furthermore, the fouling behavior during filtration and backwashing was investigated and based on re-

sults, an adaptive control algorithm was proposed and experimentally validated. The algorithm online adjusts the filtration and backwashing durations as the operating conditions change, ensuring the durations reflect the current conditions. Lastly, a power consumption model of the pumps was proposed and deployed for advanced energy-efficient scheduling of multiple parallel pumps. To test and validate the proposed solutions, the existing pilot plant is extended with a membrane filtration system which is designed and constructed during the thesis period.

It is concluded that fouling related cost can be mitigated by ensuring constant operating conditions through selecting control pairings that minimize interaction between the controllers. Fouling related cost can be further reduced by adjusting the backwashing and filtration durations to maximize fouling removal and minimize clean water spent by backwashing, thus increasing the efficiency and total throughput. Lastly, energy-efficient scheduling of multiple parallel pumps was deployed to reduce the enormous energy requirement of crossflow filtration. By reducing fouling growth, optimizing fouling removal, and reducing energy consumption, the capital and operating expenses of crossflow membrane filtration can be reduced.

Resumé

I offshore olie og gas-sektoren udvindes store mængder af gas, olie og vand fra de underjordiske reservoirer. De tre faser transporteres til separationsanlægget, hvor de adskilles. Olie- og gasfaserne transporteres til land, mens det rensede vand, som stadig indeholder olie, udledes i havet, hvor det kan påvirke nærmiljøet. Eksisterende separationsfaciliteter i den danske Nordsø kan ikke altid garantere, at det udledte vand overholder reglerne for olieudledning. En problemstilling som kun forværres yderligere af fremtidige nul-udledningspolitikker.

I denne afhandling undersøges membranfiltrering som en mulig teknologi til at forbedre separation af olie og vand. En stor udfordring med membranfiltrering er tilsmudsning af membranoverfladen, hvilket i høj grad øger investerings- og driftsomkostningerne i forhold til de almindeligt anvendte olieudskillelseshydrocykloner. Et afgørende element for omkostningseffektiv drift af membranfiltrering er at begrænse tilsmudsning af membranoverfladen. I de seneste årtier har de fleste studier arbejdet med at begrænse og modelere tilsmudsning af membranerne, men den potentielt tidsvarierende dynamiske adfærd af systemet ignoreres. Ved at ignorere den tidsvarierende adfærd i designet af kontrolsløjferne og rengøringssystemerne, kan den skiftende adfærd forårsage svingninger i driftsbetingelserne og suboptimal planlægning af rengøringsprocedurer, som derved øger tilsmudsning af membranen. En anden metode som yderligt reducere tilsmudsning er tværstrømning, men metoden komplicerer filtreringssystemet og øger energiforbruget betydeligt i forhold til dead-end konfigurationen. På baggrund af disse observationer er formålet med afhandlingen at reducere investerings- og driftsomkostningerne ved at (1) anvende avanceret styringsteknikker for at sikre driftsbetingelser, (2) benytte optimal styring af filtrerings- og tilbagespulingstiden og (3) reducere energiforbruget ved tværstrømsfiltrering.

Ved at vælge kontrolparringer, der minimerer interaktion mellem kontrolsløjferne, kan dårlige kontrolpræstationer forårsaget af interaktion undgås. Ved at undgå dårlige kontrolpræstationer kan driftsbetingelserne holdes konstante og permeabiliteten høj. Desuden blev tilsmudsningsadfærden undersøgt for både filtrerings- og tilbagespulingsfaserne og baseret på den

observerede adfærd, blev en algoritme foreslået og eksperimentelt valideret. Algoritmen justerer varigheden af filtrerings- og tilbagespulingsfaserne løbende som driftsbetingelserne ændres, hvilket sikrer at varighederne afspejler de aktuelle forhold. Derudover blev en strømforbrugsmodel for pumperne foreslået og implementeret til avanceret energieffektiv drift af flere parallelle pumper. For at teste og validere de foreslåede løsninger udvides den eksisterende testopstilling med membranfiltrering. Udvidelsen er designet og konstrueret i specialeperioden.

Det konkluderes, at omkostninger relateret til tilsmudsning kan formindskes ved at vælge kontrolparringer, der minimerer interaktion mellem kontrolsløjferne og derved sikrer konstante driftsforhold. Omkostninger forårsaget af tilsmudsning kan reduceres yderligere ved at justere tilbagespulings- og filtreringstiden for at maksimere fjernelsen af tilsmudsning og minimere forbruget af rent vand i tilbagespulingenfasen, derved øges effektiviteten og den totale gennemstrømning. Derudover blev en energieffektiv strategisk drift af flere parallelle pumper implementeret for at reducere det enorme energibehov af tværstrømningsmembranfiltrering. Ved at reducere væksten og optimere fjernelsen af tilsmudsning samt reducere energiforbruget, kan investerings- og driftsomkostningerne ved tværstrømningsmembranfiltrering reduceres.

Contents

Thesis Details

Thesis Title:	Modeling and Control of Membrane Filtration Systems for Offshore Produced Water Treatment
Ph.D. Student:	Kasper Lund Jepsen
Supervisor:	Assoc. Prof. Zhenyu Yang, Aalborg University

The body of the thesis consists of the following papers:

[A] K. L. Jepsen, L. Hansen, C. Mai and Z. Yang, "Challenges of membrane filtration for produced water treatment in offshore oil & gas production", *Proceedings of OCEANS 2016 MTS/IEEE Monterey - CA, USA, September 19-23*, pp. 1-8, 2016, https://doi.org/10.1109/OCEANS.2016.7761443.

[B] K. L. Jepsen, M. V. Bram, S. Pedersen, Z. Yang, "Membrane Fouling for Produced Water Treatment: A Review Study From a Process Control Perspective", *Water (MDPI)*, Vol. 10, No. 7, pp. 1-28, 2018, https://doi.org/10.3390/w10070847

[C] K. L. Jepsen, L. Hansen, Z. Yang, "Control parings of a de-oiling membrane process", *3rd IFAC Workshop on Automatic Control in Offshore Oil and Gas Production OOGP 2018 - Esbjerg, Denmark, 30 May - 1 June*, IFAC-PapersOnLine, Vol. 51, No. 8, pp. 126-131, 2018, https://doi.org/10.1016/j.ifacol.2018.06.366.

[D] K. L. Jepsen, S. Pedersen, Z. Yang, "Control Pairings of a Deoiling Membrane Crossflow Filtration Process based on Theoretical and Experimental Results", *submitted to Journal of Process Control, pending decision for revised version.*

[E] K. L. Jepsen, M. V. Bram, L. Hansen, S. M. Ø. Lauridsen, Z. Yang, "Online Backwash Optimization of Membrane Filtration for Produced Water Treatment", *pending approval by Total, to be submitted to Journal of Membrane Science*.

[F] K. L. Jepsen, L. Hansen, C. Mai, Z. Yang, "Power Consumption Optimization for Multiple Parallel Centrifugal Pumps", *Proceedings of IEEE Conference on Control Technology and Applications (CCTA) - Mauna Lani, HI, USA 27-30 August, 2017*, pp. 806-811, 2017, https://doi.org/10.1109/CCTA.2017.8062559

In addition the following publications have also been made:

[1] L. Hansen, P. D. Løhndorf, K. L. Jepsen, Z. Yang, "Plant-wide Optimal Control of an Offshore De-oiling Process Using MPC Technique", *3rd IFAC Workshop on Automatic Control in Offshore Oil and Gas Production OOGP 2018 - Esbjerg, Denmark, 30 May - 1 June*, IFAC-PapersOnLine, Vol. 51, No. 8, pp. 144-150, 2018, https://doi.org/10.1016/j.ifacol.2018.06.369.

[2] Z. Yang, S. Pedersen, P. D. Løhndorf, C. Mai, L. Hansen, K. L. Jepsen, A. Aillos, A. Andreasen, "Plant-wide Control Strategy for Improving Produced Water Treatment", *Proceedings of 2016 International Field Exploration and Development Conference (IFEDC) - Beijing, China, 11-12 August*, pp. 1-8, 2016, https://doi.org/10.1049/cp.2016.1388.

Other publications which are not directly relevant for this Ph.D. thesis:

[3] C. Mai, S. Pedersen, L. Hansen, K. L. Jepsen and Z. Yang, "Subsea infrastructure inspection: A review study", *Proceedings of 2016 IEEE International Conference on Underwater System Technology: Theory and Applications (USYS) - Penang, Malaysia, 13-14 December*, pp. 71-76, 2016, https://doi.org/10.1109/USYS.2016.7893928.

[4] C. Mai, S. Pedersen, L. Hansen, K. L. Jepsen and Z. Yang, "Modeling and Control of Industrial ROV's for Semi-Autonomous Subsea Maintenance Services", *Proceedings of 20th IFAC World Congress - Toulouse, France, 9-14 July*, Vol. 50, No. 1, pp. 13686-13691, 2017, https://doi.org/10.1016/j.ifacol.2017.08.2535.

[5] K. L. Jepsen, L. Hansen, C. Mai, and Z. Yang, "Emulation and Control of Slugging Flows in a Gas-Lifted Offshore Oil Production Well Through a Lab-sized Facility", *Proceedings of the 2013 IEEE International Conference on Control Applications (CCA) - Hyderabad, India, 28-30 August*. pp. 906-911, 2013, https://doi.org/10.1109/CCA.2013.6662866.

[6] C. Mai, K. L. Jepsen, Z. Yang, L. Hansen, and K. K. Madsen, "Intelligent Control of Diesel Generators Using Gain-Scheduling Based

on Online External-Load Estimation" *Proceedings of the IEEE International Power Electronics and Application Conference and Exposition (IEEE PEAC'14) - Shanghai, China, 5-8 November*. pp. 966 - 971, 2014, https://doi.org/10.1109/PEAC.2014.7037990.

Preface

This thesis is submitted as a collection of papers to fulfill the requirements for the degree of Doctor of Philosophy at the Department of Energy Technology, Aalborg University, Denmark. The work has been conducted at the Department of Energy Technology, Aalborg University, Denmark. The work was done in close collaboration with Total in the period February 2016 to February 2019 under the supervision of Assoc. Prof. Zhenyu Yang. The project has been supported by Danish Hydrocarbon Research and Technology Centre and Aalborg University joint project (Smart Water Management Systems, Aalborg University, Pr-no: 870051). I thank all the project partners, Erik Bek-Pedersen, Morten Lind, Bjarne André Asheim, and Thomas Martini Jørgensen for their support throughout the project.

I gracefully thank all the colleagues from the Department of Energy Technology, Aalborg University for providing a friendly and positive research environment. Thanks to Steven M. Ø. Lauridsen for providing a company aspect and feedback.

I would like to especially thank my supervisor Zhenyu Yang for his professional opinion and his open door policy, always finding time for discussions. Thanks to my project colleagues, Leif Hansen, Dennis S. Hansen, Mads V. Bram, Simon Pedersen, Petar D. Løhndorf, and Stefan Jespersen for proving great feedback and an open minded forum for discussions. Special thanks to former colleague Christian Mai for being a great colleague and friend.

Lastly, I express my gratitude to my family and friends, especially my girlfriend which supported me through tough times and supported my decisions, and my parents for always providing a place outside the research environment were I could relax.

Kasper Lund Jepsen
Aalborg University

Abbreviations

CAPEX	Capital expenditure
CF	Crossflow
CFV	Crossflow velocity
CiP	Cleaning in place
DIC	Decentralized integral controllability
LPV	Linear parameter-varying
MIMO	Multiple-input-multiple-output
MPC	Model predictive control
OiW	Oil-in-water
OPEX	Operational expenditure
P&ID	Piping and instrumentation diagram
PID	Proportional, integral, and derivative
PW	Produced water
PWT	Produced water treatment
RGA	Relative gain array
RHP	Right half plane
SISO	Single-input-single-output
TF	Transfer function
TMP	Transmembrane pressure
VFD	Variable frequency drive

Nomenclature

$\bar{p}_a$	Predicted power consumption based on the affinity-law (W)
$\bar{p}_b$	Predicted power consumption based on the proposed model (W)
$\boldsymbol{H}$	Hessian matrix of p_t $(-)$
ΔP	Transmembrane pressure (bar)
ΔP^*	Critical pressure (bar)
Δp_a	Difference between $\bar{p}_a$ and p_m $(\%)$
ΔP_b	Backwashing transmembrane pressure (bar)
Δp_b	Difference between $\bar{p}_b$ and p_m $(\%)$
$\Delta P_{b,ref}$	Reference for the backwashing pressure controller (bar)
ΔP_{WP1}	Pressure boost across WP_1 (bar)
Δt_{fr}	Time window used averaging (s)
η	OiW separation efficiency $(\%)$
γ	Interfacial tension (dyn/cm)
$\hat{P}_{V1}$	Estimated position of V_1 $(\%)$
$\hat{P}_{V2}$	Estimated position of V_2 $(\%)$
$\hat{P}_{V3}$	Estimated position of V_3 $(\%)$
λ	Relative gain array matrix $(-)$
λ_D	Dynamic relative gain array $(-)$
λ_E	Effective relative gain array $(-)$
λ_{Qcf}	RGA vector for the output Q_{cf} $(-)$
λ_{Qpm}	RGA vector for the output Q_{pm} $(-)$
ω	Frequency (rad/s)
Ω_c	Critical frequency/bandwidth matrix (rad/s)
ω_p	Pump speed (rpm)
$\omega_{c,zk}$	Critical frequency/bandwidth (rad/s)
ω_{max}	Maximum pump speed (rpm)

ω_{min}	Minimum pump speed (rpm)
$\omega_{p,0}$	Pump speed for the characteristic curve (rpm)
a_1	Coefficient for the function p $(-)$
a_2	Coefficient for the function p $(-)$
a_3	Coefficient for the function p $(-)$
a_4	Coefficient for the function p $(-)$
b_1	Coefficient for the function p $(-)$
b_2	Coefficient for the function p $(-)$
c_d	Mean downstream curvature (cm^{-1})
C_p	Permeate OiW concentration (mg/L)
C_r	Reject OiW concentration (mg/L)
c_u	Mean upstream curvature (cm^{-1})
$C_{V1,Qcf}$	Dynamic controller, using V_1 to control Q_{cf} $(-)$
$C_{V1,Qpm}$	Dynamic controller, using V_1 to control Q_{pm} $(-)$
$C_{WP1,Qcf}$	Dynamic controller, using WP_1 to control Q_{cf} $(-)$
$C_{WP1,Qpm}$	Dynamic controller, using WP_1 to control Q_{pm} $(-)$
CFV	Crossflow velocity (m/s)
d	Disturbance input $(-)$
d_0	Operating point for the disturbance d $(-)$
E	Effective gain matrix $(-)$
e_{zk}	Effective gain $(-)$
$f(z,d)$	Static model of the membrane process plant $(-)$
f_r	Flux recovered from backwashing $\left(\frac{L}{m^2 \cdot h}\right)$
$f_s(z,d)$	Static function calculating the scheduling variables for H_{WP1} $(-)$
G	Gain matrix of membrane process model $(-)$
$g_{\boldsymbol{H}d}$	Diagonal elements of $\boldsymbol{H}$ $(-)$
$g_{\boldsymbol{H}s}$	Non-diagonal elements of $\boldsymbol{H}$ $(-)$
g_{zk}	Transfer function between input k and output z $(-)$
g^0_{zk}	g_{zk} normalized $(-)$
h	Pump head pressure (m)
H_0	Vector of all the actuator transfer functions $(-)$
h_t	Combined head pressure over the pumps (m)
H_{V1}	Transfer function between V_1 input and valve position $(-)$
H_{V2}	Transfer function between V_2 input and valve position $(-)$
H_{V3}	Transfer function between V_3 input and valve position $(-)$

H_{WP1}	Transfer function between WP_1 input and pressure across WP_1 $(-)$
i	The complex number $(-)$
j	Flux, or permeate per membrane area $\left(\frac{L}{m^2 \cdot h}\right)$
j_b	Membrane flux during backwashing $\left(\frac{L}{m^2 \cdot h}\right)$
j_c	Total amount of permeate produced per membrane area (L/m^2)
j_f	Membrane flux during filtration $\left(\frac{L}{m^2 \cdot h}\right)$
$j_{avg\|n}$	Average flux for the cycle no. n $\left(\frac{L}{m^2 \cdot h}\right)$
k	Number of active pumps $(-)$
k_n	Number of samples for the current cycle no. n $(-)$
KV_f	Flow conductance through the membrane $\left(\frac{L}{s \cdot bar}\right)$
l_n	Number of samples for the backwashing phase no. n $(-)$
m	Index variable $(-)$
N	Total number of pumps available $(-)$
p	Pump power consumption function (W)
p_0	Pump power consumption for the characteristic curve (W)
p_m	Measured power (W)
p_s	Power saved $(\%)$
p_{tu}	A modified version of p_t, assuming identical pumps (W)
p_t	Total power consumption for the pumping system (W)
Q	Pump flow rate (L/s)
Q_f	Feed flow rate to the membrane (L/s)
Q_t	Combined flow rate from the pumps (L/s)
$Q_{1...k}$	The flow rate from pump number 1...k (L/s)
Q_{cf}	Crossflow rate (L/s)
Q_{pm}	Permeate flow rate (L/s)
$Q_{WP1,0}$	Steady-state operating point for Q_{WP1} (L/s)
Q_{WP1}	Flow rate through WP_1 (L/s)
R	Permeate flow resistance $\left(\frac{bar \cdot h \cdot m^2}{L}\right)$
R_p	Recovery percentage $(\%)$
$R_{b\|n}$	Model of the resistance development during backwashing for the cycle no. n $\left(\frac{bar \cdot m^2 \cdot h}{L}\right)$
$R_{f\|n}$	Model of the resistance development during filtration for the cycle

	no. n $\left(\frac{bar \cdot m^2 \cdot h}{L}\right)$
t	Time (s)
t_b	Duration of the backwashing phase (s)
t_f	Duration of the filtration phase (s)
T_s	Sample time (s)
$t_{b\|n}$	Backwashing duration time for the cycle no. n (s)
$t_{f\|n}$	Filtration duration for the cycle n (s)
U_{V1}	Input to V_1 $(\%)$
U_{V2}	Input to V_2 $(\%)$
U_{V3}	Input to V_3 $(\%)$
$U_{WP1,0}$	Steady-state operating point for U_{WP1} $(\%)$
U_{WP1}	Input to WP_1 $(\%)$
y_c	Output of function $f(z,d)$ $(-)$
z	Inputs to the static functions $f(z,d)$ and $f_s(z,d)$ $(-)$
z_0	Operating point in z $(-)$

Part I

Extended Summary

Chapter 1

Introduction and Motivation

In the offshore oil and gas sector, large quantities of water are extracted from the oil reservoirs. For the Danish sector, $37 \cdot 10^6 m^3$ of water was extracted in 2017, where the ratio between water and oil was approximately 4 to 1 [1]. The large quantity of water and oil must be separated offshore to avoid unnecessary transportation capacity and energy usage. If the water and oil are separated sufficiently, the water can be discharged into the sea or reinjected into the reservoirs, reducing the required transportation capacity. The main components of the offshore oil-in-water (OiW) separation train typically consist of gravity-based separators and hydrocyclones, as shown in Fig. 1.1.

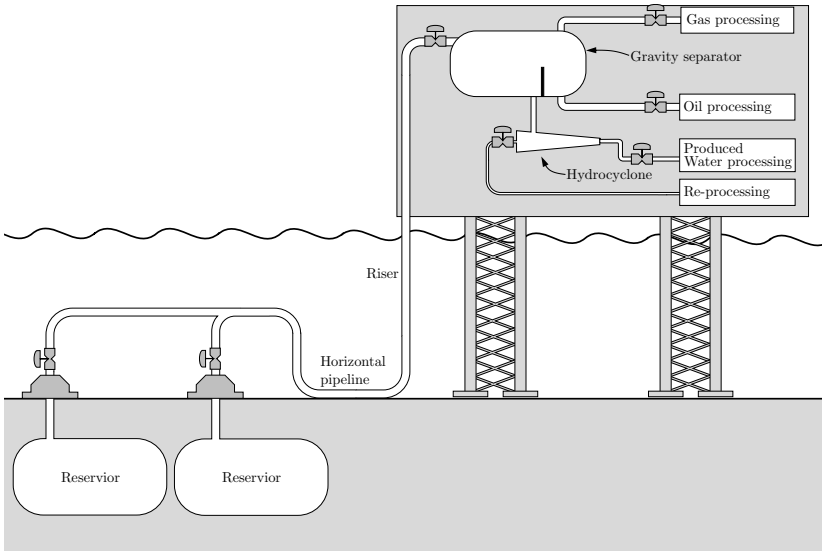

Fig. 1.1: Simplified overview of the current offshore oil extraction and separation process.

The first stage separation consists of gravity-based separators, both low and high pressure, where oil, gas, and water are separated based on density difference. In general, the gravity-based separator can reduce the dispersed OiW concentration of the produced water (PW) to 200-250mg/L [2, 3]. The separated oil and gas continue to further processing, while the PW is transported to the hydrocyclones to further reduce the OiW concentration to 20-80mg/L [4]. However, the separation efficiency of the hydrocyclone can be sensitive to fluctuating in-flow rates and care must be taken to ensure sufficient separation for discharge [5, 6]. The governmental regulations for the Danish North Sea in 2018 are as follows: (1) the discharge concentration must be below 30mg/L, and (2) the total amount of discharged dispersed oil must be below 222 tonnes annually [7, 8]. These regulations are challenging to comply with as the concentration limit in the North Sea was periodically exceeded on 16 different platforms during 2014 and in 2015 an oil producer discharged 95% of their annual limit [8, 9].

The total amount of PW is decreasing, as shown in Fig. 1.2, and increasing amounts of PW are reinjected into the reservoir (31% in 2014), consequently reducing the amount of PW discharged [10]. However, reinjecting PW into the reservoir can cause damage and block the reservoir if not cleaned sufficiently, thus the membranes can also be used to ensure high injection water quality [11, 12]. Furthermore, political tendencies towards zero-discharge policies require new technologies to be considered [13, 14]. One possible candidate for improving OiW separation efficiency which has received increasing attention is membrane filtration [15].

The remaining of this chapter is organized as follows: Firstly, the motivation for membrane filtration is described. Secondly, the motivation for improving membrane filtration performance through control is discussed. Lastly, a description of the problem and motivation for each of the papers is made. All the papers are included in Part II.

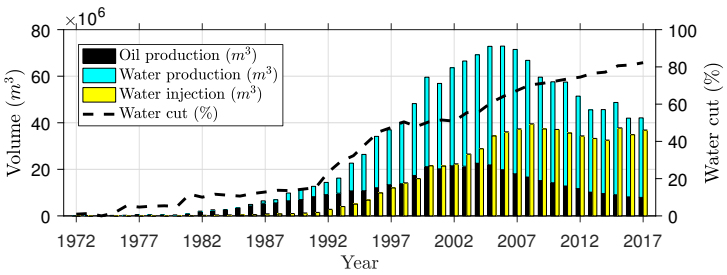

Fig. 1.2: Annually amount of oil and water production and water injection in the Danish sector of the North Sea. The dashed line is the increasing water cut. The data are based on annual reports from the Danish Energy Agency [1].

1.1 Motivation for Membrane Filtration

The environmental focus and the ability to reduce OiW concentration below what currently deployed technologies are capable of, are likely the cause of the increasing number of publications addressing membrane filtration for produced water treatment (PWT) [15]. The porous membrane wall is a selective barrier, in terms of size, that allows passage of particles or droplets with a size less than the membrane pores. Based on case studies for PWT, the considered concentration levels suggests membrane installation either downstream the gravity separators or the hydrocyclones [16–19]. However, the higher concentration after the gravity separators causes increased fouling. A typical installation downstream the hydrocyclones is shown in Fig. 1.3a, and an overview of the concept and terminology used in this thesis is presented in Fig. 1.3b. Several studies show that by deploying suitable membranes the OiW concentration can be reduced significantly as indicated by the studies shown in Table 1.1. Furthermore, separation efficiency is dependent on membrane pore size, operating conditions, and feed composition [20].

Table 1.1: Oil removal performance for different membrane filtration studies.

Membrane type	Pore size (μm)	Feed OiW concentration (mg/L)	Permeate OiW concentration (mg/L)	Source
Ceramic (ZrO_2)	0.1	25	< 3	[19]
Ceramic (α-alumina)	0.05	500	7	[21]
Ceramic (α-alumina)	0.8	250	6	[17]
Ceramic (α-alumina)	0.1	5000	< 10	[22]
NaA (zeolite)	1.2	500	< 3	[23]

Despite the focus on deploying membrane filtration for reducing harmful substances in the PW discharge, the technology is not widely deployed in the offshore sector. As the membranes require three times the footprint compared to the hydrocyclones and installation footprint offshore is extremely expensive, the lack of offshore implementation is largely caused by the capital expenditure (CAPEX) and operational expenditure (OPEX) [4]. To increase the attractiveness of membrane filtration for offshore deployment, the CAPEX and OPEX must be reduced. A common issue is the accumulation of contamination on the membranes (fouling), reducing permeability and increasing both CAPEX and OPEX [24]. Multiple approaches have been investigated to maintain permeability and capacity by removing or reducing fouling. The approaches can be categorized into chemical pretreatment, physical pretreatment, membrane materials, membrane modification, and cleaning in place (CiP) methods [24]. Chemical pretreatment is addressed in [25–27], physical

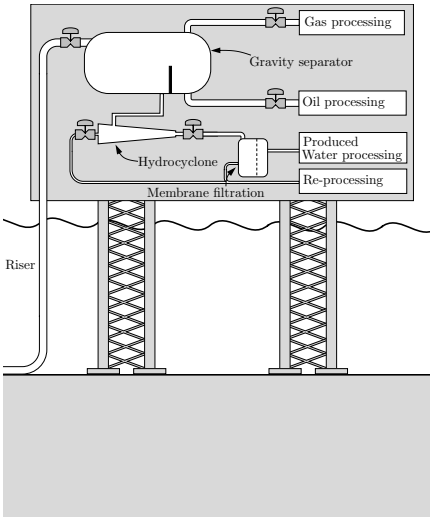

(a) Simplified overview of the offshore extraction and separation process extended with membrane filtration, where the underflow from the hydrocyclones are fed to the membranes, permeate is discharged into the sea or further processed, and reject is directed to reprocessing.

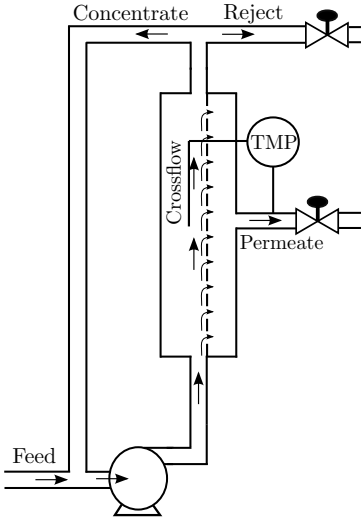

(b) Membrane terminology, showing the feed, permeate, crossflow, reject, and concentrate flow rate, as well as the transmembrane pressure (TMP). Figure from Paper B.

Fig. 1.3: A simplified overview of the offshore separation process deploying membrane filtration as the third separation stage.

pretreatment in [27], membrane materials and modification in [28, 29], and CiP methods in [30–32], where the most common CiP method is backwashing. Backwashing is a process where the permeate flow and TMP are reversed to remove fouling from the membrane. The remaining of this thesis focuses on how the CAPEX and OPEX can be reduced by improving current control strategies for membrane filtration.

1.2 Motivation for Control Improvements

The control improvements considered in this thesis are divided into two categories: (1) dynamic control of the filtration facility to maintain the desired operating point. (2) scheduling of backwashing to maintain a high net permeate production and minimize permeate spent backwashing.

1.2.1 Operating Conditions

Studies show that operating conditions of the filtration system and the preferred controlled variable, either transmembrane pressure (TMP) or flux (permeate flow rate per surface area), are essential for maximizing the overall produced permeate [20, 30, 33–37]. Few studies focus on how the dynamic controllers, maintaining the operating point, are designed with respect to control structure and tuning [38, 39]. For some applications of membrane filtration, the dynamic behavior of the controller may not be essential if the process is undisturbed and allowed to remain at steady-state. However, the design and control pairings of the dynamic controllers are crucial, as the flow rate and pressure are rarely steady for PWT [40]. Although most studies deploy proportional, integral, and derivative (PID) controllers, this thesis strives to emphasize the importance of accounting for cross couplings in the design phase, even for decentralized single-input-single-output (SISO) control, to ensure optimal reference tracking of the carefully chosen operating point [38, 41–45].

1.2.2 Backwash Scheduling

Backwashing is another topic where optimization of the scheduling algorithm can improve the capacity of the filtration system and thereby reduce CAPEX and OPEX. Often the duration of the backwashing and filtration phase are either based on an arbitrarily choice, manufacturer recommendation, or a short pre-investigation [20, 46–48]. In addition, the durations are often constant for the lifetime of the installation, rather than updated online to maintain optimality. In some cases, the duration of the filtration and backwash phase is based on the TMP or flux which, compared to fixed durations, allows for adaptation. Scheduling of backwashes based on the TMP has shown to reduce the consumption of backwashing media by 25% while maintaining identical capacity compared to fixed durations [49]. In addition, artificial neural network and response surface methodology have been applied to optimize backwash scheduling [50, 51]. Both methods estimate a model for the desired operating point, followed by optimization of the backwashing and filtration duration, not accounting for system changes occurring after identification. Furthermore, both methods select two fixed durations, one for each of the filtration phases and the backwashing phases, to be used during the lifetime of the installation. However, by applying online optimization based on current observations, optimality can be maintained throughout different conditions. The thesis aims to propose a scheduling method which can online adapt to changes in operating conditions and fouling state, ensuring optimality throughout the lifetime of the installation.

1.3 Outline of the Papers

The thesis is divided into two parts; an extended summary, and a part containing the paper contributions. The extended summary covers the background and motivation for the project and ties the contributions from each paper together. The second part consists of the contributing papers A-F. An overview of the contributions in terms of papers and how they relate is shown in Fig. 1.4. The remaining of this section describes the motivation for each of the contributing papers.

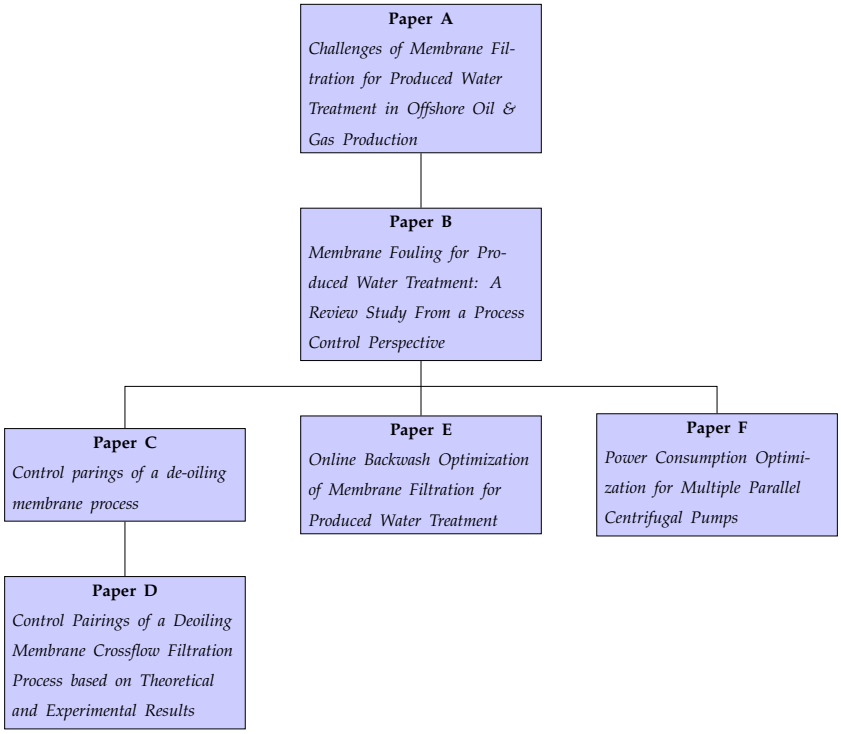

Fig. 1.4: Overview of the enclosed papers.

1.3.1 Motivation for Paper A [52] and B [24]

Firstly, the challenges for applying membrane filtration for PWT in the offshore oil and gas sector are reviewed in Paper A. Secondly, the process control related issues for membrane filtration for PWT are reviewed in Paper B. Both papers aim to highlight challenges and issues related to membrane filtration of PW, particularly as many process control related issues are unaddressed and more sophisticated control and scheduling can improve net per-

meate production. The papers are a good starting point for process engineers keen on optimizing filtration capacity through more sophisticated control and scheduling. In addition, many review membrane filtration for PWT by addressing chemical additives, PW complexity, membrane type, surface modifications, and operating parameters [25, 26, 28, 29, 53–55]. However, to the author's knowledge Paper B is currently the only review article explicitly addressing optimization of the filtration system from a process control perspective.

1.3.2 Motivation for Paper C [7] and D [56]

Much afford is used to determine the operating conditions resulting in the least amount of fouling while maintaining a high capacity [20, 57, 58]. However, the controllers actively maintaining the operating conditions are rarely mentioned nor addressed and are only deployed as a necessity for sufficient reference tracking. Based on the few studies mentioning the control structure used, the PID controllers are most frequently used [38, 41–45]. The popularity of the PID control technique is presumably a result of simplicity, transparency, and availability of simple tuning rules [39], but most tuning methods neglect to account for the cross couplings that often exist in large process systems.

Paper C identifies a static process model, which is used to predict possible interactions between the control loops based on the relative gain array (RGA) analysis. Paper D extends the model and analysis to cover the dynamic features of the system. Based on the analysis, a potential best and worst control pairing are tested and compared. Both papers aim to highlight how essential it is to account for cross couplings even if simple control structures, such as PID, are used. Results show that accounting for the cross couplings, by following the RGA pairings rules, can provide superior reference tracking, consequently reducing fouling growth.

1.3.3 Motivation for Paper E [59]

Deploying backwashing for fouling removal has shown to increase the overall permeate production of the filtration system [20, 31]. However, scheduling backwashing can be difficult as too rarely backwashing causes high permeate resistance and if done too frequently the consumption of backwashing media (often permeate) increases [49]. Often a fixed duration for each of the filtration and backwashing phase is chosen based on experience or system analysis, not allowing the durations to be online adapted even though operating conditions change.

Paper E investigates how fouling accumulates during filtration and is removed during backwashing. It was observed that fouling was removed as

quickly as the backwashing pressure could be established and prolonged backwashing resulted in no further removal. The paper aims to propose an algorithm which automatically updates the durations after each filtration cycle (filtration and backwash) to maintain optimality even when conditions change. The proposed algorithm was tested on the pilot plant where the durations were adjusted as irreversible fouling slowly accumulated.

1.3.4 Motivation for Paper F [60]

The introduction of crossflow (CF) membrane filtration results in less fouling growth, but consequently increasing pumping demand and energy consumption [61]. As membrane filtration installation increases in size and reliability is a requirement, multiple pumps must be combined for redundancy and flexibility. Scheduling of multiple pumps to maintain the desired flow and minimize energy usage is a widely discussed topic [62, 63].

Paper F proposes an alternative to the widely used affinity-law based approach. The proposed model describes the steady-state power consumption as a function of head pressure and flow rate, thus provides higher model accuracy compared to using the affinity-law. Based on the proposed model, a method for scheduling multiple identical variable frequency pumps is proposed. The method is compared to a scheduling strategy where only a single pump is equipped with a variable frequency drive (VFD).

Chapter 2

Pilot Plant Design

A large pilot plant is previously constructed to investigate current challenges related to offshore oil and water separation. The plant consists of a horizontal and vertical riser, gravity-based separators, and hydrocyclones.

The plant was initially constructed to investigate how slugging is formed and how advanced control can be deployed to negate the negative effects slugging can have on the downstream processes. In addition, advanced control and monitoring of the combined separator and hydrocyclone system have been carried out using H_∞ control and model predictive control (MPC) solutions [40, 64–68].

As a part of this thesis, the pilot plant was extended with membrane filtration units as the third separation stage, to serve as a platform for experimental validation of methods and theories proposed in this thesis.

2.1 Design Criteria

To design the pilot plant membrane extension, a set of design criteria was formulated as:

- The membrane extension should be able to process the upstream flow rate, to allow for series operation of the separation train.
- The chosen membranes should be well suited for oil removal.
- The plant extension should be very flexible and allow reconfiguration to serial or parallel operation.
- Membrane cleaning methods must be incorporated into the design.
- The OiW mixture must be well mixed to ensure consistent concentration throughout experiments.

- The extension should be adequately instrumented to allow superior insight into the filtration process.

2.2 Recreating Produced Water Mixture

Before designing the membrane extension itself, it is essential that a well-mixed OiW emulsion can be created and replicated, especially the concentration and droplet sized distribution can be a challenge to replicate. The mixing system must support multiple systems as the membranes, hydrocyclones, and gravity-based separator must be supplied from a single mixing unit. Ideally, the oil used in the pilot plant should be identical to the produced oil offshore, but because of the relatively large size of the pilot plant and the large quantity of oil required, a less volatile oil is chosen for safety reasons. Specifically, a non-detergent SAE 30 motor oil produced by Midland is used. The non-detergent feature is essential for creating a droplet size distribution similar to those offshore, as surfactant additives would reduce the droplet size distribution below desired levels.

To control the droplet size distribution and ensure a uniform distribution of oil throughout the large mixing tank, two large mechanical stirrers (variable speed) with a combined maximal mixing intensity of $1469 m^3/h$ were used. To evaluate if the artificially created emulsion has a reasonable droplet size distribution, the emulsion was analyzed using the Jorin ViPA (video microscopy) [66]. The identified droplets size distribution is illustrated in Fig. 2.1.

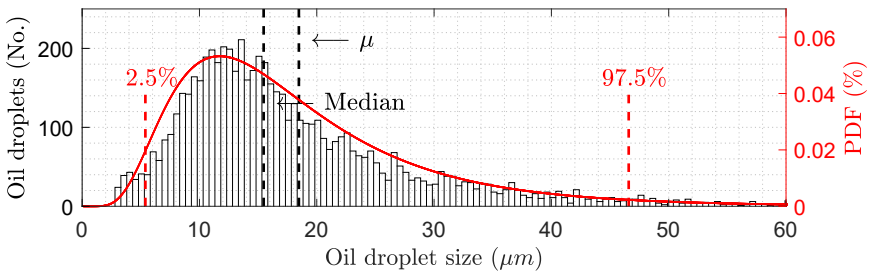

Fig. 2.1: Histogram of the oil droplet size, where the mean, median, and 95% confidence interval are marked. The mean is $18.47 \mu m$, the median is $15.47 \mu m$, and the lower and higher boundaries of the confidence interval are $5.4 \mu m$ and $46.6 \mu m$, respectively. Modified: Added the 95% confidence interval [66]. Licensed under CC BY 4.0.

It is difficult to evaluate if the droplet distribution is within a realistic range, as little information exists on droplets sizes after each separation stage. However, the droplet size range for produced water is generally between $1 \mu m$ and $1000 \mu m$, with most droplets being in the 5-50μm, but variances are to

be expected depending on oil composition [69]. As the artificial produced OiW mixture has 95% of the droplets within the 5.4-46.6μm range, the size distribution was deemed acceptable.

2.3 Membranes

In this section, the selection of membrane material, pore size, and configuration will be described.

2.3.1 Material Selection

Two types of membrane material are commonly considered; ceramic and polymeric, or a combination thereof [70]. The ceramic membranes are, compared to polymeric membranes, recognized for high resilience against temperature, pressure, cleaning agents, and for a narrower and more well-defined pore size distribution [28, 53, 71]. However, polymeric membranes are in general lighter by a factor of 10 and are less expensive to manufacture compared to ceramic membranes, especially weight is a crucial parameter for offshore deployment [16, 29, 72].

Both polymeric and ceramic membranes have been deployed for OiW separation, but ceramic membranes showed an overall higher flux compared to polymeric membranes. However, fouling remains accountable for a large reduction in flux for both ceramic and polymeric membranes [19, 73–76]. Ceramic membranes can consist of different types of ceramics, eg. SiC, TiO_2, Al_2O_3, and ZrO_2. Unfortunately, no direct comparison between all types of ceramic membranes exist, but literature agrees that SiC membranes show promising results with higher sustainable flux and strong hydrophilic properties [77, 78].

2.3.2 Pore Size Selection

Beside classification with respect to membrane material, membrane filtration is also classified into four categories based on pore size, namely: Microfiltration (MF), ultrafiltration (UF), nanofiltration (NF) and reverse osmosis (RO). The categories with respect to pore size, are defined in Table 2.1.

MF and UF have been investigated for PWT, where UF was concluded to be suitable for PWT [72]. The fact that UF is required to reliably reduce the OiW concentration below $30 mg/L$ is confirmed in [27, 46, 80–83]. Based on results in literature, UF SiC ceramic membranes were chosen for the pilot plant as they show promising results in terms of hydrophilic, high flux, and separation efficiency. The commercial selected membranes have a pore size of $40nm$ and is manufactured by LiqTech.

Table 2.1: Classification of membrane based on pore size [79].

Type	Pore size range
Microfiltration	$100nm - 2\mu m$
Ultrafiltration	$2nm - 100nm$
Nanofiltration	$1nm - 2nm$
Reverse osmosis	$\leq 1nm$

2.3.3 Configuration

Membranes are commonly configured for either dead-end or CF filtration as illustrated in Fig. 2.2. Besides the flow conditions at the membrane surface, multiple filtration units can be arranged in different configurations.

Crossflow and Dead-end Filtration

In the CF configuration, water is directed across the membrane surface, introducing shear on the membrane surface, consequently reducing the likelihood of fouling accumulating [84]. The CF configuration causes the OiW concentration to gradually increase as clean water permeates the membrane and exits the CF loop. Theoretically, the OiW concentration in the CF loop would continuously increase towards a 100% oil if only water was allowed to exit the loop, thus increasing fouling growth. To avoid this, a part of the CF is rejected from the loop as a concentrated form of the feed. The permeate and reject concentration can at steady-state be calculated using the following relationships:

$$\begin{aligned} C_p &= (1-\eta)C_f \\ C_r \cdot (1-R_p) &= C_f - R_p C_p \end{aligned} \tag{2.1}$$

where η is the separation efficiency, C_f is the OiW concentration in the feed flow, R_p is the ratio between permeate and feed (recovery percentage), C_p and C_r are the permeate and reject OiW concentrations, respectively. Eg. assuming 95% separation efficiency, 10% rejection, and $20mg/L$ feed concentration, the reject and permeate OiW concentrations are $191mg/L$ and $1mg/L$, respectively.

For dead-end filtration, the water is forced through the membrane, causing most oil to be retained by the membrane, thus the membranes foul quickly compared to CF filtration. It is not uncommon for CF filtration to increase permeate flow rate by 100% compared to dead-end filtration [85–87]. However, increasing the crossflow velocity (CFV) from $0.75m/s$ to $2.25m/s$ has shown to decrease total organic content removal efficiency and increase flux by approximately 2% and 16%, respectively [20]. The reduced removal

efficiency is presumably a consequence of high shear rates causing droplet breakup.

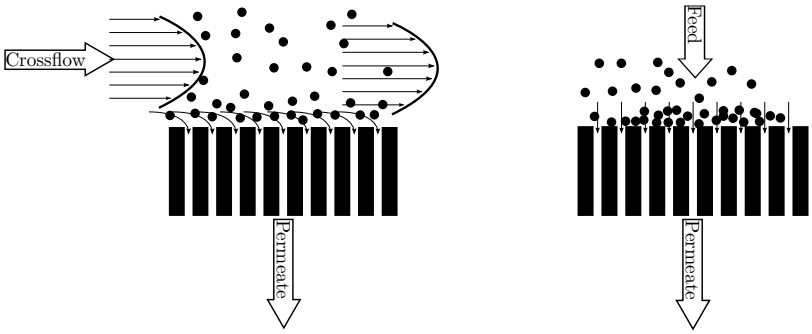

(a) Crossflow filtration. **(b)** Dead-end filtration.

Fig. 2.2: The crossflow and dead-end filtration configurations. Figure from Paper B. Licensed under CC BY 4.0.

Multi-membrane Configurations

Beside CF and dead-end configurations, multiple membrane filtration units can be arranged in different configurations. The three most common configurations are illustrated in Fig. 2.3.

Reject-feed series connected (Fig. 2.3a) membranes process only the reject from the previous stage, hence the amount of PW processed by each stage gradually decreases depending on the recovery percentage of each stage (ratio between permeate and feed). The first stage concentrates the feed to a degree specified by the recovery rate and lets the next stage deal with the condensed PW. A prototype for PWT with two stages was tested in [72] and based on results a four-stage membrane filtration unit was suggested for offshore PWT. Furthermore, in [16] two two-stage filtration units were tested offshore with promising results. As the produced water is treated by each filtration stage, the concentration in each loop gradually increases. The small concentration in the first stages ensure that fouling growth remains low and consequently the first stages can maintain higher permeate flow rates. For some membrane filtration applications, this type of configuration has shown to improve the overall capacity of the filtration system [88].

Permeate-feed series connected (Fig. 2.3b) membranes are commonly a combination of different pore size, such that each stage works as a prefilter for the downstream membranes.

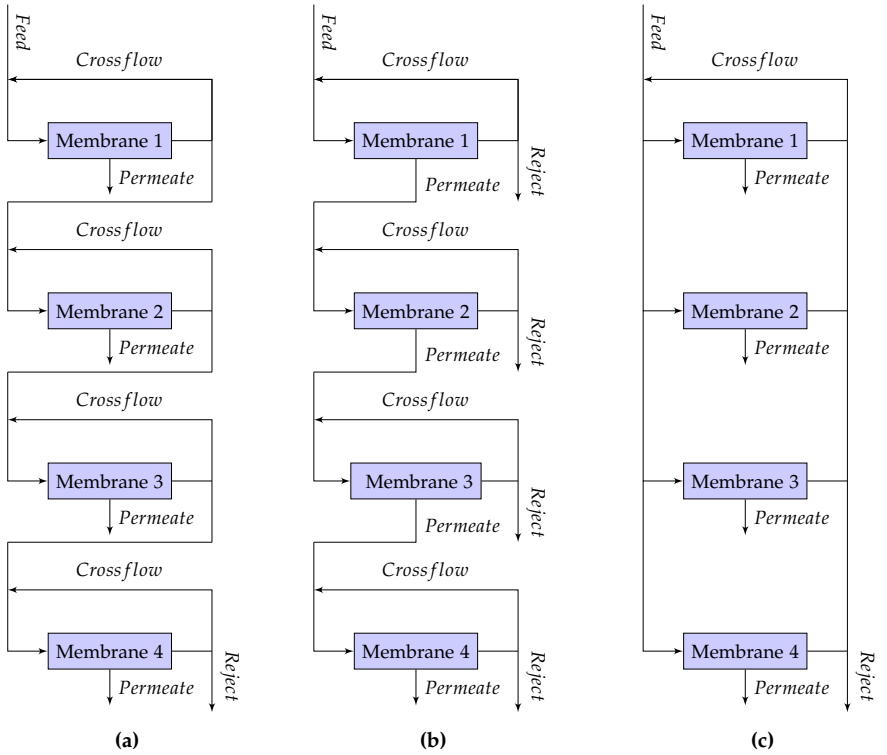

Fig. 2.3: Different membrane configurations: **(a)** illustrates the reject-feed configuration where the feed is connected to the reject from the previous stage, **(b)** illustrates the permeate-feed configuration where the feed is connected to the permeate from the previous stage, and **(c)** illustrates the feed in parallel configuration.

Feed parallel connected (Fig. 2.3c) membranes are exposed to identical concentration based on the reject percentage. Assuming identical recovery and a correlation between higher concentration and fouling growth, the membranes would be exposed to higher CF concentration and increased fouling growth compared to the reject-feed series connected membranes.

For the pilot plant, it was chosen to use CF filtration as the reduced fouling increases capacity and reduces footprint. Furthermore, it was chosen to make the filtration system highly flexible, allowing reconfiguration to all the considered configurations in Fig. 2.3, thus ensuring that each configuration can be investigated and compared. However, the system is by default configured as Fig. 2.3a.

2.4 Operational Capacity

As the membrane extension is intended to be used in series with the current first and second stage separation, it is designed to process the flow rate from the previous separation steps, which for normal conditions are 0.7-0.8L/s. The membrane manufacturer provided expected flux is 100-400$\frac{L}{h \cdot m^2}$, thus between 7.2m^2 and 28.8m^2 of membrane area is required. Due to space restrictions and availability of membrane sizes, it was chosen to use 8.16m^2 of membrane surface area. The membrane surface area is divided into eight sub-units (1.09m^2 each), see Fig. 2.4, for the following reasons: (1) to have a single unit that can operate without exposing the remaining membranes to contamination. (2) to have the possibility to reconfigure the filtration units and investigate different filtration configurations.

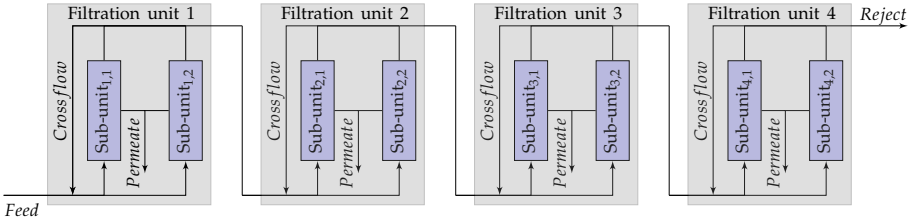

Fig. 2.4: Default membrane configuration for the pilot plant.

2.4.1 Pump Selection

The choice of pumps, e.g. centrifugal, lobe, and diaphragm can affect the shear rate and consequently the droplet size distribution and separation efficiency. Results in [89] showed that droplet breakup depends on both pump type and speed and in [90] it is shown that for a centrifugal pump the breakup is intensified by the rotational speed of the pump.

Furthermore, in [91] the droplet breakup for a coalescing centrifugal pump was analyzed with respect to both flow rate through and pressure across the pump. The results show that in general the droplet size is reduced for increased flow rate, whereas the point in pressure with the highest degree of coalescence depends on the flow rate. However, except for the coalescing centrifugal pump, the studies indicate that increased forces on the water in terms of either increased speed, flow rate, or pressure decrease droplet size.

For the pilot plant the common centrifugal pump was chosen for the following reasons; (1) it reflects what is currently deployed for oil and water separation filtration systems [20, 76, 92], and (2) low cost. Commonly the CFV is between 0.24m/s and 2.25m/s and the pumps for the pilot plant are selected with a capacity of 2.55m/s [17, 20, 93–95]. The requirements for the

feed pumps vary depending on the filtration stage, the first pump supplies the entire capacity, while the second stage feed pump supplies the three remaining stages ect. The final capacity of the pumps are:

The CF pumps: Grundfos CRNE10-02, rated 12.1m^3/h (CFV of 2.55m/s) and 22.9m.

Feed pumps: 1st and 2nd filtration unit: Grundfos CRNE3-5, rated at 3.5m^3/h and 34m.

Feed pumps: 3rd and 4th filtration unit: Grundfos CRNE1-4, rated at 2.2m^3/h and 26.8m.

2.5 Cleaning Methods

Fouling is a critical problem for offshore deployment of membrane filtration, causing the membranes to require three times the footprint compared to hydrocyclones with equal flow capacity [4]. To reduce the required installation footprint and to increase capacity, multiple CiP methods, such as ultrasonic cleaning, backwashing, and backpulsing are deployed throughout literature [32, 77, 96]. Besides the CiP methods mentioned, steam cleaning is an attractive candidate that is not widely deployed as polymeric membranes are unable to tolerate the temperatures [71, 97]. By introducing ceramic membranes with superior thermal stability (up to 800°C), steam cleaning has shown promising results for OiW separation [98]. During steam cleaning, the viscosity of the oil is reduced, allowing the oil to easier deform and dislodge from the membranes.

For the pilot plant, backwashing was chosen for its relatively low cost and popularity, hence any improvement in the backwashing technique could benefit a large range of installations [24]. By restricting backwashing to a single sub-unit at a time, a Grundfos CRNE 1-9 (rated: 61m and 2.2m^3/h) was chosen based on the assumption that the flux during backwashing and filtration are fairly identical (within a factor of 2-3). The piping and instrumentation diagram (P&ID) of the backwashing supply system is shown in Fig. 2.5. In addition, the pilot plant is equipped with a steam generator to allow further investigation into steam cleaning of the membranes, the P&ID is shown in Fig. 2.6.

2.6 Instrumentation

The instrumentation including sensors, actuators, the P&ID, and the data acquisition system are described throughout this section.

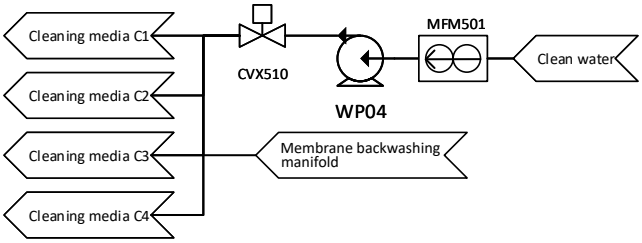

Fig. 2.5: P&ID of the backwashing system. The system pressurizes previous produced permeate and directs it to each filtration unit.

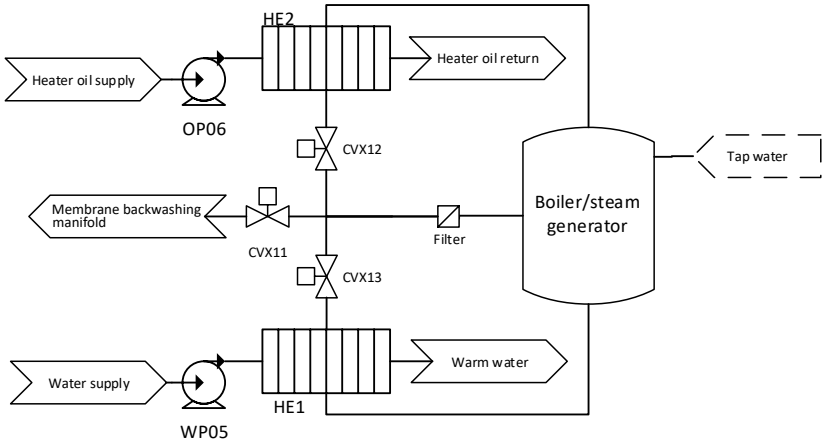

Fig. 2.6: P&ID of the steam system. The steam system can supply steam for backwashing, but can also be used to heat either the oil or the water phase.

2.6.1 Sensors and Actuators

The pressure and temperature sensors for the membrane extension are standard transmitters, measuring between 0-6*bar* and 0-100°C. Electromagnetic flow meters, based on Faraday's Law, provide cost-effective high accuracy ($\pm$0.25%) volumetric flow rate measurements. However, they rely on the fluid to be conductive, which can be problematic at high oil concentrations, but for the small OiW concentrations present in the filtration system, it is not an issue. Because of the availability of compressed air, the actuators are mainly based on pneumatics. Compared to electrical valves, the pneumatics valves provide faster responses and put less demand on the electrical power supply and cables. Lastly, several OiW monitors (Turner 4100XDC) are available to provide online OiW measurements. The OiW monitors can be connected to measure the feed, permeate outlet, and reject/crossflow OiW concentration for the membrane filtration system. The OiW measurement of the reject/crossflow is added to enable investigation of the OiW concentra-

tion for the different configurations described in section 2.3.3.

2.6.2 Pipeline and Instrumentation Diagram

The P&ID's for the filtration system are shown in Fig. 2.7 and Fig. 2.8, illustrating how the filtration units are interconnected and how each filtration unit is constructed and equipped with actuators and sensors, respectively. Most of the sensors and actuators are installed as a part of each filtration unit, see Fig. 2.8. Furthermore, the pilot plant and its key components are highlighted in Fig. 2.9 and Fig. 2.10.

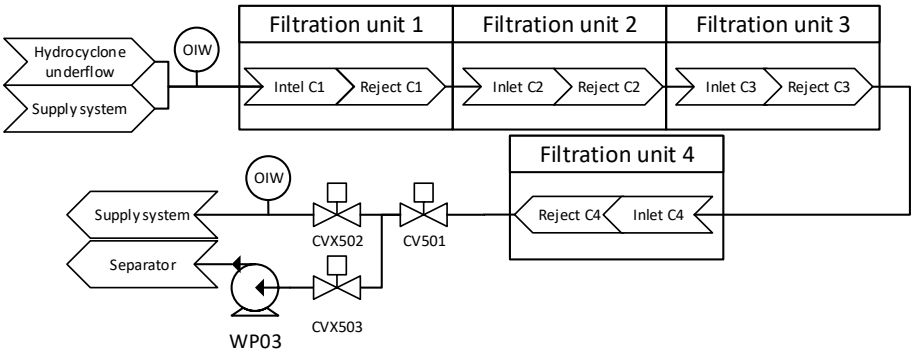

Fig. 2.7: P&ID of the filtration units, the feed flow rate can either come from the hydrocyclone or directly from the supply system. The reject can either be return to the supply system for remixing or directed to the gravity separator for reprocessing.

2.6.3 Data Acquisition System

The membrane extension is connected to the control system (MathWorks© Simulink Real-Time). All the information related to sensor and actuator offsets and gains is collected in a Microsoft Access database. Based on the database and code developed by the author, a Simulink file is auto-generated. Because of the auto-generation, sensors and actuators should only to be added to the database, whereafter the Simulink file automatically detects changes and updates accordingly. In short, the instrumentation and implementation can be simplified to the flowing components:

The pilot plant consists of approximately 300 sensors and actuators.

The host computer provides the main user interface for running highly customized experiments. Experiments are defined in a Simulink template file, where the actuators and sensors can be manipulated. Once the experiments are defined as a Simulink file, it is built and transmitted to the target PC.

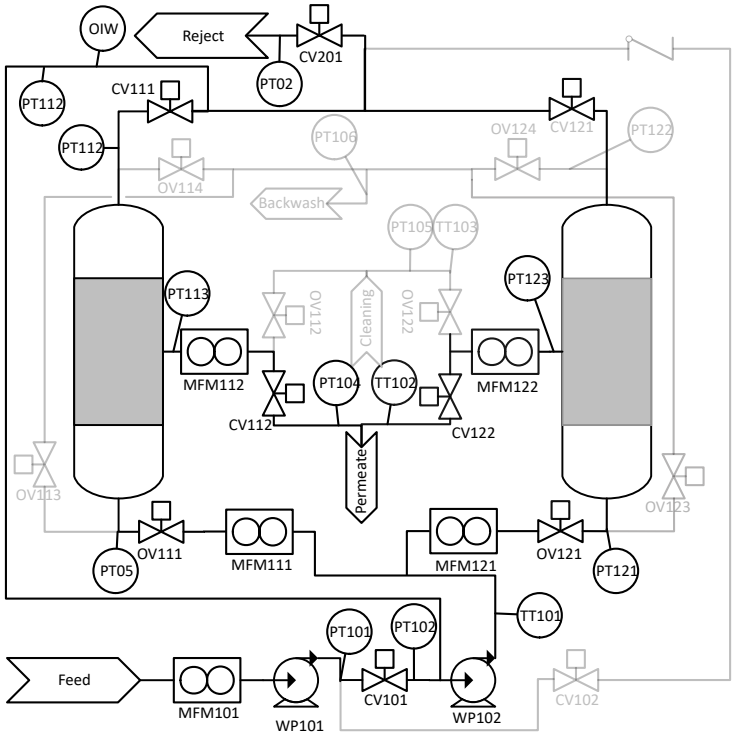

Fig. 2.8: Membrane filtration unit 1, with two membrane housings (sub-units). The bypass and backwashing instrumentation are grayed out.

Target computer The target PC is executing the Simulink file, normally at $100Hz$, and storing all sensor and actuator data on an internal hard drive.

The Matlab based acquisition system is able to transmit sensor data and receive actuator commands via ABB 800xA HMI software, allowing the system to display data according to traditional industry standards and to be controlled from a PLC-based environment. In short, the pilot plant can test both Matlab and PLC based algorithms.

2.7 Conclusion

The pilot plant has been designed and constructed to expand the current treatment train with membrane filtration. The pilot plant is equipped with pressure, temperature, and flow sensors to provide detailed data of the process, and if additional sensors are required, they are easily added with the developed Matlab script. The plant is highly flexible, allowing for reconfigu-

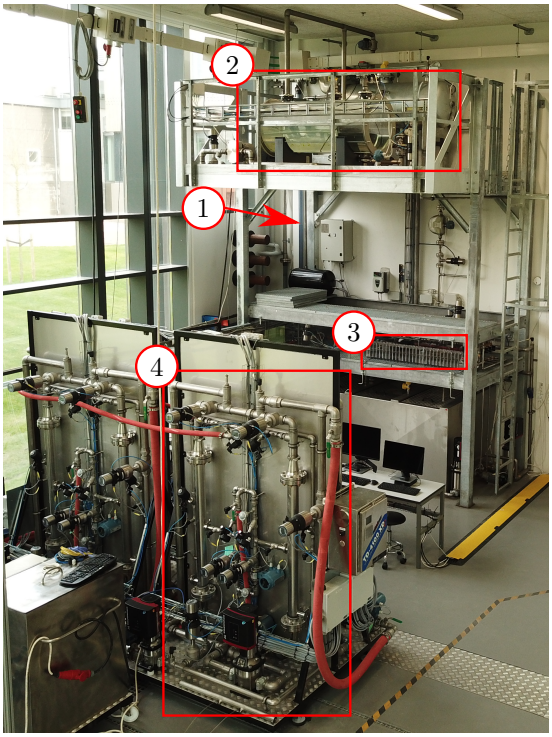

Fig. 2.9: Pilot plant: (1) is the riser pipeline, (2) are the gravity separators, (3) are the hydrocyclones, and (4) is a single membrane filtration unit.

ration for either serial or parallel operation, and both backwashing and steam cleaning have been included in the design. The flexibility, sensors, and actuators enable the pilot plant to be successfully deployed to test and validate the various methods suggested throughout the thesis. To ensure that the experimental results from the pilot plant reflect reality, the similarity between PW and the OiW emulsion used should be further investigated.

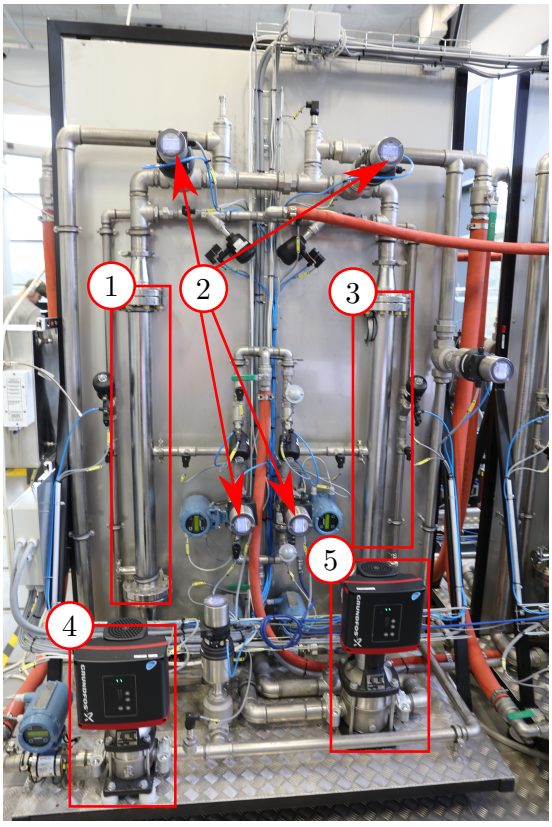

Fig. 2.10: A membrane filtration unit: (1) is the membrane housing number 1, (2) is the control valves, (3) is the membrane housing number 2, (4) is the pressure boosting pump (WP101, according to Fig. 2.8), and (5) is the CF pump (WP102, according to Fig. 2.8).

Chapter 3

State-of-the-Art Membrane Filtration for Produced Water Treatment

In this section, the main points of the review articles (Paper A and B) are summarized, covering the challenges associated with deploying membrane filtration for PWT. The section is divided into three parts, addressing filtration of PW, fouling removal and prevention techniques, and fouling models. A detailed review of the topics can be found in Paper A and B.

3.1 Complexity of Produced Water

Multiple studies review the complexity and composition of PW to enhance understanding of the fouling process [25, 28, 29, 53, 54]. PW is a composition of oil, grease, minerals, production chemicals, dissolved gases, solids, and toxicants, and the composition varies across wells, oil fields, and field maturity [99–102]. As the PW composition varies and affects membrane performance, the optimal operating point must be regularly updated to account for the time-varying behavior [101, 103, 104].

Compared to filtration of solids, oil droplets can deform and permeate the membrane even if the droplet size is larger than the pore size, consequently increasing OiW concentration in the permeate [33, 105–108]. In short, a droplet will permeate the membrane if the drive pressure is greater than the critical pressure [24]:

$$\underbrace{\Delta P^*}_{\text{Drive pressure}} > \underbrace{\gamma(c_u - c_d) \cdot 10^5}_{\text{Critical pressure}}, \tag{3.1}$$

where γ is the interfacial tension, ΔP is the TMP, and c_u and c_d are the upstream and downstream oil-water interface mean curvature, respectively. The critical pressure can be observed in several studies, where increasing pressure above a threshold increases OiW concentration in the permeate [20, 21, 109]. The critical pressures from the different OiW studies are summarized in Paper B. Besides oil droplets deforming and permeating the membrane, the deformability can be a advantages as oil trapped in the membrane can deform and dislodge from the membrane during cleaning.

For offshore oil and gas production, the complexity is not limited to the chemical composition. The multiphase flow from the well can interact and cause slugging flow, which can be problematic for the downstream separation facilities [110]. The changes in flow rate cause disturbances in pressure, consequently affecting the TMP, and if the dynamic controller does not compensate quickly, oil droplets can deform and permeate the membrane, thereby reducing permeate quality and separation efficiency. Consequently, any deployed control solution must be robust to the process disturbances to ensure optimal operation.

3.2 Fouling Removal and Prevention Techniques

Many different methods have been used to reduce, prevent, or remove fouling, they can be categorized as:

Shear on the membrane surface is used to remove or prevent the accumulation of fouling, the methods used to generate shear are:

- **Crossflow** is a well-established method, where the feed media is continuously circulated in a loop. The flow velocity over the membrane surface introduces shear preventing and removing fouling while also reducing concentration polarization (uneven distribution of the foulants over the cross-section) [16, 17, 105, 111].
- **Membrane channel modifications** have been used to increase surface shearing by creating small obstructions in the CF channel that direct the CF towards the membrane wall, also reducing concentration polarization [112, 113].
- **Rotating membranes** are an alternative to CF filtration, where the shear is introduced by rotating the membranes. Rotating the membranes, compared to CF filtration, is more energy efficient in terms of shear per energy spent but the mechanical complexity is higher [114]. Furthermore, when deploying rotating filters the TMP is independent of the shear rate, whereas for CF filtration the CFV and TMP are dependent. With TMP and shear rate decoupled, the

design of the controllers is simplified as control loop interactions are non-existing [115].

Pulsing CF is an alternative to constant CFV, the method deploys varying CFV in both directions to reduce energy usage and keep a periodic high shear rate [116–119]. However, if the dynamic controllers are not carefully designed, the coupling between CFV, TMP, and flux can cause the flux and TMP to pulsate in phase with the CFV, increasing the likelihood of oil droplets deforming and permeating the membrane [119]. Furthermore, the oscillating TMP and flux can cause increased fouling growth compared to constant flux [56].

Ultralsonic cavitation used for shear generation has shown to remove fouling while the membranes remain in operation. Ultrasonic cleaning has been deployed for different filtration application in [120–122] and for an OiW emulsion in [32, 99]. The method requires installation of an ultrasonic transmitter in each membrane housing, thus increasing the initial installation cost.

Operating conditions including CFV, temperature, and TMP are an essential part of fouling minimization [20, 29, 123–125]. However, the dynamic relationship between operating conditions and fouling rate is rarely addressed [118, 119].

Backwashing the membranes, by reversing the TMP and flux, dislodges a part of the fouling which is carried away by the backwashing media. As the permeate flow and TMP are reversed during backwashing, the membranes being backwashed are consuming produced permeate. Despite produced permeate being consumed by backwashing, backwashing has shown to increase overall permeate production [16, 20, 46–48, 126].

Pretreatment of the feed flow to the membranes can reduce fouling tendencies. Pretreatment of produced water can be divided into mechanical and chemical pretreatment, where prefilters, gravity-based separators, and hydrocyclones are considered mechanical pretreatment [54, 100, 127].

Chemical cleaning methods are required to maintain long term permeability despite the extensive effort to optimize operating conditions, membrane material, and other fouling removal methods. As such physical removal and chemical cleaning of the membranes are periodically required [128, 129].

Membrane material and surface modification affect the permeability and fouling tendency of the membranes. For PW, ceramic membranes are commonly the preferred membrane type [29, 73, 78, 130, 131].

Air sparging is a process where air is continuously or periodically injected over the membrane surface to prevent or remove fouling. The method has been proved effective when treating an OiW emulsion [102, 127].

While these methods improve the overall performance of the filtration system, most of the methods have adjustable parameters and the optimal value for each parameter must be determined. For time-varying processes, such as PWT, the optimal parameters for most of the fouling removal and prevention methods change and must be continuously updated to maintain optimality. Few studies address online optimization or adaption of the individual parameters to compensate for the time-varying behavior [38, 49, 132]. The issues of online optimization are reviewed in Paper B and an online method for adjusting the backwashing parameters are suggested in Paper E.

3.3 Review of Fouling Models

Dynamic process models are essential to facilitate advanced dynamic control and scheduling of cleaning methods. Many different model structures have been used to model the fouling behavior, namely; blocking laws [133–135], neural network [136–139], resistance [140–143], and black box/data-driven [21]. However, the remaining of the review is limited to the blocking law and resistance-based model structure. Commonly, foulant is considered to block the membrane in four different ways, as illustrated in Fig. 3.1. The

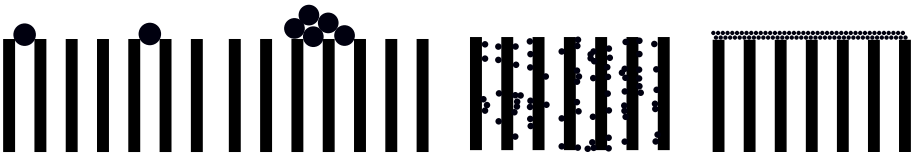

(a) Complete blockage **(b)** Intermediate blockage **(c)** Standard blockage **(d)** Cake blockage

Fig. 3.1: Four commonly accepted types of fouling. Figure from Paper B. Licensed under CC BY 4.0

blockage and resistance-based models are summarized in Table 3.1, where the difference between each model is highlighted. The resistance-based models have higher complexity and more parameters, but the blockage laws are the most frequently used model structure [134, 135, 144–150].

The blockage models were originally intended to model fouling of solid particles using dead-end filtration [133]. However, the blockage models have

Table 3.1: Overview of fouling models.

	Complete blockage, $\frac{dj}{dt}$	Intermediate blockage	Standard blockage	Cake blockage		
Blocking laws-based models						
Hermia [133]	αj	αj^2	$\alpha j^{\frac{3}{2}}$	αj^3		
De Bruijn [134]	$\alpha(j-j^*)$	$\alpha j(j-j^*)$	N/A	$\alpha j^2(j-j^*)$		
Kilduff [135]	$\alpha(j-j^*)C_b$	N/A	$\alpha j^{\frac{1}{2}}(j-j^*)C_b$	$\alpha j^2(j-j^*)C_b$		
Resistance-based models						
	Total resistance, R_t	**Cake resistance, R_c**	**Cake height development, $\frac{dh_c}{dt}$**	**Membrane resistance, $R_{m\|c}+R_b$**	**Effective pore radius, $\frac{dr_p}{dt}$**	**Fraction of open pore area, $\frac{df_o}{dt}$**
Wiesner [143]	$R_c+R_{m\|c}+R_b$	$\frac{180(1-\epsilon_c)^2}{d^2\epsilon_c^3}h_c$	$k_1 j - k_2 h_c$	$\frac{8h_m}{f_o r_p^2}$	N/A	N/A
Giraldo [142][1]	$R_c+R_{m\|c}+R_b$	$\frac{180(1-\epsilon_c)^2}{d^2\epsilon_c^3}h_c$	$\frac{jC_c - kV_{air}^{k_1}}{\rho_c}$	$\frac{8h_m}{f_o r_p^2}$	$-\alpha C_m j$	$-\alpha C_m j$
Fazana [141]	$R_c+R_{m\|c}+R_b$	$\frac{180(1-\epsilon_c)^2}{d^2\epsilon_c^3}h_c\rho_c \cdot e^{N_c t}$	$\frac{jC_c - C_c jk}{\rho_c}$	$\frac{8h_m}{f_o r_p^2}\cdot e^{N_b t}$	$-\alpha C_m j$	$-\alpha C_m j$
Busch [140][2]	$R_c(z)+R_{m\|c}+R_b(z)+R_{bo}$	$\frac{180(1-\epsilon_c)^2}{d^2\epsilon_c^3}h_c(z)$	$\frac{j(z)\alpha_c C_c}{\rho_c}$	$k\frac{(1-\epsilon_{m\|b}(z))^2}{\epsilon_{m\|b}(z)^3}$	Membrane porosity, $\frac{d\epsilon_{m\|b}(z)}{dt}$	$\frac{-k\cdot j(z)\cdot C_m \frac{A}{V}}{\rho_p}$

Symbols and descriptions

C_c	Cake forming concentration	C_m	Concentration at the membrane surface, reduced by the cake layer	C_b	Bulk concentration	α	Fouling coefficient, unique for each Eq.	k	Constant, unique for each Eq.
h_m	Effective thickness of the membrane	j	Membrane flux	j^*	Critical flux	ϵ_c	Porosity of the cake layer	d	Mean droplet diameter
ρ_c	Density of the cake	t	Time	N_c	Exponential coefficient for cake blockage	V_{air}	Cleaning air velocity	N_b	Exponential coefficient for complete blockage
$\epsilon_{m\|b}$	Porosity of the membrane given complete blockage.	A	Membrane area	V	Total processed volume of water	ρ_p	Density of the pore blocking media		

[1] Air sparging is used

[2] The bio fouling, R_{bo} model is not included in this overview.

extensively been used to describe fouling when deploying CF filtration for OiW separation [98, 124, 151–153]. Based on results, the blockage models can describe the accumulation of oil fouling, despite the deformability of oil. Even when filtration is carried out with a TMP above the critical pressure, the blockage models provide reasonable accuracy [98, 152].

Over time the blockage models have been extended to explicitly account for both feed concentration and CFV [134, 135]. To describe the effect of CF, the concept of critical flux is introduced into the models. The critical flux concept is defined as the flux limit where below nearly no fouling occurs and above a significant increase in fouling growth can be observed [149]. The critical flux is dependent on operating conditions and must be reidentified if conditions change. The fouling behavior described with critical flux is observed in [154, 155], and the concept is further investigated for an OiW emulsion in [57, 156]. The most popular method for critical flux identification is flux stepping, a method where the flux is periodically increased in steps to observe at which level of flux fouling starts to accumulate [42, 44, 154, 157–160]. Despite the popularity of the method, there are some disadvantages of the flux stepping method [161]:

- The measured critical flux is only for the dominant fouling type.
- It is dependent on stepping parameters, such as step height and length.
- It is time consuming and must be updated if the operating conditions change.

Because of the difference in feed composition, field trials and pilot plants are often used to study the fouling behavior for a specific oil composition. Based on the studies the filtration system can be tuned to the field specific conditions, maximizing permeate production or energy efficiency. However, in [28] it was proposed that by enhancing the understanding of fouling, the filtration system could be tuned without the need for pilot plants and field trials. However, it is difficult to predict the future PW composition. While membrane type should be based on the overall feed composition, operating parameters, such as backwashing interval, should be estimated online based on current conditions to allow the system to adapt and maintain optimality subject to varying conditions. For model purposes, online estimation of model parameters, including critical flux, ensures that the model is continuously updated to the current conditions and model-based optimization techniques maintain optimality despite changes in feed composition.

3.4 Conclusion

Compared to other fields, such as pharmaceutical and food industry where the feed composition is known and often constant, PW can be a challenge to treat. For PWT, the feed composition is time-varying and multiphase interactions can cause slugging flow [24, 162]. Besides the time-varying features of PW, oil droplets can easily deform and permeate the membrane if sufficient drive pressure is applied, consequently linking TMP and separation efficiency.

Methods and techniques for fouling prevention and removal exist in large quantities. However, most methods rely on parameters selected and tuned during initial configuration and installation. Consequently, the performance of the anti-fouling measures can degrade as reservoir behavior change. To compensate for the time-varying behavior, the parameters for the removal methods must be adjusted online to ensure that the prevention and cleaning methods remain efficient. Online system identification of the models reviewed in Paper B can provide a model that is continuously updated to describe the fouling behavior subject to the current reservoir behavior. The updated fouling model can be deployed to online update parameters for the prevention and cleaning methods ensuring optimality despite changes in operating conditions.

In addition to removal and prevention techniques, the fouling behavior is affected by the operating conditions. Most studies investigate the relationship between fouling and steady-state operating conditions [29, 57, 123, 156], while few consider how dynamic changes and oscillating behavior affect fouling growth [39, 118, 119]. As operating conditions affect fouling and high flux cause additional fouling to accumulate, varying flux consequently increases fouling growth compared to constant flux with identical mean, emphasizing the importance of the controllers' ability to reject disturbances and track the reference [56].

Chapter 4

RGA-based Analysis and Control

This section summarizes the results of Paper C and D, where experimental results show that fouling growth is increased subject to oscillating TMP and flux compared to a constant case. As such, the disturbance rejection and tracking performance of the dynamic controllers are essential in order to limit unnecessary fouling. For membrane filtration, decentralized control is often deployed as a necessity rather than a topic for optimization. Especially the potential performance degradation caused by cross couplings are neglected in the design phase. To minimize the cross couplings the RGA method was used to identify the control pairings and valve placement that minimizes the interaction between the control loops. The selected control pairing was compared to a potential worst pairing, the results showed a significant difference in transient performance, indicating that strong interaction do indeed exist in the considered pilot plant. Based on experimental results, it was observed that oscillating TMP and flux causes additional fouling. By considering cross couplings in the control design phase, fouling and fluctuation in TMP and flux can be reduced.

4.1 Sensitivity to Oscillating TMP and Flux

As discussed in Chapter 3, membrane performance in terms of permeability is sensitive to operating conditions. For filtration of beer, oscillating CF has shown to improve the permeate flow rate by up to 100%, but the effect on permeate quality is unaddressed [119]. During the experiment, the TMP and flux did oscillate in phase with the CFV, and according to the critical flux hypothesis and results in [156], higher flux can cause increased fouling.

Consequently, the oscillations increase fouling growth compared to constant flux. To ensure that the improved permeate flow rate was indeed caused by oscillating CFV, the flux should have been kept constant.

To investigate how oscillating TMP and flux affect the total permeate production and fouling, two experiments are carried out on the pilot plant. For the experiments both the CFV and TMP are controlled using the SISO control structure defined in Fig. 4.1 and the remaining actuators are fixed according to Table 4.1. The TMP, ΔP, is calculated according to:

$$\Delta P = \frac{PT_6 + PT_5}{2} - PT_4, \tag{4.1}$$

which assumes that the pressure drop across the length of the CF channel is linear. However, as the flow rate through the CF channel is gradually reduced as the water permeates the membrane, the pressure drop per length of CF channel is reduced. Because of the large ratio between the CF and permeate flow, the magnitude of the nonlinear effect is assumed to be negligible [56].

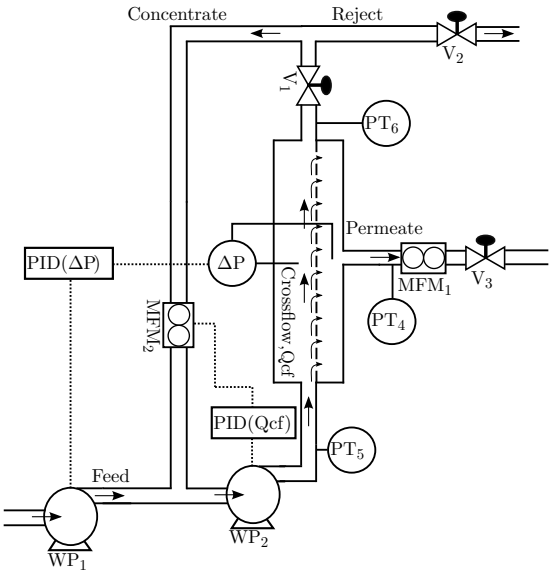

Fig. 4.1: Overview of the piping and instrumentation of the considered system, where the syntax PID(Q_{cf}) means that Q_{cf} is the controlled variable for that control loop. Figure from Paper D.

The valves for the permeate and CF loop are fully open to allow easy passage of permeate and CF, while the reject valve is 30% open to ensure that the permeate flow do not significantly increase the concentration in the CF loop. The two experiments are divided into a constant and oscillating case. For the constant case both CFV and TMP are controlled with a constant reference of $2m/s$ and $0.6bar$, respectively. For the oscillating case the TMP reference

Table 4.1: Actuator configuration during the experiment.

Actuator	Controlled/fixed	Position
V_1	Fixed	100% open
V_2	Fixed	30% open
V_3	Fixed	100% open
WP_1	Controlled	See Fig 4.1
WP_2	Controlled	See Fig 4.1

is switching between $0.4bar$ and $0.8bar$ every $10s$, while the reference for the CFV controller is $2m/s$ constantly. To ensure that the results are comparable, it is crucial that the conditions, except for the TMP and flux, are identical for each case. For most variables, this is easily achieved within a small margin of error by using feedback control. However, the OiW concentration is difficult to recreate accurately. To ensure that the OiW concentration do not favor the expected best case (constant), the OiW concentration for the constant case is intentionally higher.

The results from 10 hours of filtration without any cleaning action are shown in Fig. 4.2. For the oscillating case the CFV should ideally be relatively constant throughout the experiment. However, measurements show that during the initial 1-2 hours the CFV controller was unable to maintain a constant CFV, whereas for the constant case the TMP and CFV are constant throughout the experiment.

Based on flow measurement it can be difficult to determine which of the cases have the highest average flux, therefore the total produced permeate, defined as:

$$j_c(t) = \int_0^t j(\tau) d\tau, \tag{4.2}$$

is shown in Fig. 4.3. Based on j_c, the oscillating case initially produces higher flux, but after around 1-2 hours the constant case maintains a higher flux and after just 4.3 hours the constant case overtakes the oscillating case in permeate production. The results from the experiments are summarized in Table 4.2.

As OiW concentration is difficult to measure accurately and reliably, two different Turner 4100XDC's were used in series to ensure that the constant case was indeed exposed to a higher OiW concentration. The difference in concentration is according to measurements between 2% and 8.6%. The mean TMP and CFV were for the two cases identical within a reasonable margin, and after 10 hours of filtration, the constant case produced 8.49% more permeate and the final flux was 20.5% higher compared to the oscillating case.

It is only after approximately 1-2 hours and 4 hours that the constant case surpasses the oscillating case in flux and total permeate production, respectively. As oscillating CFV can increase flux compared to constant CFV [119].

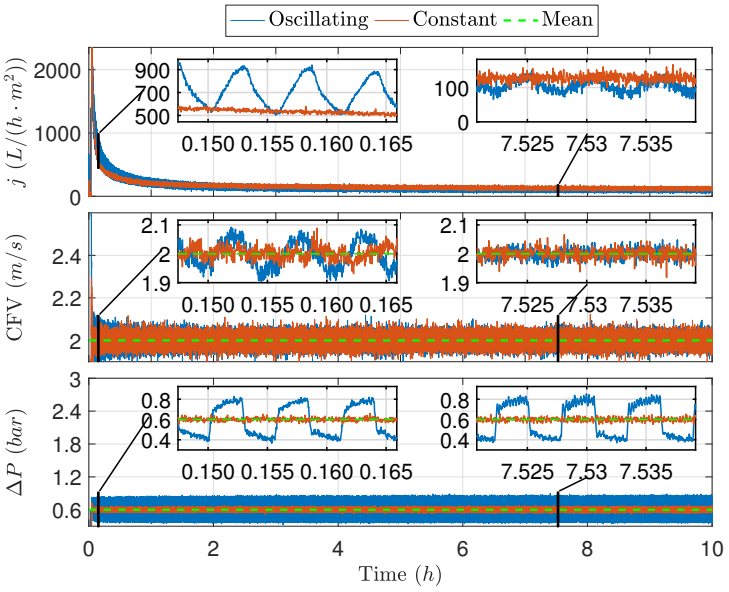

Fig. 4.2: Flux, CFV, and TMP for the constant and oscillating experiments. Figure from Paper D.

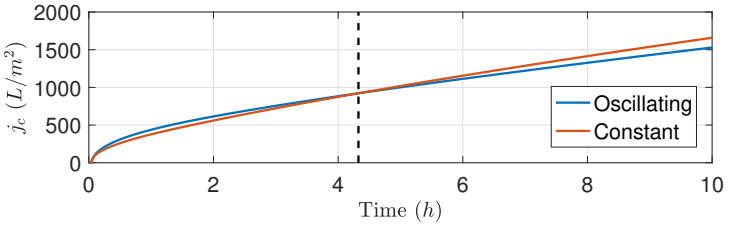

Fig. 4.3: Total produced permeate for both the oscillating and constant case.

It is conceivable that the inability of the CFV controller to maintain a constant CFV provides an unfair advantage to the oscillating case. As the flux is reduced by fouling, the CFV controller regain the ability to maintain a constant CFV despite of the oscillating flux and TMP. Once the oscillating CFV is eliminated the constant case relatively quickly surpasses the oscillating case in both flux and net permeate production. Overall it is clear that once oscillating CFV is eliminated the constant case produces less fouling and higher flux compared to the oscillating case.

Possible sources of errors are variance in membrane production affecting initial resistance and inaccurate OiW concentration measurements. As the oscillating case initially produced a higher flow rate, it is unlikely that variance in production caused an unfair advantage to the constant case. Furthermore, to compensate for the inaccuracy regarding OiW measurements, the concen-

Table 4.2: The mean flux, CFV, TMP, and OiW concentration for the oscillating and constant case. The OiW concentration is measured before each experiment. Table from Paper D.

	Constant	Oscillating	Difference[a]
OiW1[b]	$3213PPM$	$2960PPM$	8.6%
OiW2[b]	$2911PPM$	$2854PPM$	2%
Final j[c]	$118.7Lh^{-1}m^{-2}$	$98.5Lh^{-1}m^{-2}$	20.5%
CFV	$1.9941m/s$	$1.9943m/s$	-0.01%
ΔP	$0.5972bar$	$0.5977bar$	-0.08%
j_c	$1658L/m^2$	$1528L/m^2$	8.49%
Permeate/reject ratio	295%	293%	0.7331%
Recovery (R_p)	25.2890%	25.4272%	-0.5434%

[a] Calculated by $(Constant/Oscillating \cdot 100) - 100$
[b] The concentration is measured using two serial connected Turner 4100XDC's.
[c] Final flux is the average flux for the last $6mins$ of the experiment.

tration for the constant case was intentionally higher to eliminate any unfair advantage.

Based on the results, the oscillating CFV and TMP deployed in [119] could be further improved by deploying control to maintain a steady TMP and flux subject to oscillating CFV. Even if the CFV is constant, the designs of the controllers are essential to ensure that the TMP and flux are kept constant subject to upstream disturbance.

4.2 System Analysis and Control Pairings

Oscillating TMP and flux can cause additional fouling, consequently increasing the required membrane area and footprint. To enhance the cost-effectiveness of the membranes, it is crucial that the dynamic controller, maintaining the flux or TMP, is designed to reject disturbances caused by upstream processes. Commonly the membrane filtration systems are controlled by a set of PID controllers that individually and uncoordinated manipulate different actuators to control the defined variables. For CF membrane filtration, two controllers are commonly applied to control the CFV and either the TMP or flux [38, 41–45]. However, the design of the dynamic controllers is often deployed as a necessity and the potential for optimization is ignored [24]. An issue often neglected by most PID tuning rules are the interactions between the multiple control loops. By ignoring possible cross couplings, a designed controller can by itself be stable, but when multiple controllers are enabled, the interaction between control loops can cause system instability or poor performance in terms of disturbance rejection and reference tracking.

Cross couplings between the control loops can be accounted for by deploying advanced multiple-input-multiple-output (MIMO) control strategies, such as MPC. However, MPC is rarely deployed for membrane filtration, conceivably because of its reliance on an accurate model and complex tuning, compared to the PID structure [56, 163]. Alternatively, the RGA method can be used to design a SISO control system where the control pairings can be selected to minimize interaction between the individual control loops [164].

In Paper C a RGA analysis is carried out for the pilot plant, and in Paper D the analysis is extended to cover the frequency domain. Commonly, the RGA analysis is carried out at a single operating point, but as the feed flow rate and fouling state of the membranes are time-varying, the RGA analysis considers a range of operating points.

4.3 Dynamic Process Model of the Membrane Filtration System

For the RGA analysis, a model of the considered filtration system is required. In Paper C a static model of the filtration system is developed, identified, and described, and in Paper D the model is extended with dynamics. The model is divided into dynamic and static parts, the structure of the extended model is shown in Fig 4.4.

The model includes the dynamic relationship between valve inputs (U_{V1}, U_{V3}) and the placement of each valve seat ($\hat{P}_{V1}$, $\hat{P}_{V3}$). As the orifice of V_2 was found too large to reliably control the reject flow rate, the dynamic relationship between U_{V2} and $\hat{P}_{V2}$ is not included in the model. Furthermore, the dynamic relationship between pump input (U_{WP1}) and pressure across the pump (ΔP_{WP1}) is also included. As the relationships are identified through flow and pressure measurements, some hydrodynamics are also captured by the valve and pump models. The static model estimates the considered output based on the current valve positions, pump pressure, and disturbance inputs. As upstream conditions and fouling can cause feed flow rate (Q_f) and the membrane conductance (KV_f) to vary during operation, they are considered as input disturbance. To account for the varying conditions, the RGA analysis is carried out at different Q_f and KV_f to highlight any potential pairing issues at different operating points. The considered outputs for the RGA analysis are the CFV (Q_{cf}) and the permeate flow rate (Q_{pm}). The flow through WP_1 (Q_{WP1}) is used as a scheduling variable for the linear parameter-varying (LPV) transfer function (TF) (H_{WP1}).

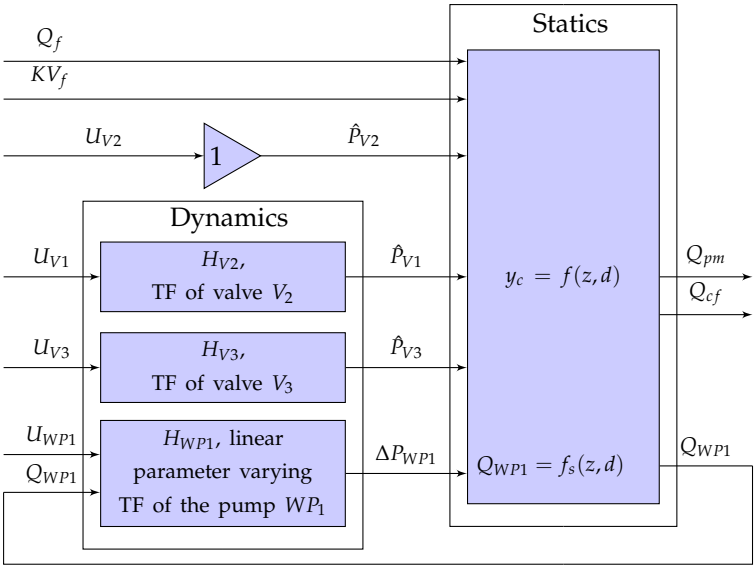

Fig. 4.4: The model structure proposed in Paper D. Note that the transfer function H_{WP1} is a linear parameter varying transfer function with U_{WP1} and Q_{WP1} as scheduling variables, where $d = [Q_f, KV_f]^T$ and $z = [\hat{P}_{V1}, \hat{P}_{V2}, \hat{P}_{V3}, \Delta P_{WP1}]^T$. Figure from Paper D.

4.4 Relative Gain Array

The RGA method was proposed in [164] as a measure of interactions. The method has extensively been used for decentralized control to select control pairings that minimize control loop interactions [165, 166]. Furthermore, the method was also used to determine which system configuration provided the best decoupling potential [167]. The RGA method is defined as:

$$\lambda = G(0) \times (G(0)^{-1})^T, \tag{4.3}$$

where

$$G(s) = \begin{bmatrix} g_{11}(s) & g_{12}(s) & g_{13}(s) & \dots & g_{1n}(s) \\ g_{21}(s) & g_{22}(s) & g_{23}(s) & \dots & g_{2n}(s) \\ \vdots & \vdots & \vdots & \ddots & \vdots \\ g_{m1}(s) & g_{m2}(s) & g_{m3}(s) & \dots & g_{mn}(s) \end{bmatrix} \tag{4.4}$$

and $g_{zk}(s)$ is the TF between input k and output z, and $\times$ is element by element multiplication. A limitation of the RGA method is that it is based on steady-state gains of the considered system and ignores dynamic information, potentially causing misleading results [168].

4.4.1 Dynamic Relative Gain Array

An alternative, accounting for the dynamics, is dynamic RGA (DRGA) which was proposed in [169], and later deployed in [170]. DRGA uses the same method as RGA but extends the analysis to cover the frequency domain. The DRGA is defined as:

$$\lambda_D(i\omega) = G(i\omega) \times (G(i\omega)^{-1})^T, \tag{4.5}$$

where i is the imaginary number, and ω is the frequency. The DRGA method can be difficult to interpret, as the method produces an RGA matrix for each considered frequency.

4.4.2 Effective Relative Gain Array

To simplify the interpretation and to account for the dynamic features, the effective RGA (ERGA) method was proposed in [168]. The effective gain is defined as the integral from zero to the bandwidth of the normalized TF times the steady-state gain [171]:

$$e_{zk} = g_{zk}(0) \int_0^{\omega_{c,zk}} |g^0_{zk}(i\omega)| d\omega \quad \forall\, z \in m \wedge k \in n, \tag{4.6}$$

where $g_{zk}(0)$ is the steady-state gain, $g^0_{zk}(i\omega)$ is the normalized TF, $\omega_{c,zk}$ is the critical frequency, commonly interpreted as the bandwidth frequency. The normalized TF is defined as:

$$g_{zk}(i\omega) = g_{zk}(0) g^0_{zk}(i\omega), \tag{4.7}$$

where $g_{zk}(i\omega)$ is the TF between input k and output z. The integral in Eq. (4.6) can be approximated as a rectangular area and calculated as:

$$e_{zk} = g_{zk}(0) \omega_{c,zk}, \tag{4.8}$$

and the ERGA can be interpreted as the regular RGA scaled with the bandwidth. Eq. (4.8) can be written in matrix format:

$$E = G(0) \times \Omega_c, \tag{4.9}$$

where

$$\Omega_c = \begin{bmatrix} \omega_{c,11} & \omega_{c,12} & \omega_{c,13} & \dots & \omega_{c,1n} \\ \omega_{c,21} & \omega_{c,22} & \omega_{c,23} & \dots & \omega_{c,2n} \\ \vdots & \vdots & \vdots & \ddots & \vdots \\ \omega_{c,m1} & \omega_{c,m2} & \omega_{c,m3} & \dots & \omega_{c,mn} \end{bmatrix}. \tag{4.10}$$

The ERGA can then be calculated as:

$$\lambda_E = E \times (E^{-1})^T. \tag{4.11}$$

Compared to DRGA, ERGA compresses the dynamic features of the system down to a single matrix, consequently reducing the complexity in the pairing selection process. However, as the frequency features are compressed and expressed in terms of bandwidth, peaks in the magnitude of the bode plot below the bandwidth would be unaccounted for, consequently hiding potential pairings issues.

4.4.3 Dynamic RGA Analysis for Membrane Filtration Control

The work in Paper C is based on RGA, while Paper D accounts for the dynamic features by deploying the DRGA method. Based on the model structure defined in Fig. 4.4, the dynamic gain is calculated as:

$$G(z_0, d_0, \omega) = \left.\frac{\partial f(z, d_0)}{\partial z}\right|_{z=z_0} \cdot diag(H_0(i\omega)), \tag{4.12}$$

where

$$H_0(i\omega) = [H_{V1}(i\omega), H_{V2}(i\omega), H_{V3}(i\omega), H_{WP1}(Q_{WP1,0}, U_{WP1,0}, i\omega)]^T, \tag{4.13}$$

ω is the considered frequency, z_0, d_0, $Q_{WP1,0}$, and $U_{WP1,0}$ are the steady-state operating conditions chosen for z, d, Q_{WP1}, and U_{WP1}, respectively. The RGA matrix can then be calculated according to:

$$\lambda_D(G(z_0, d_0, \omega)) = G(z_0, d_0, \omega) \times (G(z_0, d_0, \omega)^{-1})^T. \tag{4.14}$$

As V_2 is unsuitable for control, only U_{V1}, U_{V3}, and U_{WP1} are considered as inputs for the RGA analysis, thus the RGA matrix has the following format:

$$\begin{array}{c} \\ Q_{pm} \\ Q_{cf} \end{array} \begin{array}{c} \begin{array}{ccc} V_1 & V_3 & WP_1 \end{array} \\ \begin{bmatrix} \lambda_{D,1,1}(\bullet) & \lambda_{D,1,2}(\bullet) & \lambda_{D,1,3}(\bullet) \\ \lambda_{D,2,1}(\bullet) & \lambda_{D,2,2}(\bullet) & \lambda_{D,2,3}(\bullet) \end{bmatrix} \end{array} \tag{4.15}$$

where $\bullet$ indicates dependencies on operating condition and frequency, $\lambda_{D,1,1}$ represents the interaction between V_1 and Q_{pm}, and $\lambda_{D,2,3}$ represents the interaction between WP_1 and Q_{cf} ect. The RGA analysis assumes perfect control, where the reference is equal to the output, which is only true for steady-state. However, it is a good approximation for frequencies below the bandwidth [172]. For the analysis, the RGA values are defined as two vectors:

$$\begin{aligned} \lambda_{Qpm} &= [\lambda_{D,1,1},\ \lambda_{D,1,2},\ \lambda_{D,1,3}]^T \\ \lambda_{Qcf} &= [\lambda_{D,2,1},\ \lambda_{D,2,2},\ \lambda_{D,2,3}]^T, \end{aligned} \tag{4.16}$$

where λ_{Qpm} and λ_{Qcf} are the RGA vectors for the considered outputs.

4.4.4 Interpretation of the Relative Gain Array

The RGA pairing rules are described in Paper C and D, but can briefly be summarized as:

- The rearranged system (preferred pairings on the diagonal) should be as close as possible to the identity matrix.
- Negative pairings should be avoided, as they indicate that the sign for the considered loop changes as the other control loops are closed with feedback.
  - Negative RGA elements indicate the existences of a right half plane (RHP) zero in either the considered loop, the combined system, or in the open-loop combined system.
  - Negative RGA elements must be avoided if decentralized integral controllability (DIC) is a requirement, ensuring the system remains stable even if controllers are disabled or the actuators saturate.
- Large elements (>5) should be avoided, as they indicate controllability problems, strong interactions, and sensitivity to input uncertainty (e.g. neglected actuator dynamics).
- For frequency dependent RGA, pairings close to one at the closed-loop bandwidth, are preferred.

4.5 Results

The results of this study are divided into two parts; the analytical and experimental results. The analytic results present the results from the RGA analysis, and the experimental results compare the preferred control pairing with a possible worst pairing.

4.5.1 Analytic Results

The results from the RGA analysis are divided into two parts, firstly the RGA values for the different operating conditions are considered at steady-state, and secondly the frequency domain is inspected for any potential pairing issues. Beside considering different control pairings, the RGA considers three different valve placements, namely V_1, V_2, and V_3 as shown in Fig. 4.1. However, V_2 proved to be uninteresting and was excluded from the RGA analysis as the orifice of the valve was designed too large to reliably control the small flow rates. The results at steady-state are shown in Fig. 4.5 (V_1 and WP_1) and Fig. 4.6 (V_3 and WP_1), where the dashed black line is the desired operating point. As the considered system has more actuators than considered

outputs, the valves not considered are fixed, and across the considered operating range, the equilibrium is estimated for the considered actuators. As such, each figure provides an indication of how well the considered pairings are decoupled throughout the considered operating range.

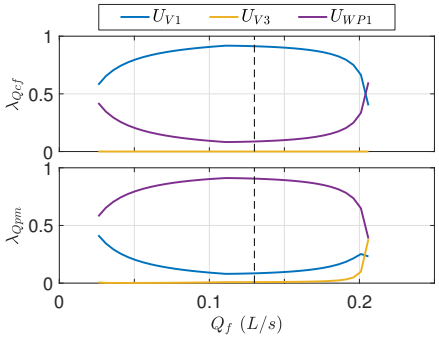

(a) RGA values at different feed flow rates.

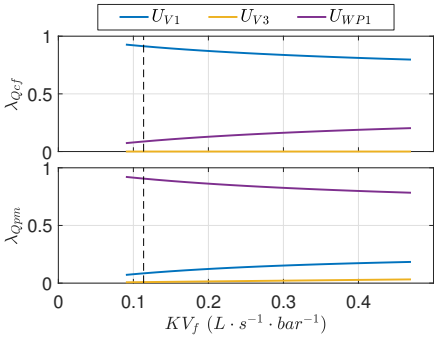

(b) RGA values at different membrane permeate conductances.

Fig. 4.5: RGA values when using V_1 and WP_1 to control the process at different feed flow rates and membrane conductances. The non-controlled valves are fixed at: $U_{V2} = 30\%$ and $U_{V3} = 50\%$. Figure from Paper D

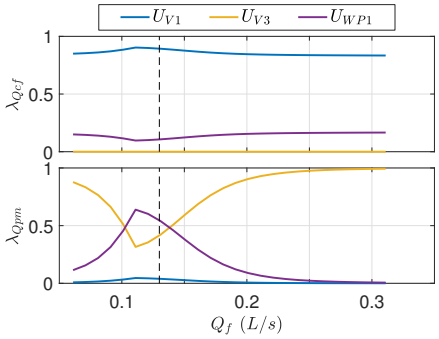

(a) RGA values at different feed flow rates.

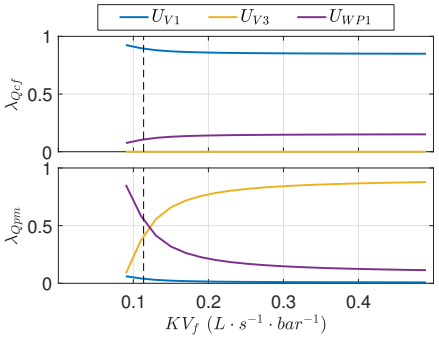

(b) RGA values at different membrane permeate conductances.

Fig. 4.6: RGA values when using V_3 and WP_1 to control the process at different feed flow rates and membrane conductances. The non-controlled valves are fixed at: $U_{V1} = 40\%$ and $U_{V2} = 30\%$. Figure from Paper D.

Based on the steady-state results, the combination of V_1 and WP_1 provide good decoupling around the operating point, and only at very high feed flow rates, the preferred control pairing changes. For the case of V_3 and WP_1, the pairing is more complicated. At the operating point, the RGA values for Q_{pm}

are very close to 0.5 indicating strong interaction, additionally the preferred pairing switches just around the operating point. Nonetheless, the results show that V_1 and WP_1 are good candidates for controlling Q_{cf} and Q_{pm}, respectively. However, the analysis is extended to the frequency domain to investigate if any potential problems exist at different frequencies. For the V_1 and WP_1 combination, no problems were observed. However, for the V_3 and WP_1 combination illustrated in Fig. 4.7, the preferred pairing changes as frequency increases, highlighting the need to consider the frequency domain. The remaining RGA plots, covering the frequency domain, are illustrated in Paper D [56].

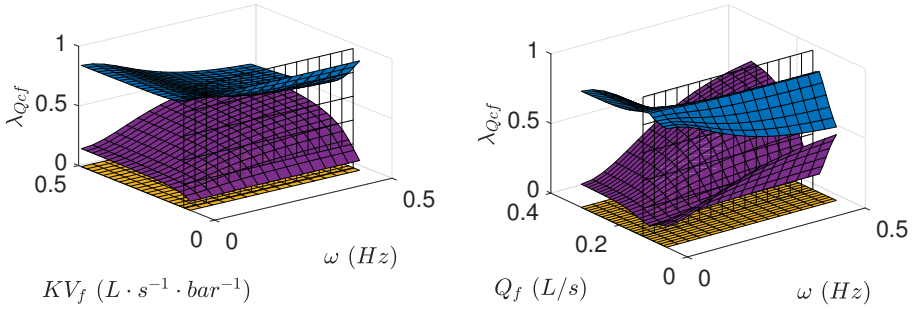

(a) RGA values for Q_{cf} when using V_3 and WP_1 across different membrane conductances and frequencies.

(b) RGA values for Q_{cf} when using V_3 and WP_1, across different feed flow rates and frequencies.

Fig. 4.7: RGA analysis extended to the frequency domain. Figure from Paper D.

4.5.2 Experimental Results

To confirm the RGA results, four controllers are designed:

- Preferred:
  - $C_{V1,Qcf}$
  - $C_{WP1,Qpm}$
- Unpreferred:
  - $C_{V1,Qpm}$
  - $C_{WP1,Qcf}$

where the notation $C_{V1,Qcf}$ is the controller using V_1 to control Q_{cf}. The preferred controllers are based on the RGA analysis, and the unpreferred are the reversed version of the preferred pairings. The controllers are designed based

on the model and tuned to perform identically to give each output a similar responses regardless of controller. Details regarding controller tuning are presented in Paper D [56]. The controllers are then tested on the pilot plant, and the results are shown in Fig. 4.8. Based on the experiment, there is a

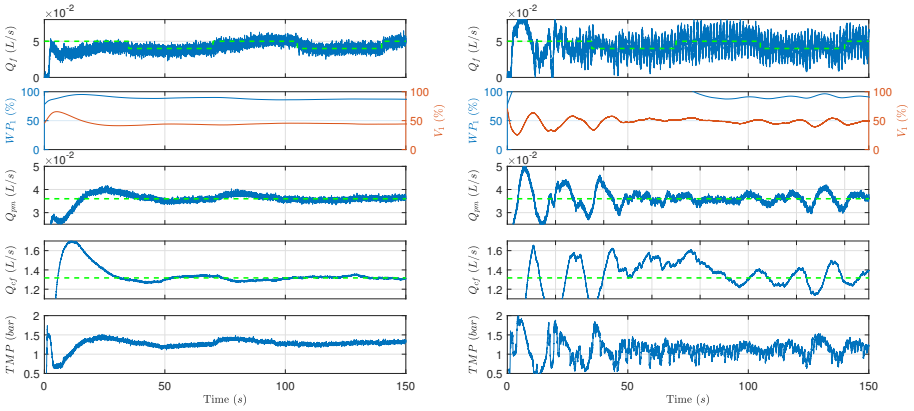

(a) Preferred control pairing. **(b)** Unpreferred control pairing.

Fig. 4.8: Experimental comparison between the preferred and unpreferred control pairings. Figure from Paper D.

huge difference in controller performance in terms of reference tracking and disturbance rejection, despite the controllers being tuned to perform identically based on the SISO models. The difference between the controllers is conceivably caused by interaction between the control loops, as each controller was individually tested and confirmed to have the desired performance. The difference in performance is also reflected on the control effort, where the unpreferred controllers are manipulating the actuators more in an attempt to keep the reference, consequently increasing the wear and energy consumptions of the actuators. Furthermore, it was observed that controller interaction also affected the upstream feed controller, indicating that poor controller performance may not only affect the process which they control but can also affect up- and down-stream processes. Accounting for the fouling behavior observed in section 4.1, poor control design and interaction between control loops can indeed cause increased fouling.

4.6 Conclusion

It was theorized that oscillating flux and TMP caused additional fouling to accumulate compared to constant flux. During periods with above average flux, additional fouling accumulates and the fouling is not completely removed during the periods with below average flux. Through experiments, it was

observed that oscillating flux did indeed cause more fouling to accumulate and the difference in flux after just 10 hours of filtration was 20.5%. If the exact OiW concentration could be recreated for each case it is conceivable that the difference would further increase, as the OiW concentration did favor the oscillating case.

As fouling is accelerated by oscillating flux compared to a constant level, poor control design can contribute to fouling growth. Often decentralized control is deployed without accounting for the strong interactions that exist in the process system, which can potentially cause system instability. By analyzing the interaction and selecting the control pairings and actuator placements that minimizes the interaction, the robustness to external disturbance can be improved significantly. Furthermore, the interaction between the controllers not only affects the filtration process but can also affect the upstream processes.

The identified control pairings were experimentally compared to a possible worst pairing. The results confirmed that selecting control pairings to minimize the control loop interaction can indeed improve the tracking and disturbance rejection performance. With better tracking and disturbance rejection, the oscillating tendency can be eliminated, and oil droplets are less likely to deform and permeate the membrane. Consequently, fouling is reduced and the attractiveness of membrane filtration for offshore PWT is increased, hence control design is essential for efficient operation.

Chapter 5

Optimization and Scheduling of Backwashing

Fouling is responsible for reducing the permeability and permeate flow rate of the membranes by a factor of 20 according to the results presented in section 4.1. The significant reduction in permeability caused by fouling leaves enormous potential for improving the attractiveness of membrane filtration for PWT by reducing membrane fouling. Backwashing, a method where the flow direction is reversed, is one of the most commonly applied methods for reducing the fouling issue. Because of its popularity, any improvement to the backwashing technique has huge potential to improve the cost-effectiveness of both current and future membrane filtration installations [113, 173].

During backwashing, the membranes are isolated, permeate production is halted, and the permeate from the previous filtration cycle is used as the backwashing media. As such, it is crucial that the backwashing frequency and duration are chosen such that permeate production time and permeate are not unnecessary used. Commonly the duration of the filtration and backwashing phases are based on either background knowledge or manufacture provided recommendations, both are ineffective from a permeate production point of view [20, 47, 174]. In some cases, the durations are based on a pilot study of a limited set of different durations [46, 48]. However, often the considered range of different durations are relatively small and the chosen durations are fixed for the backwashing and the filtration phase. Fixed durations for the backwashing and the filtration phase is sub-optimal as the optimal duration could change as irreversible fouling accumulates and process conditions change. Alternatively, backwashing can be initiated by a rise in TMP compared to fixed durations. The TMP-based method automatically adjusts the duration if fouling behavior suddenly changes. Alternatively, backwashing can also be triggered based on the produced permeate, allo-

wing for the backwashing duration to be online adjusted [175]. However, both methods only determine the duration of the filtration phase, leaving the backwashing duration fixed [16, 49, 174, 176].

In addition to measurement-based triggers, the following model-based optimization methods have also been deployed; artificial neural network [50], response surface methodology [51], and ordinary differential equations model with MATLAB based optimization [173]. However, none of the methods address the time-varying behavior nor the necessity to reestimate or train the model to ensure optimality is maintained. In [38, 132] run-to-run control is deployed, which optimizes permeate production and accounts for time-varying behavior. However, in the implementation phase, the authors were unable to describe the fouling removal, consequently a fixed backwashing duration was chosen and the loss in performance is claimed to be limited as the filtration phase is significantly longer than the backwashing phase. However, results in this study show the backwashing flow rate can be eight times larger than the filtration flow rate, making the backwashing duration essential for maximizing net permeate production.

The remaining of this section summarizes the results from Paper E, where the fouling behavior of an OiW emulsion during backwashing was studied. The study concludes that removable fouling was very quickly ($10s$) removed, and the fouling behavior during backwashing can be difficult to isolate, as the removal happens in the transient transition between filtration and backwashing. Based on the observed behavior, a scheduling algorithm maximizing the net permeate production for a filtration cycle, subject to constant TMP, is suggested. The suggested algorithm is implemented and tested on the pilot plant, where the duration of backwashing and filtration phases are automatically adjusted as irreversible fouling accumulates.

5.1 Optimization Problem

The objective is to maximize the net permeate production defined as:

$$\max_{t_{f|n}, t_{b|n} \in [0,\infty)} j_{avg|n}(t_{f|n}, t_{b|n}), \tag{5.1}$$

where $t_{f|n}$ is the filtration duration for cycle no. n, $t_{b|n}$ is the backwashing duration for cycle n, and $j_{avg|n}$ is the average flux for the entire cycle n. The maximization problem can be solved by modeling how the fouling resistance develops during the backwashing and filtration phase. To ensure that the method can adapt to changes, the resistance model during filtration ($R_{f|n}$) and during backwashing ($R_{b|n}$) should be based on measurements from the previous cycle ($n-1$), as illustrated in Fig. 5.1.

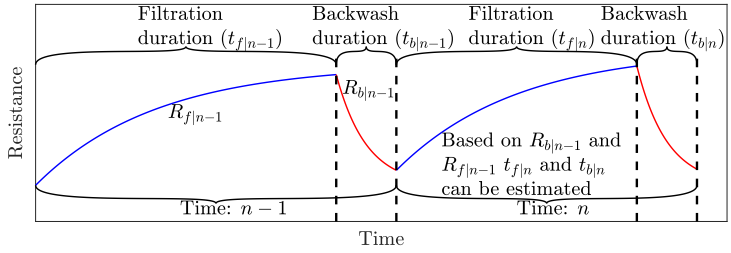

Fig. 5.1: Resistance trend and notations during filtration and backwashing. Figure from Paper E.

5.1.1 Observed Backwashing Behavior

While the estimated resistance could be observed to increase during filtration, the resistance during backwashing did not behave as theorized in Fig. 5.1. It is likely that the fouling removal was concealed by the valve, pump, and hydro-dynamics, making identification of the dynamic related to fouling difficult. Furthermore, during prolonged backwashing, as shown in Fig. 5.2, the resistance seems to slowly increase, indicating fouling of the membrane during backwashing. The slow fouling tendency is likely caused by a small degree of oil in the permeate. The issue of isolating the dynamic

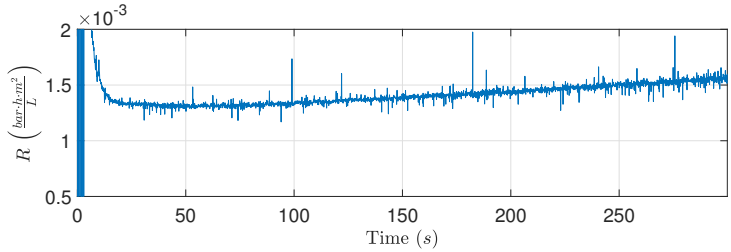

Fig. 5.2: Estimated resistance during backwashing, a slight increase in resistance during backwashing was observed, indicating fouling from the permeate side of the membrane. Figure from Paper E.

development of resistance during backwashing from the pump-, valve-, and hydro-dynamic originates from Darcy's law used to estimate the resistance:

$$j = \frac{\Delta P}{R}. \tag{5.2}$$

Darcy's law is often used to estimate the permeate flow resistance [20, 177]. However, Darcy's law does not account for transient conditions and is therefore unable to accurately describe resistance during the transition between filtration and backwashing, which is problematic as the fouling removal coincide with the transient period. To study how fast fouling is removed, a series

of steady-state experiments were conducted to map the relationship between backwashing duration and the amount of recovered flux, where the recovered flux is defined as [59]:

$$f_r = \frac{\int_{t_{b|n}}^{t_{b|n}+\Delta t_{fr}} j_{f|n}(t)dt}{\Delta t_{fr}} - \frac{\int_{t_{f|n-1}-\Delta t_{fr}}^{t_{f|n-1}} j_{f|n-1}(t)dt}{\Delta t_{fr}}, \tag{5.3}$$

where $j_{f|n}$ and $j_{f|n-1}$ is the filtration flux for the current and previous cycle respectively, and Δt_{fr} is the time window used to reduce the effect of measurement noise, which was chosen as $10s$. The recovered flux for different backwashing durations are shown in Fig. 5.3. While the data points have a

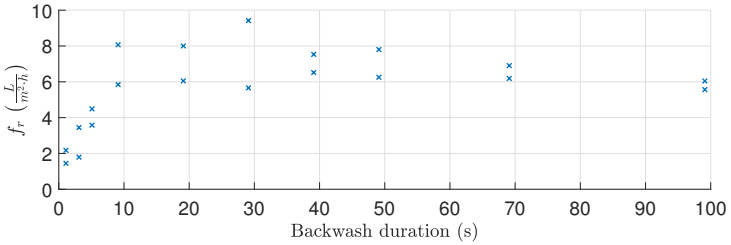

Fig. 5.3: Recovered flux from different backwashing durations. Before each backwash, the membranes were fouled by a 1000s of filtration, with TMP of $0.55bar$ and a backwashing pressure of $-2.2bar$. Figure from Paper E.

high variance, the tendency indicates that around $10s$ of backwashing is sufficient and extending the duration has little to no effect. $10s$ is also the time required for the backwashing pressure to be established, indicating that all removable fouling has been removed once the backwashing pressure is achieved. Assuming that fouling is indeed removed as quickly as the backwashing pressure can be established, $t_{b|n}$ is independent on $t_{f|n}$ and can be determined online by monitoring the pressure.

5.1.2 Scheduling Algorithm

Based on the observed fouling behavior during both filtration and backwashing, a scheduling algorithm is proposed in this section. For the purpose of easy notation, two discrete time variables are defined as:

$$t_{b|n} = l_n \cdot T_s \qquad l_n \in \mathbb{N}, \tag{5.4a}$$

$$t_{b|n} + t_{f|n} = k_n \cdot T_s \qquad k_n \in \mathbb{N}, \tag{5.4b}$$

where the sample time, T_s, is $0.1s$. The backwashing duration is assumed independent on the filtration duration but to maximize the net permeate production, the filtration duration is dependent on the volume of permeate

used for backwashing. Therefore, the backwashing is considered the first step in the cycle, and to ensure the inability of the controller to track the exact reference does not postpone the termination, backwashing is terminated as soon as 95% of the desired pressure is achieved. The backwashing algorithm is formulated as:

Algorithm 1 Backwashing phase. Modified from Paper E.

1: **while** $0.95\Delta P_b > \Delta P_{b,ref}$ **do**
2: Backwash ▷ Continue backwashing
3: $V_{b|n} = V_{b|n} + j_{b|n}(l_n T_s)T_s$ ▷ Updated the backwashing volume
4: $t_{b|n} = t_{b|n} + T_s$ ▷ Updated the time spent backwashing
5: $l_n = l_n + 1$ ▷ Increment the index variables
6: $k_n = k_n + 1$

where ΔP_b is the measurement of the backwashing pressure, $\Delta P_{b,ref}$ is the reference for the backwashing pressure controller, $V_{b|n}$ is the volume permeate spent backwashing. After the backwashing is carried out, the average flux for a filtration cycle can be calculated as:

$$j_{avg|n}(t_{f|n}) = \frac{\int_{t_{b|n}}^{t_{f|n}+t_{b|n}} j_{f|n}(t)\, dt - V_{b|n}}{t_{f|n} + t_{b|n}}, \tag{5.5}$$

where $V_{b|n}$ and $t_{b|n}$ are the volume of permeate and time spent backwashing, respectively. As the objective is to maximize the average permeate production defined in Eq. (5.5), the permeate produced in the filtration cycle can be defined as the sum of $j_{f|n}$ for the entire filtration phase:

$$V_{f|n}(k_n) = \sum_{i=l_n}^{k_n} j_{f|n}(iT_s)T_s. \tag{5.6}$$

The average flux is increasing while the current flux is higher than the previous average, as such filtration is continued while

$$j_{f|n}(k_n T_s) > \frac{V_{f|n}(k_n - 1) + V_{b|n}}{(k_n - 1)T_s} \tag{5.7}$$

is true. The filtration phase algorithm can be defined as:

Algorithm 2 Filtration phase. Modified from Paper E.

1: $j_{avg|n} = 0$ ▷ Initialization
2: **while** $j_{f|n}(k_n T_s) > j_{avg|n}$ **do** ▷ Implements Eq. (5.7)
3: Filtration ▷ Continue filtration
4: $V_{f|n} = V_{f|n} + j_{f|n}(k_n T_s) T_s$ ▷ Updated the total produced permeate
5: $j_{avg|n} = \frac{V_{f|n} + V_{b|n}}{k_n T_s}$ ▷ Update the average flux
6: $k_n = k_n + 1$ ▷ Increment k_n

The proposed algorithm for the backwashing and filtration phases (Algorithm 1 and 2) ensures that the net permeate production is optimized for the entire cycle. However, measurement noise can cause early termination of either phase. The two algorithms are combined and extended with both initialization and anti-noise measures:

Algorithm 3 Proposed scheduling algorithm, modified from Paper E.

1: **while** true **do**
2: $V_{b|n} = 0$ ▷ Initialization and/or reset the variables
3: $V_{f|n} = 0$
4: $t_{b|n} = 0$
5: $j_{avg|n} = 0$
6: $k_n = 0$
7: $l_n = 0$
8: **while** $0.95 \cdot min(\Delta P_b(l_n T_s), \Delta P_b(l_n T_s - 30 T_s)) > \Delta P_{b,ref}(t)$ **do**
9: Backwash
10: $V_{b|n} = V_{b|n} + j_{b|n}(l_n T_s) T_s$
11: $t_{b|n} = t_{b|n} + T_s$
12: $l_n = l_n + 1$
13: $k_n = k_n + 1$
14: **while** $j_{f|n}(k_n T_s) > j_{avg|n}$ **or** $(k_n - l_n) T_s < 50$ **do**
15: Filtration
16: $V_{f|n} = V_{f|n} + j_{f|n}(k_n T_s) T_s$
17: $j_{avg|n} = \frac{V_{f|n} + V_{b|n}}{k_n T_s}$
18: $k_n = k_n + 1$

The initialization is carried out in line no. 2-7, and anti-noise measures are added in line no. 8 and 14. Line no. 8 is modified such that backwashing pressure must be above 95% of the reference for both the current sample ($\Delta P_b(t)$) and three seconds ago ($\Delta P_b(t - 3s)$) before the backwashing phase is terminated. Line no. 14 is modified such that a minimum filtration duration of $50s$ is enforced. To further reduce any measurement noise related issues, a lowpass FIR filter is deployed with a bandwidth of $0.1Hz$, for detailed

specification see Paper E.

5.2 Experimental Results

To test the developed and described algorithm (Algorithm 3), it is implemented on the pilot plant, and new membranes are installed to better highlight the adaptability of the algorithm as irreversible fouling accumulates. To accelerate the experiment, the initial OiW concentration is intentionally above $1000 mg/L$ according to measurements. The backwashing scheduler was allowed to run for over 5 hours, where a total of 19 backwashes were carried out. The resulting flux, TMP, and backwashing flux are shown in Fig. 5.4, and filtration and backwashing durations are shown as a function of the cycle number in Fig. 5.5.

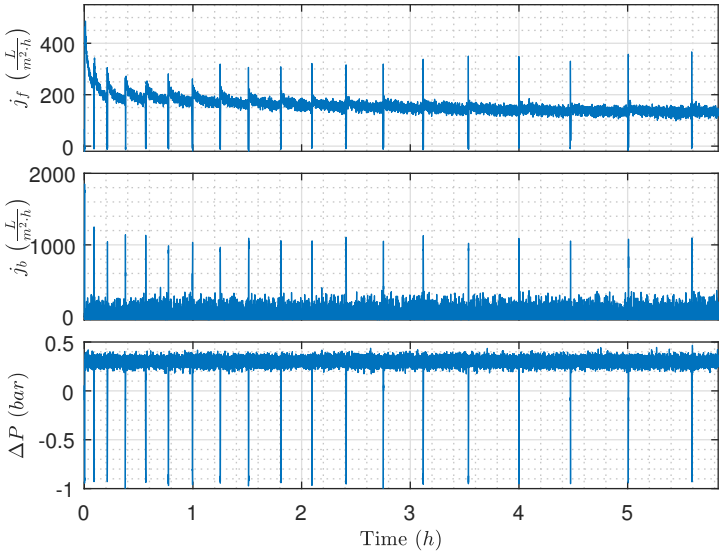

Fig. 5.4: Flow rates and pressure measurements while testing the proposed algorithm. The experimental conditions were: $1\frac{m}{s}$ CFV, $0.33 bar$ TMP, and $-1 bar$ backwashing pressure. Figure from Paper E.

As the membranes suffer from irreversible fouling, the frequency of backwashes is slowly reduced, while the backwashing duration remains relatively constant, see Fig. 5.5. The experiments showed that the backwashing flux could be up to eight times higher than the filtration flux [59]. Because of the high backwashing flux, the backwashing duration is critical in order to reduce permeate consumed by backwashing. To approximate the potential loss of extending the backwashing duration $5s$ beyond what is proposed in Alg. 3, it is assumed that the extended duration has no effect on the recovered flux

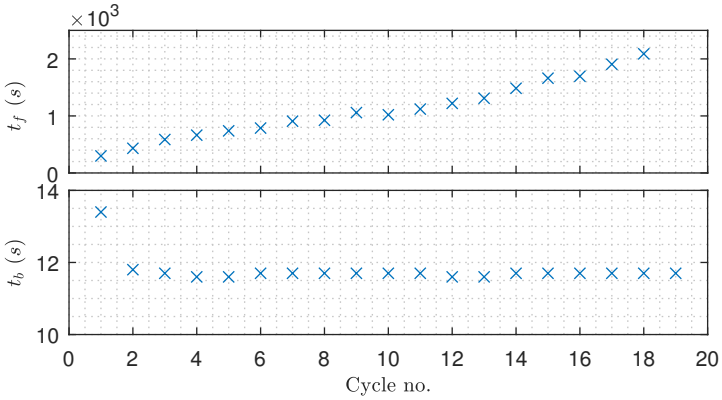

Fig. 5.5: Filtration and backwashing duration as a function of filtration cycle number, based on the experiments shown in Fig. 5.4. Figure from Paper E.

and that the backwashing flux present at the end of the backwashing phase is maintained for the extended duration. Based on these approximations, extending the backwashing duration by 5s causes a 3.5% reduction in permeate production.

Besides the backwashing duration, the filtration duration also affects the net permeate production. Based on the results in Paper E, where a filtration cycle was allowed to run for an extended period of time, the filtration duration is less time critical compared to the backwashing duration. For the considered case, the average flux peaked at 17.2min and if 3% production loss is allowed, the filtration duration interval becomes [11min, 30.6min]. Compared with the backwashing case where 5s caused a 3.5% reduction in permeate production, the backwashing duration is evidently more time critical.

5.3 Conclusion

Based on the observed fouling behavior during filtration and backwashing, an algorithm is proposed and tested on the pilot plant. Compared to the fixed durations commonly applied, the proposed algorithm adapts the filtration and backwashing duration online to account for time-varying features such as irreversible fouling. Extending the backwashing duration by 5s can cause up to 3.5% loss in average flux whereas 13min extension or 6min reduction are required to create identical losses by adjusting the filtration duration. Furthermore, the backwashing flux was observed to be up to eight times higher than the filtration flux, depending on the fouling state of the membranes. With the extremely high backwashing flux, permeate can quickly be consumed by backwashing. Both the high backwashing flow rate and the relatively

high production loss caused by extending the backwashing duration, indicating that the backwashing duration is critical for optimizing the permeate production.

The algorithm suggested do not necessarily guarantee optimal operating throughout the lifetime of the membranes, as irreversible fouling is unaccounted for in the optimization. It is possible that more frequent backwashing results in less irreversible fouling. To apply this algorithm and enforce more frequent backwashing, Eq. (5.7) can be modified with a tuning parameter.

For PWT, the OiW concentration after the hydrocyclones are typical 20-80mg/L [4]. However, for this study, the OiW concentration was intentionally mixed oil-rich (above 1000mg/L) to accelerate fouling and thereby test the proposed algorithm in hours instead of days. The OiW emulsion used in the pilot plant is artificially produced and the chemical complexity differs from offshore produced water. To ensure that the backwashing scheduling algorithm is applicable for offshore deployment, future work should compare the fouling behavior of the PW and artificial PW.

Chapter 6

Energy Optimization of Multi-Pump system

Despite the fact that CF membrane filtration has high specific energy consumption (energy consumed per cubic meter of permeate produced) [178], CF filtration remains the preferred configuration for separating oil and water [76, 179–182]. CF can increase the membrane flux by more than 100% depending on CFV and is therefore preferred above dead-end filtration in applications where installation footprint is in short supply, which is the case for offshore PWT [85]. Based on the manufacturer specification for the membranes, the ratio between CF and expected flux is between 11 and 46, emphasizing the pumping capacity and energy requirements of CF filtration, which is confirmed in [183]. In [178] where surface water is treated, results showed that the specific energy consumption for UF CF filtration was $0.54 kWh/m^3$ and in [184] where produced water with an OiW concentration of $12 mg/L$ to $84 mg/L$ was treated using UF CF filtration, the specific energy consumption was $0.84 kWh/m^3$. With a yearly produced water quantity of around $37 \cdot 10^6 m^3$ for the Danish North Sea, the yearly energy requirement of CF filtration would be approximately $33600 MWh$, assuming the specific energy consumption to be $0.84 kwh/m^3$ [1].

The enormous specific energy consumption introduced by CF can be reduced by minimizing fouling, thus increasing membrane flux. However, optimizing the pumping system can also reduce the operating cost through reduced energy consumption. The offshore PWT train must have high reliability and scalability to remain operational and comply with the varying flow rates caused by reservoir maturity or facility shutdown. A system equipped with a single CF pump is neither reliable nor energy efficient if operated in a wide operating range [185]. To increase reliability and efficiency at different operating conditions, multiple pumps with variable frequency drives (VFD)

can be connected in parallel and scheduled to maintain high efficiency in a broader operating range [185, 186].

Many methods have been used to schedule parallel connected pumps to maximize energy efficiency. However, most of the methods rely on the affinity-law to approximate the pump behavior at different pump speeds [185–190]. While the affinity-law is accurate at high pump speed, the accuracy is diminished as the pump speed is reduced and at 40% pump speed the prediction error can be above 20% [60]. The relative high prediction error of the affinity-law at low pump speeds can potentially cause suboptimal scheduling with respect to energy efficiency.

The remaining of this section summarizes results from Paper F, where an alternative to the widely used affinity-law based model is proposed. The proposed model showed improved prediction accuracy, especially below 50% pump speed but additional data is required by the model estimation process. Furthermore, the proposed model is used to schedule multiple identical pumps such that energy efficiency is maximized and the proposed method is compared to an affinity-law based scheduling method.

6.1 Power Consumption Model

To schedule multiple identical parallel pumps energy efficiently, a power consumption model of the pumps are essential. The proposed power consumption model is defined as:

$$p(h, Q) = a_1 \cdot h^{b_1} + a_2 \cdot Q^{b_2} + h \cdot Q \cdot a_3 + a_4, \tag{6.1}$$

where a_1, a_2, a_3, a_4, b_1, and b_2 are coefficients of the function, Q is the flow rate, and h is the head pressure. The proposed model function in Eq. (6.1) is chosen for its monotonic features and fitness to data. The estimated function coefficients and the adjusted coefficient of determination ($\bar{R}^2$) for the pumping station, described in Paper F, are listen in Table 6.1

Table 6.1: Estimated model coefficients and the adjusted coefficient of determination for the three pumps.

	a_1	a_2	b_1	b_2	a_3	a_4	$\bar{R}^2$
Pump 1	2.29	45.24	1.38	2.86	10.84	34.3	0.9994
Pump 2	1.73	34.93	1.45	2.93	10.37	27.1	0.9997
Pump 3	1.21	38.94	1.54	2.93	11.16	39.3	0.9994

6.1.1 Model Accuracy

The proposed model structure and the affinity-law are compared with respect to power consumption prediction accuracy. According to the affinity-law, the

relationship between pump speed and power consumption is defined as:

$$p = p_0 \cdot \left(\frac{\omega_p}{\omega_{p,0}} \right)^3, \tag{6.2}$$

where p is the electrical power, ω_p is the pump speed, and the subscript 0 denotes the base value given by the characteristic curves [185]. The power consumption of the pumps are measured using the Zimmer power analyzer LMG670. In Fig. 6.1 the prediction accuracy of both models, as defined in Eq. (6.3), is shown.

$$\Delta p_a = \frac{|(\bar{p}_a - p_m)|}{p_m} \cdot 100\%, \qquad \Delta p_b = \frac{|(\bar{p}_b - p_m)|}{p_m} \cdot 100\%, \tag{6.3}$$

where p_m is the measured power, $\bar{p}_a$ and $\bar{p}_b$ are the predicted power based on the affinity-law and the proposed model in Eq. (6.1), respectively. The

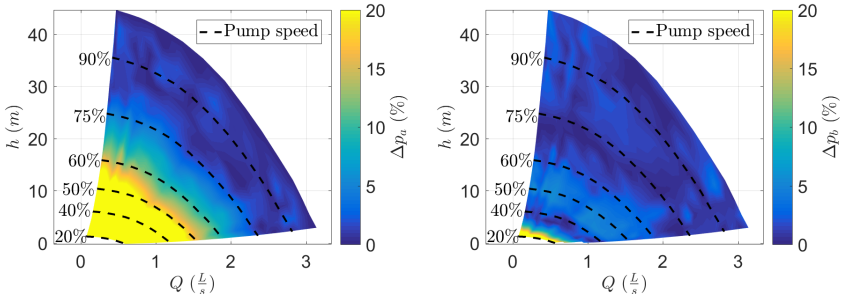

(a) Error between power measurement and prediction based on the affinity-law, for pump 1.

(b) Error between power measurement and prediction based on the proposed model, for pump 1.

Fig. 6.1: Comparison between the affinity-law and the proposed model, where the dashed black lines indicate different pump speeds. Figure modified from Paper F. © **2017 IEEE.**

prediction accuracy from either model is good at high pump speed, but once below 60% pump speed, the prediction performance of the affinity-law degrades and below 50% pump speed the error between measured and predicted power is around 20%. Based on these results, the power prediction performance of the proposed model is far better at lower pump speeds compared to the affinity-law, but does require additional data for the model estimate process.

6.2 Scheduling of Identical Pumps

Optimal scheduling of multiple identical parallel pumps with respect to power consumption is investigated based on the proposed model. The total

predicted power of multiple identical parallel pumps can be described as:

$$\begin{aligned} &p_t(h_t, Q_t, Q_1, Q_2 \cdots Q_{k-1}) = p(h_t, Q_1) + p(h_t, Q_2) + \cdots \\ &p(h_t, Q_{k-1}) + p(h_t, Q_t - Q_1 - Q_2 \cdots Q_{k-1}), \end{aligned} \tag{6.4}$$

where h_t is the pressure over the pumps, Q_t is the combined flow rate, k is the number of active pumps, and Q_1, Q_2, and Q_k are the flow rates delivered by pump 1, 2, and k, respectively. For the parallel configuration the pressure over each pump is identical, and the flow rate from the last pump can be expressed as Q_t minus the flow rates from the remaining active pumps. If h_t is the setpoint for the pump system, Q_t can be estimated based on system curve or directly obtained from measurements. The objective is defined as minimizing the total power by adjusting the flow rate from each pump, subject to a given Q_t and h_t:

$$\begin{aligned} \underset{Q_1, Q_2 \cdots Q_{k-1}}{\text{minimize}} \quad & p_t(h_t, Q_t, Q_1, Q_2 \cdots Q_{k-1}) \\ \text{subject to:} \quad & (h_t, Q_t) \in \mathbb{R}^2_{>0}, \\ & (Q_1, Q_2 \cdots Q_{k-1}) \in \mathbb{R}^{(k-1)}_{\geq 0} \\ & k \in \mathbb{N}, \end{aligned} \tag{6.5}$$

where the notation $\mathbb{R}_{>0}$ is the set of positive real numbers ($\mathbb{R}_{>0} = \{x \in \mathbb{R} | x > 0\}$). To facilitate the defined objective, it would be beneficial if the function p_t is convex. To evaluate if the function is convex, the Hessian with respect to $Q_1 \cdots Q_{k-1}$ is calculated:

$$\boldsymbol{H} = \begin{bmatrix} g_{\boldsymbol{H}d}(1) & g_{\boldsymbol{H}s} & \cdots & g_{\boldsymbol{H}s} \\ g_{\boldsymbol{H}s} & g_{\boldsymbol{H}d}(2) & \cdots & g_{\boldsymbol{H}s} \\ \vdots & \vdots & \ddots & \vdots \\ g_{\boldsymbol{H}s} & g_{\boldsymbol{H}s} & \cdots & g_{\boldsymbol{H}d}(k-1) \end{bmatrix} \tag{6.6}$$

where the diagonal elements are:

$$\begin{gathered} g_{\boldsymbol{H}d}(m) = a_2 \cdot b_2 \cdot (b_2 - 1) \cdot \left(Q_m^{b_2 - 2} + (Q_t - Q_1 \cdots Q_{k-1})^{b_2 - 2} \right) \\ \forall m \in \{x \in \mathbb{N} | x \leq k-1\}, \end{gathered} \tag{6.7}$$

and the off-diagonal elements are all identical and calculated as:

$$g_{\boldsymbol{H}s} = a_2 \cdot b_2 \cdot (b_2 - 1) \cdot (Q_t - Q_1 \cdots Q_{k-1})^{b_2 - 2}. \tag{6.8}$$

In order for $p_t(h_t, Q_t, Q_1, Q_2 \cdots Q_{k-1})$ to be convex or strictly convex, the Hessian of the function must be positive semidefinite (PSD) or positive definite (PD), respectively. To show that the Hessian is PD, the Hessian matrix can be divided into two parts:

$$\boldsymbol{H} = \boldsymbol{A} + \boldsymbol{B} \tag{6.9}$$

where

$$\boldsymbol{B} = \begin{bmatrix} g_{\boldsymbol{Hs}} & \cdots & g_{\boldsymbol{Hs}} \\ \vdots & \ddots & \vdots \\ g_{\boldsymbol{Hs}} & \cdots & g_{\boldsymbol{Hs}} \end{bmatrix} \tag{6.10}$$

and

$$\boldsymbol{A} = \boldsymbol{H} - \boldsymbol{B} = \begin{bmatrix} g_{\boldsymbol{Hd}}(1) - g_{\boldsymbol{Hs}} & 0 & \dots & 0 \\ 0 & g_{\boldsymbol{Hd}}(2) - g_{\boldsymbol{Hs}} & \dots & 0 \\ \vdots & \vdots & \ddots & \vdots \\ 0 & 0 & \dots & g_{\boldsymbol{Hd}}(k-1) - g_{\boldsymbol{Hs}} \end{bmatrix} \tag{6.11}$$

and by restricting the function coefficients to $a_1, b_1, a_3, a_4 \in \mathbb{R}$, $a_2 \in \mathbb{R}_{>0}$, $b_2 \in \{x \in \mathbb{R} | x > 1\}$ and assuming positive flow rates and pressure, the following is true for the Hessian matrix elements:

$$\begin{array}{ll} & g_{\boldsymbol{Hs}} > 0 \\ g_{\boldsymbol{Hd}}(m) > g_{\boldsymbol{Hs}} & \forall m \in \{x \in \mathbb{N} | x \leq k-1\} \end{array} \tag{6.12}$$

Provided the relationships defined in Eq. (6.12), the matrix $\boldsymbol{B}$ is PSD:

$$\boldsymbol{x}^T \boldsymbol{B} \boldsymbol{x} = g_{\boldsymbol{Hs}}(x_1 + \cdots x_{k-1})^2 \geq 0 \quad \forall \boldsymbol{x} \in \mathbb{R}^{k-1} \backslash \boldsymbol{0} \Leftrightarrow \boldsymbol{B} \succeq 0, \tag{6.13}$$

where $\boldsymbol{x} = [x_1\ x_2 \cdots x_{k-1}]$ and the notation $\succeq 0$ and $\succ 0$ are used for PSD and PD, respectively. Furthermore, with the relationships defined in Eq. (6.12) the matrix $\boldsymbol{A}$ is PD:

$$\begin{array}{c} \boldsymbol{x}^T \boldsymbol{A} \boldsymbol{x} = (g_{\boldsymbol{Hd}}(1) - g_{\boldsymbol{Hs}}) x_1^2 + \cdots (g_{\boldsymbol{Hd}}(k-1) - g_{\boldsymbol{Hs}}) x_{k-1}^2 \geq 0 \\ \forall \boldsymbol{x} \in \mathbb{R}^{k-1} \backslash \boldsymbol{0} \Leftrightarrow \boldsymbol{A} \succ 0. \end{array} \tag{6.14}$$

As $\boldsymbol{A}$ is PD and $\boldsymbol{B}$ is PSD, the sum of both matrices must also be greater than zero, hence $\boldsymbol{H}$ is PD:

$$0 < \boldsymbol{x}^T \boldsymbol{A} \boldsymbol{x} + \boldsymbol{x}^T \boldsymbol{B} \boldsymbol{x} = \boldsymbol{x}^T \cdot \underbrace{(\boldsymbol{A} + \boldsymbol{B})}_{\boldsymbol{H}} \cdot \boldsymbol{x} \Leftrightarrow \boldsymbol{H} \succ 0. \tag{6.15}$$

Provided that the Hessian matrix is PD, the total power function p_t is strictly convex, hence only a single minimum exists. The global minimum is where the partial derivative is equal to zero. The partial derivative of p_t with respect to the flow rates can be simplified to:

$$\frac{\partial}{\partial Q_m} p_t(\cdots) = Q_t - Q_1 \cdots - Q_{k-1} = Q_k = Q_m \quad \forall m \in \{x \in \mathbb{N} | x \leq k-1\}, \tag{6.16}$$

showing that for identical parallel pumps, the flow rate from each pump is identical at the global minimum. Based on the location of the global minimum, the total power usage can be reformulated in terms of pressure, total flow rate, and number of active pumps:

$$p_{tu}(h_t, Q_t, k) = p\left(h_t, \frac{Q_t}{k}\right) \cdot k \quad k \in [1...N], \tag{6.17}$$

where N is the total number of identical pumps available. Based on the previous defined bounds for Q_t, h_t, the function coefficients, and relaxing k to $k \in \mathbb{R}_{\geq 1}$ the reformulated total power function is convex with respect to k:

$$\frac{\partial^2}{\partial k^2} p_{tu}(h_t, Q_t, k) = \frac{a_2 b_2 \left(\frac{Q_t}{k}\right)^{b_2} (b_2 - 1)}{k} > 0. \tag{6.18}$$

The minimization objective can be redefined in terms of the updated power function p_{tu}:

$$\begin{aligned} \underset{k}{\text{minimize}} \quad & p_{tu}(h_t, Q_t, k) \\ \text{subject to:} \quad & (h_t, Q_t) \in \mathbb{R}^2_{>0} \\ & k \in \left\{ x \in \mathbb{R}_{\geq 1} \middle| \omega_{min} \leq \omega_p\left(h_t, \frac{Q_t}{x}\right) \leq \omega_{max} \right\}, \end{aligned} \tag{6.19}$$

where $\omega_p(h, Q)$ is a function describing the relationship between flow rate, pressure and pump speed, ω_{min} and ω_{max} are the minimum and maximum pump speed, respectively. Applying convex optimization to the problem defined in Eq. (6.19) results in a non-integer number of pumps. However, the two nearest integers can be checked for optimality. Ignoring the slight difference between the pumps and assuming identical performance, the power minimization problem is reduced to only depend on the number of pumps given that the required head pressure and total flow rate are known.

6.3 Scheduling Results

The accuracy of scheduling method defined in Eq. (6.19) is evaluated, and the results are presented in Fig. 6.2a. The result of the proposed scheduling method is compared to the affinity-law based scheduling method, illustrated in Fig. 6.2b. The non-optimal points for the proposed method are caused by the model predicting that the pumps are unable to deliver the pressure and flow rate, whereas, in reality, the pumps are barely able to supply the pressure and flow rate. The affinity-law based method is resulting in sub-optimal scheduling at low flow rates and pressures, as a consequence of model inaccuracy at low pump speeds. For identical pumps, the difference in power

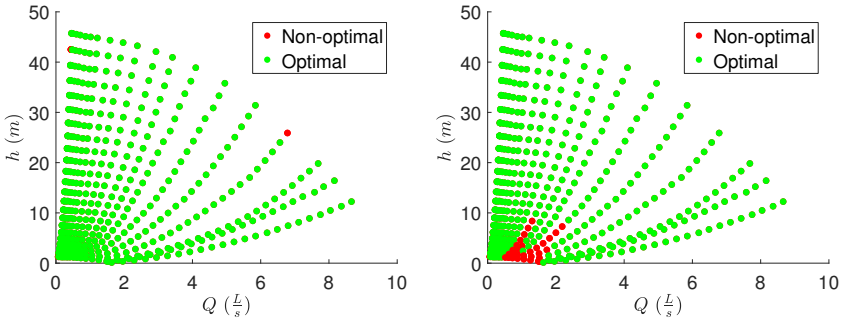

(a) Proposed optimization according to Eq. (6.19). Modified from Paper F, the maximum speed allowed according to the model is adjusted from 3500RPM to 3486RPM, which is the maximum pump speed measured.

(b) Pump scheduling based on the affinity-law, see Eq. (6.2). Based on data from Paper F.

Fig. 6.2: Optimal (green) and sub-optimal (red) pump scheduling. Figure modified from Paper F. © **2017 IEEE.**

between different numbers of pumps are fairly well distributed, thus the model inaccuracy can be relatively large before sub-optimal scheduling occurs. However, for non-identical pumps (a combination of different sizes) the minimum distance in power between the different configurations are reduced, consequently requiring better model accuracy to ensure optimal scheduling, thus increasing the region of sub-optimal scheduling for the affinity-law based method.

Fig. 6.3 shows the increased power usage caused by the sub-optimal scheduling of the affinity-law based method, where only non-zero elements are shown. Based on the results, sub-optimal scheduling of the affinity-law based method can increase power consumption by up to 70% in the relatively small region where sub-optimal scheduling occurs.

The proposed optimal pump scheduling strategy (mode 1) is compared to the configuration where only a single pump is equipped with VFD while the remaining pumps are subject to on/off control (mode 2). Based on experimental results, VFD combined with intelligent control can reduce energy consumption with over 30%, depending on the flow and pressure demands, as illustrated in Fig. 6.4. However, as results for mode 2 are based on pumps with VFD, the efficiency of the VFD should be subtracted for the pumps operated in no/off mode. But as the power efficiency for a reasonable sized VFD is above 90%, the potential power savings, for a pumping system with a large operating range, by applying VFD and intelligent control is still significant [191].

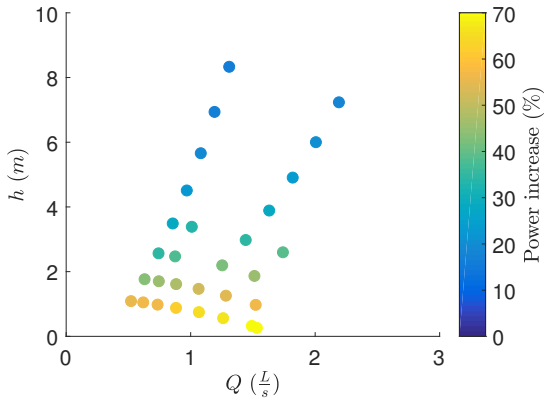

Fig. 6.3: Increased power consumption caused by sub-optimal scheduling of the affinity-law based method. Based on data from Paper F.

6.4 Conclusion

The model structure proposed was able to describe the relationship between power, flow rate, and pressure with high accuracy compared to the commonly applied affinity-law based model. Especially at pump speeds below 60%, the accuracy of the affinity-law based model degraded rapidly, while the proposed model structure was able to maintain high accuracy above 30% pump speed. However, the proposed model structure requires significantly more data points for the model estimation process compared to the affinity-law based model.

Based on the proposed model, a scheduling strategy for identical pumps is proposed and the minimization problem is reduced to a 1-D convex optimization problem. Comparing the proposed scheduling strategy to the affinity-law based scheduling strategy showed that the proposed method was able to predict the optimal number of pumps more consistently than the affinity-law based method. Furthermore, the deployed scheduling strategy was compared to a strategy deploying a single VFD and on/off control. Results showed that despite the efficiency loss caused by the VFD, the total system efficiency can be increased depending on flow rate and pressure.

To ensure that the pump scheduling remains efficient throughout time, the pump models must be periodically updated as wear and cavitation can affect pump performance characteristics. In addition, the scheduling strategy should be extended to cover non-identical pumps, especially as manufacturing variance and uneven wear can cause pumps of identical model to operate differently.

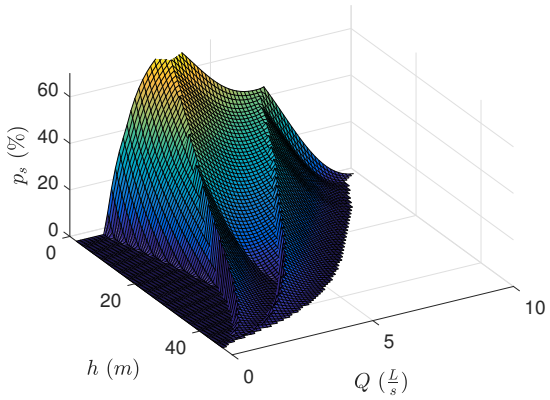

Fig. 6.4: Power saved by deploying mode 1 to schedule pumps compared to mode 2. Figure from F.

Chapter 7

Closing Remarks

7.1 Conclusion

In this thesis, the challenges associated with cost-effective membrane filtration of PW are addressed with emphasis on process control. The thesis aims to increase the attractiveness of membrane filtration by deploying advanced process control and scheduling techniques to reduce fouling of the membranes. This consequently reduces the capital and operating expenses.

The main thesis contributions are the literature review, reviewing challenges related to membrane filtration with emphasis on process control in Paper A and B, the system cross couplings analysis in Paper C and D, scheduling of backwashing in Paper E, modeling and scheduling of multiple pumps in parallel in Paper F, and lastly the construction and design of the pilot plant membrane extension.

The designed and constructed membrane extension was successfully integrated with the pilot plant and extensively used to investigate the fouling behavior and validate the various proposed control solutions. The extension is equipped with several flow meters, pressure and temperature transmitters, providing valuable insight into the filtration process. However, the fluorescence-based OiW monitors installed require further investigation to evaluate if and how varying flow conditions affect the OiW measurement.

Based on the literature review of membrane filtration with focus on PWT and process control, it was concluded that operating conditions greatly affect the fouling rate. While the relationship between operating conditions and fouling was comprehensively investigated, most studies neglect the design of the dynamic controllers maintaining the crucially selected operating conditions. Furthermore, the filtration duration and the backwashing duration are often fixed throughout time based on an initial study, neglecting the opportunity to online adapt the durations to ensure optimality despite irreversible

fouling or unforeseen behavioral changes. Thus, scheduling of backwashing and improved dynamic control to maintain operating conditions are topics where advanced control and scheduling techniques could potentially reduce fouling related cost.

Results from the pilot plant indicate that oscillating operating conditions in terms of flux and TMP cause increased fouling growth compared to non-oscillating operating conditions. Specifically 10 hours of oscillating TMP and flux caused a 20% reduction in flux compared to the case of constant TMP and flux. Often decentralized control is deployed for controlling and maintaining the selected operating point for the filtration system. However, control is often deployed for necessity rather than a topic for optimization, consequently the cross couplings in the filtration system are neglected or underestimated. The neglected and underestimated cross couplings can cause oscillating operating conditions which increase fouling growth. A dynamic RGA analysis of the considered pilot plant revealed that severe interaction between the CFV and flux exists. Furthermore, the analysis predicted that interaction between the control loops are minimized by selecting V_1 to control Q_{cf} and WP_1 to control Q_{pm}. The preferred control pairing is compared to a potential worst pairing, and experimental results showed that by selecting poor control pairings, controller interaction severely degraded the reference tracking and disturbance rejection performance. As poorly maintained operating conditions can increase fouling growth, control design is a crucial factor for efficient membrane filtration.

The fouling behavior during filtration and backwashing was examined, and results indicate that the removable fouling was removed as quickly as the backwashing pressure could be established. In addition, the backwashing flux was up to eight times higher than the subsequent filtration cycle, indicating that especially the backwashing duration is a crucial factor for maximizing the net permeate production. Based on the observed behavior a scheduling algorithm online adapting to process changes and maximizing net permeate production over a filtration cycle, is proposed. The proposed algorithm was tested on the pilot plant and results confirmed that the backwashing duration was indeed critical, as prolonging the backwashing duration from around $10s$ to $15s$ could cause a 3.5% reduction in net permeate production.

To operate the crossflow pumps energy efficiently, a new power consumption model describing the relationship between flow, pressure, and power consumption is proposed as an alternative to the affinity-based model commonly used. The proposed model provides much higher accuracy below 60% pump speed compared to the affinity-based model but does require a more extensive model estimation process. Furthermore, based on the newly developed power consumption model, a scheduling strategy for multiple parallel variable speed pumps is proposed and compared to an on/off configuration

with a single variable speed pump. Results showed that despite the efficiency loss caused by the VFD, proper scheduling of multiple variable speed pumps can increase the overall pumping efficiency when a wide pumping range is required.

The overall conclusion is that it is difficult to develop a solution that ensures optimality for all applications of membrane filtration with the large variance in feed composition. Even within PW, the composition varies with respect to well, reservoir, and field maturity, and multiphase interaction can cause oscillating feed flow rate and TMP. To compensate for the time varying behavior, the backwashing and filtration durations must be selected online based on measurement to guarantee optimality regardless of operating conditions. In addition, the dynamic controllers must be designed to account for cross couplings, thus ensuring proper reference tracking subject to disturbances in inlet OiW concentration, pressure, and flow rate. Lastly, the high energy consumption of the CF system and the requirements to scalability and reliability require advanced pump scheduling to ensure high energy efficiency. By addressing these topics, the overall fouling resistance and energy consumption can be reduced, consequently reducing the capital and operating expenses, and increasing the attractiveness of membrane filtration for PWT.

7.2 Future Work

The work in this thesis addresses some of the challenges with membrane filtration for offshore PWT from a process control perspective. However, for future work the difference between the artificial and offshore PW should be investigated and depending on the difference, the suggested methods should be adjusted.

For the RGA analysis, a pre-investigation confirmed that the membranes are sensitive to oscillating conditions, leading to an extensive analysis of the cross couplings in order to select the control pairings that minimize control loop interaction and thereby fouling. However, the difference in fouling rate between the preferred and the unpreferred case was not investigated. Further work should quantify the difference in fouling rate caused by the preferred and unpreferred pairings. For the backwashing scheduling algorithm, the method assumed that irreversible fouling is uncorrelated to the backwashing and filtration durations which is unlikely. Further research is required to investigate the relationship between backwashing and filtration durations and irreversible fouling. For scheduling of multiple pumps, the work should be extended to cover scheduling of multiple non-identical parallel pumps, as uneven wear and tear on the pumps can cause a difference in performance despite the pumps being initial identical.

References

[1] The Danish Energy Agency, "Yearly production, injection, flare, fuel and export in si units 1972-2017," 2018. [Online]. Available: https://ens.dk/sites/ens.dk/files/OlieGas/1972-2017.xlsx

[2] J. Coca-Prados and G. Gutiérrez-Cervelló, *Water Purification and Management*. Springer, 2009, vol. 119. ISBN 9789400750784

[3] S. Nesic and V. Streletskaya, "An integrated approach for produced water treatment and injection," *Georesursy*, vol. 20, no. 1, pp. 25–31, 2018. doi: 10.18599/grs.2018.1.25-31

[4] S. Judd, H. Qiblawey, M. Al-Marri, C. Clarkin, S. Watson, A. Ahmed, and S. Bach, "The size and performance of offshore produced water oil-removal technologies for reinjection," *Separation and Purification Technology*, vol. 134, pp. 241–246, 2014. doi: 10.1016/j.seppur.2014.07.037

[5] S. Amini, D. Mowla, M. Golkar, and F. Esmaeilzadeh, "Mathematical modelling of a hydrocyclone for the down-hole oil-water separation (DOWS)," *Chemical Engineering Research and Design*, vol. 90, no. 12, pp. 2186–2195, 2012. doi: 10.1016/j.cherd.2012.05.007

[6] Q. Huang, C. Li, and P. Li, "A mathematical model for predicting oil-water separation efficiency in a de-oiling hydrocyclone," *Journal of Dispersion Science and Technology*, vol. 38, no. 9, pp. 1319–1324, 2017. doi: 10.1080/01932691.2016.1236266

[7] K. L. Jepsen, L. Hansen, and Z. Yang, "Control parings of a de-oiling membrane process," *IFAC-PapersOnLine*, vol. 51, no. 8, pp. 126–131, 2018. doi: 10.1016/j.ifacol.2018.06.366

[8] Danish Environmental Protection Agency, "General authorization for Maersk Oil and Gas," 2016. [Online]. Available: http://mst.dk/media/92144/20161221-ann-generel-udledningstilladelse-for-maersk-olie-og-gas-2017-18.pdf

[9] A. Taylor, M. Malinovsky, H. Nielsen, E. Garland, K. Machetanz, M. Cronin, I. Abdoellakhan, T. Sørgård, and I. Rønning, "OSPAR report on discharges, spills and emissions from offshore oil and gas installations in 2014," OSPAR, Tech. Rep., 2016. [Online]. Available: https://www.ospar.org/documents?d=35364

[10] OSPAR-Commission, "OSPAR report on discharges, spills and emissions from offshore oil and gas installations in 2014," p. 55, 2016. [Online]. Available: https://www.ospar.org/documents?d=35364 (Accessed 2018-12-09).

[11] M. Bader, "Seawater versus produced water in oil-fields water injection operations," *Desalination*, vol. 208, no. 1-3, pp. 159–168, 2007. doi: 10.1016/j.desal.2006.05.024

[12] C. C. Patton, "Injection-Water Quality," *Journal of Petroleum Technology*, vol. 42, no. 10, pp. 1238–1240, 1990. doi: 10.2118/21300-PA

[13] E. Lystad and I. Nilssen, "Monitoring and Zero Discharge," in *SPE International Conference on Health, Safety, and Environment in Oil and Gas Exploration and Production*, no. March 2004. Society of Petroleum Engineers, 2004, pp. 1305–1310. doi: 10.2118/86799-MS

[14] S. Jiménez, M. Micó, M. Arnaldos, F. Medina, and S. Contreras, "State of the art of produced water treatment," *Chemosphere*, vol. 192, pp. 186–208, 2018. doi: 10.1016/j.chemosphere.2017.10.139

[15] U. W. Siagian, S. Widodo, Khoiruddin, A. K. Wardani, and I. G. Wenten, "Oilfield Produced Water Reuse and Reinjection with Membrane," *MATEC Web of Conferences*, vol. 156, p. 08005, 2018. doi: 10.1051/matecconf/201815608005

[16] I. Dunsmuir, G. Guthrie, T. Cottrell, A. Nijmeijer, and B. G. Reck, "The Deployment of Ceramic Membrane Technology to Treat Stable Oil in Emulsions in Produced Water Offshore," in *SPE Offshore Europe Conference & Exhibition*. Aberdeen, United Kingdom: Society of Petroleum Engineers, 2017, pp. 1–8. doi: 10.2118/186131-MS

[17] J. Mueller, "Crossflow microfiltration of oily water," *Journal of Membrane Science*, vol. 129, no. 2, pp. 221–235, 1997. doi: 10.1016/S0376-7388(96)00344-4

[18] T. Zsirai, A. Al-Jaml, H. Qiblawey, M. Al-Marri, A. Ahmed, S. Bach, S. Watson, and S. Judd, "Ceramic membrane filtration of produced water: Impact of membrane module," *Separation and Purification Technology*, vol. 165, no. March 2018, pp. 214–221, 2016. doi: 10.1016/j.seppur.2016.04.001

[19] S. E. Weschenfelder, A. M. Louvisse, C. P. Borges, E. Meabe, J. Izquierdo, and J. C. Campos, "Evaluation of ceramic membranes for oilfield produced water treatment aiming reinjection in offshore units," *Journal of Petroleum Science and Engineering*, vol. 131, pp. 51–57, 2015. doi: 10.1016/j.petrol.2015.04.019

[20] S. R. H. Abadi, M. R. Sebzari, M. Hemati, F. Rekabdar, and T. Mohammadi, "Ceramic membrane performance in microfiltration of oily wastewater," *Desalination*, vol. 265, no. 1-3, pp. 222–228, 2011. doi: 10.1016/j.desal.2010.07.055

[21] F. Hua, Y. Tsang, Y. Wang, S. Chan, H. Chua, and S. Sin, "Performance study of ceramic microfiltration membrane for oily wastewater treatment," *Chemical Engineering Journal*, vol. 128, no. 2-3, pp. 169–175, 2007. doi: 10.1016/j.cej.2006.10.017

[22] C. Yang, G. Zhang, N. Xu, and J. Shi, "Preparation and application in oil–water separation of ZrO2/α-Al2O3 MF membrane," *Journal of Membrane Science*, vol. 142, no. 2, pp. 235–243, 1998. doi: 10.1016/S0376-7388(97)00336-0

[23] J. Cui, X. Zhang, H. Liu, S. Liu, and K. L. Yeung, "Preparation and application of zeolite/ceramic microfiltration membranes for treatment of oil contaminated water," *Journal of Membrane Science*, vol. 325, no. 1, pp. 420–426, 2008. doi: 10.1016/j.memsci.2008.08.015

[24] K. Jepsen, M. Bram, S. Pedersen, and Z. Yang, "Membrane Fouling for Produced Water Treatment: A Review Study From a Process Control Perspective," *Water*, vol. 10, no. 7, p. 847, 2018. doi: 10.3390/w10070847

[25] S. Munirasu, M. A. Haija, and F. Banat, "Use of membrane technology for oil field and refinery produced water treatment—A review," *Process Safety and Environmental Protection*, vol. 100, pp. 183–202, 2016. doi: 10.1016/j.psep.2016.01.010

[26] S. N. W. Ikhsan, N. Yusof, F. Aziz, and N. Misdan, "A Review of Oilfield Wastewater Treatment using Membrane Filtration over Conventional Technology," *Malaysian Journal of Analytical Science*, vol. 21, no. 3, pp. 643–658, 2017. doi: 10.17576/mjas-2017-2103-14

[27] A. Fakhru'l-Razi, A. Pendashteh, L. C. Abdullah, D. R. A. Biak, S. S. Madaeni, and Z. Z. Abidin, "Review of technologies for oil and gas produced water treatment," *Journal of Hazardous Materials*, vol. 170, no. 2-3, pp. 530–551, 2009. doi: http://dx.doi.org/10.1016/j.jhazmat.2009.05.044

[28] J. M. Dickhout, J. Moreno, P. M. Biesheuvel, L. Boels, R. G. Lammertink, and W. M. de Vos, "Produced water treatment by membranes: A review from a colloidal perspective," *Journal of Colloid and Interface Science*, vol. 487, pp. 523–534, 2017. doi: 10.1016/j.jcis.2016.10.013

[29] M. Padaki, R. Surya Murali, M. S. Abdullah, N. Misdan, A. Moslehyani, M. A. Kassim, N. Hilal, and A. F. Ismail, "Membrane technology enhancement in oil-water separation. A review," pp. 197–207, 2015. [Online]. Available: http://dx.doi.org/10.1016/j.desal.2014.11.023

[30] K. Guerra, J. Pellegrino, and J. E. Drewes, "Impact of operating conditions on permeate flux and process economics for cross flow ceramic membrane ultrafiltration of surface water," *Separation and Purification Technology*, vol. 87, pp. 47–53, 2012. doi: 10.1016/j.seppur.2011.11.019

[31] S. Weschenfelder, C. Borges, and J. Campos, "Oilfield produced water treatment by ceramic membranes: Bench and pilot scale evaluation," *Journal of Membrane Science*, vol. 495, pp. 242–251, 2015. doi: 10.1016/j.memsci.2015.08.028

[32] W. L. L. Thiam Teik Wan, "Experimental Study of the Separation of Oil in Water Emulsions by Tangential Flow Microfiltration Process. Part 1: Analysis of Oil Rejection Efficiency and Flux Decline," *Journal of Membrane Science & Technology*, vol. 05, no. 01, pp. 1–6, 2015. doi: 10.4172/2155-9589.1000130

[33] M. A. Monfared, N. Kasiri, and T. Mohammadi, "Microscopic modeling of critical pressure of permeation in oily waste water treatment via membrane filtration," *RSC Adv.*, vol. 6, no. 75, pp. 71 744–71 756, 2016. doi: 10.1039/C6RA12266C

[34] L. Defrance and M. Jaffrin, "Comparison between filtrations at fixed transmembrane pressure and fixed permeate flux: application to a membrane bioreactor used for wastewater treatment," *Journal of Membrane Science*, vol. 152, no. 2, pp. 203–210, 1999. doi: 10.1016/S0376-7388(98)00220-8

[35] E. K. Lee, V. Chen, and A. Fane, "Natural organic matter (NOM) fouling in low pressure membrane filtration — effect of membranes and operation modes," *Desalination*, vol. 218, no. 1-3, pp. 257–270, 2008. doi: 10.1016/j.desal.2007.02.021

[36] X. Guo, Z. Zhang, L. Fang, and L. Su, "Study on ultrafiltration for surface water by a polyvinylchloride hollow fiber membrane," *Desalination*, vol. 238, no. 1-3, pp. 183–191, 2009. doi: 10.1016/j.desal.2007.11.064

[37] D. J. Miller, S. Kasemset, D. R. Paul, and B. D. Freeman, "Comparison of membrane fouling at constant flux and constant transmembrane pressure conditions," *Journal of Membrane Science*, vol. 454, pp. 505–515, 2014. doi: 10.1016/j.memsci.2013.12.027

[38] J. Busch and W. Marquardt, "Run-to-run control of membrane filtration in wastewater treatment - an experimental study," *IFAC Proceedings Volumes*, vol. 40, no. 5, pp. 195–200, 2007. doi: 10.3182/20070606-3-MX-2915.00080

[39] A. Abbas, "Model predictive control of a reverse osmosis desalination unit," *Desalination*, vol. 194, no. 1-3, pp. 268–280, 2006. doi: 10.1016/j.desal.2005.10.033

[40] S. Pedersen, "Plant-Wide Anti-Slug Control for Offshore Oil and Gas Processes," Ph.D. thesis, Aalborg Universitet, 2016. doi: 10.5278/vbn.phd.engsci.00183

[41] M. Stoller and R. S. Mendes, "Advanced control system for membrane processes based on the boundary flux model," *Separation and Purification Technology*, vol. 175, pp. 527–535, 2017. doi: 10.1016/j.seppur.2016.09.049

[42] B. Espinasse, P. Bacchin, and P. Aimar, "On an experimental method to measure critical flux in ultrafiltration," *Desalination*, vol. 146, no. 1-3, pp. 91–96, 2002. doi: 10.1016/S0011-9164(02)00495-2

[43] S. G. Lehman and L. Liu, "Application of ceramic membranes with preozonation for treatment of secondary wastewater effluent," *Water Research*, vol. 43, no. 7, pp. 2020–2028, 2009. doi: 10.1016/j.watres.2009.02.003

[44] B. Espinasse, P. Bacchin, and P. Aimar, "Filtration method characterizing the reversibility of colloidal fouling layers at a membrane surface: Analysis through critical flux and osmotic pressure," *Journal of Colloid and Interface Science*, vol. 320, no. 2, pp. 483–490, 2008. doi: 10.1016/j.jcis.2008.01.023

[45] M. Hung and J. Liu, "Microfiltration for separation of green algae from water," *Colloids and Surfaces B: Biointerfaces*, vol. 51, no. 2, pp. 157–164, 2006. doi: 10.1016/j.colsurfb.2006.07.003

[46] P. Srijaroonrat, E. Julien, and Y. Aurelle, "Unstable secondary oil / water emulsion treatment using ultrafiltration : fouling control by backflushing," *Journal of Membrane Science*, vol. 159, pp. 11–20, 1999. doi: https://doi.org/10.1016/j.jwpe.2014.09.007

[47] S. E. Weschenfelder, A. M. T. Louvisse, C. P. Borges, and J. C. Campos, "Preliminary Studies on the Application of Ceramic Membranes for Oilfield Produced Water Management," in *OTC Brasil*. Offshore Technology Conference, 2013, pp. 1–10. doi: https://doi.org/10.4043/24465-MS

[48] J. Wu, P. Le-Clech, R. M. Stuetz, A. G. Fane, and V. Chen, "Effects of relaxation and backwashing conditions on fouling in membrane bioreactor," *Journal of Membrane Science*, vol. 324, no. 1-2, pp. 26–32, 2008. doi: 10.1016/j.memsci.2008.06.057

[49] S. Vigneswaran, W. Guo, P. Smith, and H. Ngo, "Submerged membrane adsorption hybrid system (SMAHS): process control and optimization of operating parameters," *Desalination*, vol. 202, no. 1-3, pp. 392–399, 2007. doi: 10.1016/j.desal.2005.12.079

[50] A. Aidan, N. Abdel-Jabbar, T. H. Ibrahim, V. Nenov, and F. Mjalli, "Neural network modeling and optimization of scheduling backwash for membrane bioreactor," *Clean Technologies and Environmental Policy*, vol. 10, no. 4, pp. 389–395, 2008. doi: 10.1007/s10098-007-0129-0

[51] F. Z. Slimane, F. Ellouze, G. Ben miled, and N. Ben Amar, "Physical backwash optimization in membrane filtration processes: Seawater Ultrafiltration case," *Membrane Processes Research Laboratory (MPRL)*, vol. 0, no. 0, pp. 63–68, 2017. doi: 10.22079/JMSR.2017.66624.1145

[52] K. L. Jepsen, L. Hansen, C. Mai, and Z. Yang, "Challenges of Membrane Filtration for Produced Water Treatment in Offshore Oil & Gas Production," *OCEANS 2016 MTS/IEEE Monterey*, pp. 1–8, 2016. doi: 10.1109/oceans.2016.7761443

[53] K. S. Ashaghi, M. Ebrahimi, and P. Czermak, "Ceramic Ultra- and Nanofiltration Membranes for Oilfield Produced Water Treatment: A Mini Review," *Open Environmental Sciences*, vol. 1, no. 1, pp. 1–8, 2008. doi: 10.2174/1876325100701010001

[54] S. Alzahrani and A. W. Mohammad, "Challenges and trends in membrane technology implementation for produced water treatment: A review," *Journal of Water Process Engineering*, vol. 4, pp. 107–133, 2014. doi: 10.1016/j.jwpe.2014.09.007

[55] N. Ahmad, P. Goh, Z. Abdul Karim, and A. Ismail, "Thin Film Composite Membrane for Oily Waste Water Treatment: Recent Advances and Challenges," *Membranes*, vol. 8, no. 4, p. 86, 2018. doi: 10.3390/membranes8040086

[56] K. L. Jepsen, S. Pedersen, and Z. Yang, "Control Pairings of a Deoiling Membrane Crossflow Filtration Process based on Theoretical and Experimental Results," *Submitted to Journal of Process Control, pending decision for revised version.*, 2019.

[57] H. J. Tanudjaja, V. V. Tarabara, A. G. Fane, and J. W. Chew, "Effect of cross-flow velocity, oil concentration and salinity on the critical flux of an oil-in-water emulsion in microfiltration," *Journal of Membrane Science*, vol. 530, no. February, pp. 11–19, 2017. doi: 10.1016/j.memsci.2017.02.011

[58] A. Ezzati, E. Gorouhi, and T. Mohammadi, "Separation of water in oil emulsions using microfiltration," *Desalination*, vol. 185, no. 1-3, pp. 371–382, 2005. doi: 10.1016/j.desal.2005.03.086

[59] K. L. Jepsen, M. V. Bram, L. Hansen, Z. Yang, and S. M. Ø. Lauridsen, "Online Backwash Optimization of Membrane Filtration for Produced Water Treatment ." *Pending approval by Total, to be submitted to Journal of Membrane Science.*, 2019.

[60] K. Jepsen, L. Hansen, C. Mai, and Z. Yang, "Power consumption optimization for multiple parallel centrifugal pumps," in *1st Annual IEEE Conference on Control Technology and Applications, CCTA 2017*, vol. 2017-Janua, 2017. ISBN 9781509021826. doi: 10.1109/CCTA.2017.8062559

[61] M. Jaffrin, B. Gupta, and P. Paullier, "Energy saving pulsatile mode cross flow filtration," *Journal of Membrane Science*, vol. 86, no. 3, pp. 281–290, 1994. doi: 10.1016/0376-7388(93)E0151-9

[62] Z. Yang and H. Børsting, "Optimal scheduling and control of a multi-pump boosting system," in *2010 IEEE International Conference on Control Applications*, no. i. IEEE, 2010. ISBN 978-1-4244-5362-7. ISSN 1085-1992 pp. 2071–2076. doi: 10.1109/CCA.2010.5611177

[63] P. W. Jowitt and G. Germanopoulos, "Optimal Pump Scheduling in Water-Supply Networks," *Journal of Water Resources Planning and Management*, vol. 118, no. 4, pp. 406–422, 1992. doi: 10.1061/(ASCE)0733-9496(1992)118:4(406)

[64] L. Hansen, P. D. Løhndorf, K. L. Jepsen, and Z. Yang, "Plant-wide Optimal Control of an Offshore De-oiling Process Using MPC Technique," *IFAC-PapersOnLine*, vol. 51, no. 8, pp. 144–150, 2018. doi: 10.1016/j.ifacol.2018.06.369

[65] D. S. Hansen, M. V. Bram, P. D. Løhndorf, and Z. Yang, "Efficiency Evaluation of Offshore Deoiling Applications utilizing Real-Time Oil-in-Water Monitors," in *OCEANS 2017 - Anchorage*, Anchorage, AK, USA, 2017, pp. 1–6.

[66] P. Durdevic and Z. Yang, "Dynamic Efficiency Analysis of an Off-Shore Hydrocyclone System, Subjected to a Conventional PID- and Robust-Control-Solution," *Energies*, vol. 11, no. 9, p. 2379, 2018. doi: 10.3390/en11092379

[67] P. D. Løhndorf, "Real-Time Monitoring and Robust Control of Offshore De-oiling Processes," PhD Thesis, Aalborg University. ISBN 9788771129304 2017.

[68] M. V. Bram, L. Hansen, D. S. Hansen, and Z. Yang, "Hydrocyclone Separation Efficiency Modeled by Flow Resistances and Droplet Trajectories," *IFAC-PapersOnLine*, vol. 51, no. 8, pp. 132–137, 2018. doi: 10.1016/j.ifacol.2018.06.367

[69] H. B. Bradley and F. W. Gipson, *Petroleum engineering handbook*, F. W. Gipson, A. S. Odeh, P. S. Sizer, M. Mortada, L. L. Raymer, and G. L. Smith, Eds. Society of Petroleum Engineers, Richardson, TX, 1987. ISBN 1-55563-010-3

[70] R. Faibish, "Fouling-resistant ceramic-supported polymer membranes for ultrafiltration of oil-in-water microemulsions," *Journal of Membrane Science*, vol. 185, no. 2, pp. 129–143, 2001. doi: 10.1016/S0376-7388(00)00595-0

[71] M. Bader, "Seawater versus produced water in oil-fields water injection operations," *Desalination*, vol. 208, no. 1-3, pp. 159–168, 2007. doi: 10.1016/j.desal.2006.05.024

[72] T. Bilstad and E. Espedal, "Membrane separation of produced water," *Water Science and Technology*, vol. 34, no. 9, pp. 239–246, 1996. doi: 10.1016/S0273-1223(96)00810-4

[73] M. Ebrahimi, K. S. Ashaghi, L. Engel, D. Willershausen, P. Mund, P. Bolduan, and P. Czermak, "Characterization and application of different ceramic membranes for the oil-field produced water treatment," *Desalination*, vol. 245, no. 1-3, pp. 533–540, 2009. doi: 10.1016/j.desal.2009.02.017

[74] A. B. Koĺtuniewicz and R. W. Field, "Process factors during removal of oil-in-water emulsions with cross-flow microfiltration," *Desalination*, vol. 105, no. 1-2, pp. 79–89, 1996. doi: 10.1016/0011-9164(96)00061-6

[75] P. Pedenaud, E. Wayne, H. Samuel, and B. Didier, "Ceramic Membrane And Core Pilot Results For Produced Water Management," in *Offshore Technology Conference, Brasil*, vol. 1. Offshore Technology Conference, 2011. ISBN 9781618392770. ISSN 01603663 pp. 385–400. doi: 10.4043/22371-MS

[76] M. Ebrahimi, D. Willershausen, K. S. Ashaghi, L. Engel, L. Placido, P. Mund, P. Bolduan, and P. Czermak, "Investigations on the use of different ceramic membranes for efficient oil-field produced water treatment," *Desalination*, vol. 250, no. 3, pp. 991–996, 2010. doi: 10.1016/j.desal.2009.09.088

[77] B. Hofs, J. Ogier, D. Vries, E. F. Beerendonk, and E. R. Cornelissen, "Comparison of ceramic and polymeric membrane permeability and fouling using surface water," *Separation and Purification Technology*, vol. 79, no. 3, pp. 365–374, 2011. doi: 10.1016/j.seppur.2011.03.025

[78] T. Zsirai, A. Al-Jaml, H. Qiblawey, M. Al-Marri, A. Ahmed, S. Bach, S. Watson, and S. Judd, "Ceramic membrane filtration of produced water: Impact of membrane module," *Separation and Purification Technology*, vol. 165, pp. 214–221, 2016. doi: 10.1016/j.seppur.2016.04.001

[79] K. C. Khulbe, C. Feng, and T. Matsuura, "Pore Size, Pore Size Distribution, and Roughness at the Membrane Surface," in *Synthetic Polymeric Membranes*. Berlin, Heidelberg: Springer Berlin Heidelberg, 2008, pp. 101–139. ISBN 978-3-540-73994-4

[80] Y. He and Z.-W. Jiang, "Technology review: Treating oilfield wastewater," *Filtration & Separation*, vol. 45, no. 5, pp. 14–16, 2008. doi: 10.1016/S0015-1882(08)70174-5

[81] M. Cheryan and N. Rajagopalan, "Membrane processing of oily streams. Wastewater treatment and waste reduction," *Journal of Membrane Science*, vol. 151, no. 1, pp. 13–28, 1998. doi: 10.1016/S0376-7388(98)00190-2

[82] S. M. Santos, M. R. Weisner, and M. R. Wiesner, "Ultrafiltration of water generated in oil and gas production," *Water Environment Research*, vol. 69, no. 6, pp. 1120–1127, 1997. doi: 10.2175/106143097X125858

[83] A. Chen, J. Flynn, R. Cook, and A. Casaday, "Removal of Oil, Grease, and Suspended Solids From Produced Water With Ceramic Crossflow Microfiltration," *SPE Production Engineering*, vol. 6, no. 02, pp. 131–136, 1991. doi: 10.2118/20291-PA

[84] R. R. Bhave, "Cross-Flow Filtration," in *Fermentation and Biochemical Engineering Handbook*, 2nd ed., H. C. Vogel and C. L. Todaro, Eds. Elsevier, 1996, ch. Cross-flow, pp. 271–347. ISBN 978-0-8155-1407-7. [Online]. Available: https://linkinghub.elsevier.com/retrieve/pii/B9780815514077500106

[85] T. Arnot, R. Field, and A. Koltuniewicz, "Cross-flow and dead-end microfiltration of oily-water emulsions," *Journal of Membrane Science*, vol. 169, no. 1, pp. 1–15, 2000. doi: 10.1016/S0376-7388(99)00321-X

[86] A. Koltuniewicz, R. Field, and T. Arnot, "Cross-flow and dead-end microfiltration of oily-water emulsion. Part I: Experimental study and analysis of flux decline," *Journal of Membrane Science*, vol. 102, no. C, pp. 193–207, 1995. doi: 10.1016/0376-7388(94)00320-X

[87] N. Shamsuddin, C. Cao, V. M. Starov, and D. B. Das, "A comparative study between stirred dead end and circular flow in microfiltration of China clay suspensions," *Water Science and Technology: Water Supply*, vol. 16, no. 2, pp. 481–492, 2016. doi: 10.2166/ws.2015.158

[88] V. V. Bobinkin, S. Y. Larionov, A. A. Panteleev, D. A. Shapovalov, and M. M. Shilov, "Optimization of membrane elements' array in industrial reverse osmosis units," *Thermal Engineering*, vol. 62, no. 10, pp. 735–740, 2015. doi: 10.1134/S0040601515100031

[89] D. Flanigan, J. Stolhand, M. Scribner, and E. Shimoda, "Droplet Size Analysis: A New Tool for Improving Oilfield Separations," in *SPE Annual Technical Conference and Exhibition*. Houston, Texas: Society of Petroleum Engineers, 1988. ISBN 978-1-55563-578-7 p. 7. doi: 10.2118/18204-MS

[90] R. Morales, E. Pereyra, S. Wang, and O. Shoham, "Droplet Formation Through Centrifugal Pumps for Oil-in-Water Dispersions," *SPE Journal*, vol. 18, no. 01, pp. 172–178, 2012. doi: 10.2118/163055-PA

[91] R. Husveg, T. Husveg, N. V. Teeffelen, M. Ottestad, and M. R. Hansen, "Performance of a Coalescing Multistage Centrifugal Produced Water Pump with Respect to Water Characteristics and Point of Operation," in *Tuv Nel Produced Water Workshop*, Aberdeen, 2016, pp. 1–14.

[92] R. Sondhi and R. Bhave, "Role of backpulsing in fouling minimization in crossflow filtration with ceramic membranes," *Journal of Membrane Science*, vol. 186, no. 1, pp. 41–52, 2001. doi: 10.1016/S0376-7388(00)00663-3

[93] M. Abbasi, A. Salahi, M. Mirfendereski, T. Mohammadi, and A. Pak, "Dimensional analysis of permeation flux for microfiltration of oily wastewaters using mullite ceramic membranes," *Desalination*, vol. 252, no. 1-3, pp. 113–119, 2010. doi: 10.1016/j.desal.2009.10.015

[94] A. Reyhani and H. Mashhadi Meighani, "Optimal operating conditions of micro- and ultra-filtration systems for produced-water purification: Taguchi method and economic investigation," *Desalination and Water Treatment*, vol. 57, no. 42, pp. 19 642–19 654, 2016. doi: 10.1080/19443994.2015.1101714

[95] L. G. Fernandez, C. O. Soria, C. A. Garcia Tourn, and M. S. Izquierdo, "The Study of Oil/Water Separation in Emulsion by Membrane Technology," in *SPE Latin American and Caribbean Petroleum Engineering Conference*, no. v. Society of Petroleum Engineers, 2001. doi: 10.2118/69554-MS

[96] H. Liang, W. Gong, J. Chen, and G. Li, "Cleaning of fouled ultrafiltration (UF) membrane by algae during reservoir water treatment," *Desalination*, vol. 220, no. 1-3, pp. 267–272, 2008. doi: 10.1016/j.desal.2007.01.033

[97] D. R. Woods, *Rules of Thumb in Engineering Practice*. Wiley, 2007. ISBN 9783527312207

[98] H. Peng and A. Y. Tremblay, "Membrane regeneration and filtration modeling in treating oily wastewaters," *Journal of Membrane Science*, no. 324, pp. 59–66, 2008. doi: 10.1016/j.memsci.2008.06.062

[99] A. Agi, R. Junin, A. Yahya, A. Gbadamosi, and A. Abbas, "Comparative study of continuous and intermittent ultrasonic ultrafiltration membrane for treatment of synthetic produced water containing emulsion," *Chemical Engineering and Processing - Process Intensification*, vol. 132, no. August, pp. 137–147, 2018. doi: 10.1016/j.cep.2018.08.016

[100] E. T. Igunnu and G. Z. Chen, "Produced water treatment technologies," *International Journal of Low-Carbon Technologies*, vol. 9, no. 3, pp. 157–177, 2014. doi: 10.1093/ijlct/cts049

[101] Y. Thibault, J. Gamage McEvoy, S. Mortazavi, D. Smith, and A. Doiron, "Characterization of fouling processes in ceramic membranes used for the recovery and recycle of oil sands produced water," *Journal of Membrane Science*, vol. 540, no. June, pp. 307–320, 2017. doi: 10.1016/j.memsci.2017.06.065

[102] A. Motta, C. Borges, K. Esquerre, and A. Kiperstok, "Oil Produced Water treatment for oil removal by an integration of coalescer bed and microfiltration membrane processes," *Journal of Membrane Science*, vol. 469, pp. 371–378, 2014. doi: 10.1016/j.memsci.2014.06.051

[103] J. F. Martel-Valles, R. Foroughbakchk-Pournavab, and A. Benavides-Mendoza, "Produced Waters of the Oil Industry as an Alternative Water Source for Food Production," *Revista Internacional de Contaminación Ambiental*, vol. 32, no. 4, pp. 463–475, 2016. doi: 10.20937/RICA.2016.32.04.10

[104] J. Guo, J. Cao, M. Li, and H. Xia, "Influences of water treatment agents on oil-water interfacial properties of oilfield produced water," *Petroleum Science*, vol. 10, no. 3, pp. 415–420, 2013. doi: 10.1007/s12182-013-0290-5

[105] T. Darvishzadeh and N. V. Priezjev, "Effects of crossflow velocity and transmembrane pressure on microfiltration of oil-in-water emulsions," *Journal of Membrane Science*, vol. 423-424, pp. 468–476, 2012. doi: 10.1016/j.memsci.2012.08.043

[106] F. F. Nazzal and M. R. Wiesner, "Microfiltration of oil-in-water emulsions," *Water environment research*, pp. 1187–1191, 1996.

[107] I. W. Cumming, R. G. Holdich, and I. D. Smith, "The rejection of oil by microfiltration of a stabilised kerosene/water emulsion," *Journal of Membrane Science*, vol. 169, no. 1, pp. 147–155, 2000. doi: 10.1016/S0376-7388(99)00338-5

[108] T. Darvishzadeh, V. V. Tarabara, and N. V. Priezjev, "Oil droplet behavior at a pore entrance in the presence of crossflow: Implications for microfiltration of oil-water dispersions," *Journal of Membrane Science*, vol. 447, pp. 442–451, 2013. doi: 10.1016/j.memsci.2013.07.029

[109] J. Zhong, X. Sun, and C. Wang, "Treatment of oily wastewater produced from refinery processes using flocculation and ceramic membrane filtration," *Separation and Purification Technology*, vol. 32, no. 1-3, pp. 93–98, 2003. doi: 10.1016/S1383-5866(03)00067-4

[110] S. Pedersen, P. Durdevic, and Z. Yang, "Review of Slug Detection, Modeling and Control Techniques for Offshore Oil & Gas Production Processes," *IFAC-PapersOnLine*, vol. 48, no. 6, pp. 89–96, 2015. doi: 10.1016/j.ifacol.2015.08.015

[111] B. Hu and K. Scott, "Microfiltration of water in oil emulsions and evaluation of fouling mechanism," *Chemical Engineering Journal*, vol. 136, no. 2-3, pp. 210–220, 2008. doi: 10.1016/j.cej.2007.04.003

[112] M. Wiese, O. Nir, D. Wypysek, L. Pokern, and M. Wessling, "Fouling minimization at membranes having a 3D surface topology with microgels as soft model colloids," *Journal of Membrane Science*, vol. 569, no. September 2018, pp. 7–16, 2018. doi: 10.1016/j.memsci.2018.09.058

[113] N. Hilal, O. O. Ogunbiyi, N. J. Miles, and R. Nigmatullin, "Methods employed for control of fouling in MF and UF membranes: A comprehensive review," *Separation Science and Technology*, vol. 40, no. 10, pp. 1957–2005, 2005. doi: 10.1081/SS-200068409

[114] M. Ebrahimi, O. Schmitz, S. Kerker, F. Liebermann, and P. Czermak, "Dynamic cross-flow filtration of oilfield produced water by rotating ceramic filter discs," *Desalination and Water Treatment*, vol. 51, no. 7-9, pp. 1762–1768, 2013. doi: 10.1080/19443994.2012.694197

[115] B. Schnabel, M. Ebrahimi, O. Schmitz, S. Kerker, J. Hild, C. Gutmann, M. Aden, F. Liebermann, and P. Czermak, "Enhanced oil recovery monitoring for oilfield produced water treatment using rotating ceramic membranes," *FILTECH 2013*, 2013.

[116] T. J. Kennedy, R. L. Merson, and B. J. McCoy, "Improving permeation flux by pulsed reverse osmosis," *Chemical Engineering Science*, vol. 29, no. 9, pp. 1927–1931, 1974. doi: 10.1016/0009-2509(74)85010-4

[117] E. Spiazzi, J. Lenoir, and A. Grangeon, "A new generator of unsteady-state flow regime in tubular membranes as an anti-fouling technique: A hydrodynamic approach," *Journal of Membrane Science*, vol. 80, no. 1, pp. 49–57, 1993. doi: 10.1016/0376-7388(93)85131-F

[118] B. B. Gupta, P. Blanpain, and M. Y. Jaffrin, "Permeate flux enhancement by pressure and flow pulsations in microfiltration with mineral membranes," *Journal of Membrane Science*, vol. 70, no. 2-3, pp. 257–266, 1992. doi: 10.1016/0376-7388(92)80111-V

[119] P. Blanpain-Avet, N. Doubrovine, C. Lafforgue, and M. Lalande, "The effect of oscillatory flow on crossflow microfiltration of beer in a tubular mineral membrane system - Membrane fouling resistance decrease and energetic considerations," *Journal of Membrane Science*, vol. 152, no. 2, pp. 151–174, 1999. doi: 10.1016/S0376-7388(98)00214-2

[120] T. T. Kobayashi, T. T. Kobayashi, Y. Hosaka, and N. Fujii, "Ultrasound-enhanced membrane-cleaning processes applied water treatments: Influence of sonic frequency on filtration treatments," *Ultrasonics*, vol. 41, no. 3, pp. 185–190, 2003. doi: 10.1016/S0041-624X(02)00462-6

[121] L. Borea, V. Naddeo, M. S. Shalaby, T. Zarra, V. Belgiorno, H. Abdalla, and A. M. Shaban, "Wastewater treatment by membrane ultrafiltration enhanced with ultrasound: Effect of membrane flux and ultrasonic frequency," *Ultrasonics*, vol. 83, pp. 42–47, 2018. doi: 10.1016/j.ultras.2017.06.013

[122] H. M. Kyllönen, P. Pirkonen, and M. Nyström, "Membrane filtration enhanced by ultrasound: A review," *Desalination*, vol. 181, no. 1-3, pp. 319–335, 2005. doi: 10.1016/j.desal.2005.06.003

[123] S. M. Seyed Shahabadi and A. Reyhani, "Optimization of operating conditions in ultrafiltration process for produced water treatment via the full factorial design methodology," *Separation and Purification Technology*, vol. 132, pp. 50–61, 2014. doi: 10.1016/j.seppur.2014.04.051

[124] M. Abbasi, R. S. Mohammad, A. Salahi, and B. Mirza, "Modeling of membrane fouling and flux decline in microfiltration of oily wastewater using ceramic membranes," *Chemical Engineering Communications*, vol. 199, no. 1, pp. 78–93, 2012. doi: 10.1080/00986445.2011.570391

[125] A. Lobo, Á. Cambiella, J. M. Benito, C. Pazos, and J. Coca, "Ultrafiltration of oil-in-water emulsions with ceramic membranes: Influence of pH and crossflow velocity," *Journal of Membrane Science*, vol. 278, no. 1-2, pp. 328–334, 2006. doi: 10.1016/j.memsci.2005.11.016

[126] B. M. Aumeier, S. Yüce, and M. Wessling, "Temperature Enhanced Backwash," *Water Research*, vol. 142, pp. 18–25, 2018. doi: 10.1016/j.watres.2018.05.007

[127] H. Huang, K. Schwab, and J. G. Jacangelo, "Pretreatment for low pressure membranes in water treatment: A review," *Environmental Science and Technology*, vol. 43, no. 9, pp. 3011–3019, 2009. doi: 10.1021/es802473r

[128] S. Ebrahim, "Cleaning and regeneration of membranes in desalination and wastewater applications: State-of-the-art," *Desalination*, vol. 96, no. 1-3, pp. 225–238, 1994. doi: 10.1016/0011-9164(94)85174-3

[129] Q. Li and M. Elimelech, "Organic fouling and chemical cleaning of nanofiltration membranes: Measurements and mechanisms," *Environmental Science and Technology*, vol. 38, no. 17, pp. 4683–4693, 2004. doi: 10.1021/es0354162

[130] S.-J. Lee, M. Dilaver, P.-K. Park, and J.-H. Kim, "Comparative analysis of fouling characteristics of ceramic and polymeric microfiltration membranes using filtration models," *Journal of Membrane Science*, vol. 432, pp. 97–105, 2013. doi: 10.1016/j.memsci.2013.01.013

[131] X. Hu, Y. Yu, J. Zhou, Y. Wang, J. Liang, X. Zhang, Q. Chang, and L. Song, "The improved oil/water separation performance of graphene oxide modified Al2O3microfiltration membrane," *Journal of Membrane Science*, vol. 476, pp. 200–204, 2015. doi: 10.1016/j.memsci.2014.11.043

[132] J. Busch and W. Marquardt, "Run-to-run control of membrane filtration processes," *IFAC Proceedings Volumes*, vol. 39, no. 2, pp. 1003–1008, 2006. doi: 10.3182/20060402-4-BR-2902.01003

[133] J. Hermia, "Constant pressure blocking filtration law: Application to power law non-Newtonian fluids," *Trans. Inst. Chem. Eng.*, 1982.

[134] J. De Bruijn, F. Salazar, and R. Bórquez, "Membrane Blocking In Ultrafiltration," *Food and Bioproducts Processing*, vol. 83, no. September, pp. 211–219, 2005. doi: 10.1205/fbp.04012

[135] J. E. Kilduff, S. Mattaraj, J. Sensibaugh, J. P. Pieracci, Y. Yuan, and G. Belfort, "Modeling flux decline during nanofiltration of NOM with poly(arylsulfone) membranes modified using UV-assisted graft polymerization." *Environmental Engineering Science*, vol. 19, no. 6, pp. 477–495, 2002. doi: 10.1089/109287502320963454

[136] B. K. Nandi, A. Moparthi, R. Uppaluri, and M. K. Purkait, "Treatment of oily wastewater using low cost ceramic membrane: Comparative assessment of pore blocking and artificial neural network models," *Chemical Engineering Research and Design*, vol. 88, no. 7, pp. 881–892, 2010. doi: 10.1016/j.cherd.2009.12.005

[137] S. Chellam, "Artificial neural network model for transient crossflow microfiltration of polydispersed suspensions," *Journal of Membrane Science*, vol. 258, no. 1-2, pp. 35–42, 2005. doi: 10.1016/j.memsci.2004.11.038

[138] M. Dornier, M. Decloux, G. Trystram, and A. Lebert, "Dynamic modeling of crossflow microfiltration using neural networks," *Journal of Membrane Science*, vol. 98, no. 3, pp. 263–273, 1995. doi: 10.1016/0376-7388(94)00195-5

[139] W. R. Bowen, M. G. Jones, and H. N. S. Yousef, "Prediction of the rate of crossflow membrane ultrafiltration of colloids: A neural network approach," *Chemical Engineering Science*, vol. 53, no. 22, pp. 3793–3802, 1998. doi: 10.1016/S0009-2509(98)00183-3

[140] J. Busch, A. Cruse, and W. Marquardt, "Modeling submerged hollow-fiber membrane filtration for wastewater treatment," *Journal of Membrane Science*, vol. 288, no. 1-2, pp. 94–111, 2007. doi: 10.1016/j.memsci.2006.11.008

[141] M. F. R. Zuthi, W. Guo, H. H. Ngo, D. L. Nghiem, F. I. Hai, S. Xia, J. Li, J. Li, and Y. Liu, "New and practical mathematical model of membrane fouling in an aerobic submerged membrane bioreactor," *Bioresource Technology*, vol. 238, pp. 86–94, 2017. doi: 10.1016/j.biortech.2017.04.006

[142] E. Giraldo, N. Systems, L. A. Water, and E. Giraldo, "Dynamic Mathematical Modeling of Membrane Fouling in Submerged Membrane Bioreactors," *Proceedings of the Water Environment Federation*, vol. 2006, no. January 2006, 2006. doi: 10.2175/193864706783762959

[143] M. R. Wiesner and P. Aptel, *Water Treatment Membrane Processes*. American Water Works Association, 1996. ISBN 978-0070015593

[144] R. Badrnezhad and A. H. Beni, "Ultrafiltration membrane process for produced water treatment: experimental and modeling," *Journal of Water Reuse and Desalination*, pp. 249–259, 2013. doi: 10.2166/wrd.2013.092

[145] M. Sampath, A. Shukla, and A. Rathore, "Modeling of Filtration Processes - Microfiltration and Depth Filtration for Harvest of a Therapeutic Protein Expressed in Pichia pastoris at Constant Pressure," *Bioengineering*, vol. 1, no. 4, pp. 260–277, 2014. doi: 10.3390/bioengineering1040260

[146] W. R. Bowen, J. I. Calvo, and A. Hernández, "Steps of membrane blocking in flux decline during protein microfiltration," *Journal of Membrane Science*, vol. 101, no. 1-2, pp. 153–165, 1995. doi: 10.1016/0376-7388(94)00295-A

[147] M. C. Vincent Vela, S. Álvarez Blanco, J. Lora García, and E. Bergantiños Rodríguez, "Analysis of membrane pore blocking models adapted to crossflow ultrafiltration in the ultrafiltration of PEG," *Chemical Engineering Journal*, vol. 149, no. 1-3, pp. 232–241, 2009. doi: 10.1016/j.cej.2008.10.027

[148] G. Bolton, D. LaCasse, and R. Kuriyel, "Combined models of membrane fouling: Development and application to microfiltration and ultrafiltration of biological fluids," *Journal of Membrane Science*, vol. 277, no. 1-2, pp. 75–84, 2006. doi: 10.1016/j.memsci.2004.12.053

[149] R. W. Field, D. Wu, J. A. Howell, and B. B. Gupta, "Critical flux concept for microfiltration fouling," *Journal of Membrane Science*, vol. 100, no. 3, pp. 259–272, 1995. doi: 10.1016/0376-7388(94)00265-Z

[150] A. Maiti, M. Sadrezadeh, S. Guha Thakurta, D. J. Pernitsky, and S. Bhattacharjee, "Characterization of boiler blowdown water from steam-assisted gravity drainage and silica-organic coprecipitation during acidification and ultrafiltration," *Energy and Fuels*, vol. 26, no. 9, pp. 5604–5612, 2012. doi: 10.1021/ef300865e

[151] D. Vasanth, G. Pugazhenthi, and R. Uppaluri, "Cross-flow microfiltration of oil-in-water emulsions using low cost ceramic membranes," *Desalination*, vol. 320, pp. 86–95, 2013. doi: 10.1016/j.desal.2013.04.018

[152] A. Salahi, M. Abbasi, and T. Mohammadi, "Permeate flux decline during UF of oily wastewater: Experimental and modeling," *Desalination*, vol. 251, no. 1-3, pp. 153–160, 2010. doi: 10.1016/j.desal.2009.08.006

[153] T. Mohammadi, M. Kazemimoghadam, and M. Saadabadi, "Modeling of membrane fouling and flux decline in reverse osmosis during separation of oil in water emulsions," *Desalination*, vol. 157, no. 1-3, pp. 369–375, 2003. doi: 10.1016/s0011-9164(03)00419-3

[154] F. Wicaksana, A. G. Fane, P. Pongpairoj, and R. Field, "Microfiltration of algae (Chlorella sorokiniana): Critical flux, fouling and transmission," *Journal of Membrane Science*, vol. 387-388, no. 1, pp. 83–92, 2012. doi: 10.1016/j.memsci.2011.10.013

[155] M. Gander, B. Jefferson, and S. Judd, "Aerobic MBRs for domestic wastewater treatment: A review with cost considerations," *Separation and Purification Technology*, vol. 18, no. 2, pp. 119–130, 2000. doi: 10.1016/S1383-5866(99)00056-8

[156] X. Yi, Y. Wang, L. Jin, and W. Shi, "Critical flux investigation in treating o/w emulsion by TiO2 /Al2O3 -PVDF UF membrane," *Water Science and Technology*, vol. 76, no. 10, pp. 2785–2792, 2017. doi: 10.2166/wst.2017.445

[157] S. Metsämuuronen, J. Howell, and M. Nyström, "Critical flux in ultrafiltration of myoglobin and baker's yeast," *Journal of Membrane Science*, vol. 196, no. 1, pp. 13–25, 2002. doi: 10.1016/S0376-7388(01)00572-5

[158] Y. Ye, P. L. Clech, V. Chen, and A. G. Fane, "Evolution of fouling during crossflow filtration of model EPS solutions," *Journal of Membrane Science*, vol. 264, no. 1-2, pp. 190–199, 2005. doi: 10.1016/j.memsci.2005.04.040

[159] R. Chan and V. Chen, "The effects of electrolyte concentration and pH on protein aggregation and deposition: critical flux and constant flux membrane filtration," *Journal of Membrane Science*, vol. 185, no. 2, pp. 177–192, 2001. doi: 10.1016/S0376-7388(00)00645-1

[160] P. van der Marel, A. Zwijnenburg, A. Kemperman, M. Wessling, H. Temmink, and W. van der Meer, "An improved flux-step method to determine the critical flux and the critical flux for irreversibility in a membrane bioreactor," *Journal of Membrane Science*, vol. 332, no. 1-2, pp. 24–29, 2009. doi: 10.1016/j.memsci.2009.01.046

[161] S. P. Beier and G. Jonsson, "Critical flux determination by flux-stepping," *AIChE Journal*, vol. 56, no. 7, pp. 1739–1747, 2009. doi: 10.1002/aic.12099

[162] S. Pedersen, P. Durdevic Løhndorf, and Z. Yang, "Influence of riser-induced slugs on the downstream separation processes," *Journal of Petroleum Science and Engineering*, vol. 154, pp. 337–343, 2017. doi: 10.1016/j.petrol.2017.04.042

[163] A. M. H. Kadhim, W. Birk, and T. Gustafsson, "Relative gain array estimation based on non-parametric frequency domain system identification," in *2014 IEEE Conference on Control Applications (CCA)*, no. i. IEEE, 2014. ISBN 978-1-4799-7409-2 pp. 110–115. doi: 10.1109/CCA.2014.6981337

[164] E. Bristol, "On a new measure of interaction for multivariable process control," *IEEE Transactions on Automatic Control*, vol. 11, no. 1, pp. 133–134, 1966. doi: 10.1109/TAC.1966.1098266

[165] M. F. Islam Zahran, M. Z. Nordin, A. N. Rahimi, M. A. Zubir, M. Z. Shahruddin, K. A. Ibrahim, and M. K. Abd Hamid, "Control properties of driving force based distillation columns design," *Energy Procedia*, vol. 142, pp. 2965–2970, 2017. doi: 10.1016/j.egypro.2017.12.315

[166] S. Amal Shekhar, R. Balaji, and R. Jeyanthi, "Study of Control Strategies for a Non-Linear Benchmark Boiler," in *2018 International CET Conference on Control, Communication, and Computing (IC4)*. IEEE, 2018. ISBN 978-1-5386-4966-4 pp. 5–10. doi: 10.1109/CETIC4.2018.8530959

[167] M. F. Islam Zahran, A. N. Rahimi, M. A. Zubir, M. Z. Shahruddin, K. A. Ibrahim, and M. K. Abd Hamid, "Relative gain analysis of energy efficient hydrocarbon separation sequence," *Energy Procedia*, vol. 142, pp. 2624–2629, 2017. doi: 10.1016/j.egypro.2017.12.202

[168] Q. Xiong, W. J. Cai, and M. J. He, "A practical loop pairing criterion for multivariable processes," *Journal of Process Control*, vol. 15, no. 7, pp. 741–747, 2005. doi: 10.1016/j.jprocont.2005.03.008

[169] M. Witcher and T. J. McAvoy, "Interacting Control Systems: Steady State and Dynamic Measurement of Interaction," *ISA Transactions*, pp. 35–41, 1977.

[170] T. Mc Avoy, Y. Arkun, R. Chen, D. Robinson, and P. Schnelle, "A new approach to defining a dynamic relative gain," *Control Engineering Practice*, vol. 11, no. 8, pp. 907–914, 2003. doi: 10.1016/S0967-0661(02)00207-1

[171] N. Monshizadeh-Naini, A. Fatehi, and A. Khaki-Sedigh, "Input-Output Pairing Using Effective Relative Energy Array," *Industrial & Engineering Chemistry Research*, vol. 48, no. 15, pp. 7137–7144, 2009. doi: 10.1021/ie801667s

[172] S. Skogestad and I. Postlethwaite, *Multivariable Feedback Control: Analysis and Design*, 2nd ed. Wiley & Sons, 2005. ISBN 978-0-470-01167-6

[173] N. Kalboussi, J. Harmand, A. Rapaport, T. Bayen, F. Ellouze, and N. Ben Amar, "Optimal control of physical backwash strategy - towards the enhancement of membrane filtration process performance," *Journal of Membrane Science*, vol. 545, no. September 2017, pp. 38–48, 2018. doi: 10.1016/j.memsci.2017.09.053

[174] R. Villarroel, S. Delgado, E. González, and M. Morales, "Physical cleaning initiation controlled by transmembrane pressure set-point in a submerged membrane bioreactor," *Separation and Purification Technology*, vol. 104, pp. 55–63, 2013. doi: 10.1016/j.seppur.2012.10.047

[175] P. Lipp, G. Baldauf, A. Schmitt, and B. Theis, "Long-term behaviour of UF membranes treating surface water," *Water Science and Technology: Water Supply*, vol. 3, no. 5-6, pp. 31–37, 2003. doi: 10.2166/ws.2003.0147

[176] P. J. Smith, S. Vigneswaran, H. H. Ngo, R. Ben-Aim, and H. Nguyen, "A new approach to backwash initiation in membrane systems," *Journal of Membrane Science*, vol. 278, no. 1-2, pp. 381–389, 2006. doi: 10.1016/j.memsci.2005.11.024

[177] S. Mahesh Kumar, G. M. Madhu, and S. Roy, "Fouling behaviour, regeneration options and on-line control of biomass-based power plant effluents using microporous ceramic membranes," *Separation and Purification Technology*, vol. 57, no. 1, pp. 25–36, 2007. doi: 10.1016/j.seppur.2007.03.002

[178] K. Glucina, J. M. Laine, and L. Durand-Bourlier, "Assessment of filtration mode for the ultrafiltration membrane process," *Desalination*, vol. 118, no. 1-3, pp. 205–211, 1998. doi: 10.1016/S0011-9164(98)00131-3

[179] K. Suresh and G. Pugazhenthi, "Cross flow microfiltration of oil-water emulsions using clay based ceramic membrane support and TiO2composite membrane," *Egyptian Journal of Petroleum*, vol. 26, no. 3, pp. 679–694, 2017. doi: 10.1016/j.ejpe.2016.10.007

[180] B. Chakrabarty, A. K. Ghoshal, and M. K. Purkait, "Cross-flow ultrafiltration of stable oil-in-water emulsion using polysulfone membranes," *Chemical Engineering Journal*, vol. 165, no. 2, pp. 447–456, 2010. doi: 10.1016/j.cej.2010.09.031

[181] A. S. C. Chen, J. T. Flynn, R. G. Cook, and A. L. Casaday, "Removal of Oil, Grease, and Suspended-Solids from Produced Water Using Ceramic Cross-Flow Microfiltration," *Advances in Filtration and Separation Technology, Vol 3*, no. May, pp. 292–317, 1990. doi: 10.2118/20291-PA

[182] B. A. Farnand and T. A. Krug, "Oil Removal From Oilfield-Produced Water By Cross Flow Ultrafiltration," *Journal of Canadian Petroleum Technology*, vol. 28, no. 06, pp. 18–24, 1989. doi: 10.2118/89-06-01

[183] M. Y. Jaffrin, "Dynamic shear-enhanced membrane filtration: A review of rotating disks, rotating membranes and vibrating systems," *Journal of Membrane Science*, vol. 324, no. 1-2, pp. 7–25, 2008. doi: 10.1016/j.memsci.2008.06.050

[184] Z. Xiang-hua, Y. Shui-li, W. Bei-fu, and Z. Hai-feng, "Flux enhancement during ultrafiltration of produced water using turbulence promoter," *Journal of Environmental Sciences*, vol. 18, no. 6, pp. 1077–1081, 2006. doi: 10.1016/S1001-0742(06)60042-9

[185] Z. Tianyi, Z. Jili, and M. Liangdong, "On-line optimization control method based on extreme value analysis for parallel variable-frequency hydraulic pumps in central air-conditioning systems," *Building and Environment*, vol. 47, pp. 330–338, 2012. doi: 10.1016/j.buildenv.2011.07.007

[186] J. Viholainen, J. Tamminen, T. Ahonen, J. Ahola, E. Vakkilainen, and R. Soukka, "Energy-efficient control strategy for variable speed-driven parallel pumping systems," *Energy Efficiency*, vol. 6, no. 3, pp. 495–509, 2012. doi: 10.1007/s12053-012-9188-0

[187] Z. Yang and H. Børsting, "Energy efficient control of a boosting system with multiple variable-speed pumps in parallel," in *49th IEEE Conference on Decision and Control (CDC)*. IEEE, 2010. ISBN 978-1-4244-7745-6 pp. 2198–2203. doi: 10.1109/CDC.2010.5717312

[188] Z. Ma and S. Wang, "Energy efficient control of variable speed pumps in complex building central air-conditioning systems," *Energy and Buildings*, vol. 41, no. 2, pp. 197–205, 2009. doi: 10.1016/j.enbuild.2008.09.002

[189] T. Westerlund, F. Pettersson, and I. E. Grossmann, "Optimization of pump configurations as a MINLP problem," *Computers & Chemical Engineering*, vol. 18, no. 9, pp. 845–858, 1994. doi: 10.1016/0098-1354(94)e0006-9

[190] F. Pettersson and T. Westerlund, "Global optimization of pump configurations using binary separable programming," *Computers & Chemical Engineering*, vol. 21, no. 5, pp. 521–529, 1997. doi: 10.1016/s0098-1354(96)00285-2

[191] P. Waide and C. U. Brunner, "Energy-Efficiency Policy Opportunities for Electric Motor-Driven Systems," *International Energy Agency*, vol. 7, pp. 1–132, 2011. doi: 10.1787/5kgg52gb9gjd-en

Part II

Papers

Paper A

Challenges of Membrane Filtration for Produced Water Treatment in Offshore Oil & Gas Production

Kasper L. Jepsen, Leif Hansen, Christian Mai and Zhenyu Yang.

The paper has been published in the proceedings of
Proceedings of OCEANS'16 MTS/IEEE, Monterey, USA, pp. 1-8, 2016

The layout has been revised.

Paper B

Membrane Fouling for Produced Water Treatment: A Review Study From a Process Control Perspective

Kasper L. Jepsen, Mads Valentin Bram, Simon Pedersen and Zhenyu Yang.

The paper has been published in
Water (MDPI) Vol. 10(7), pp. 1-28, 2018.

The layout has been revised.

Paper C

Control parings of a de-oiling membrane process

Kasper L. Jepsen, Leif Hansen and Zhenyu Yang.

The paper has been published in the
Proceedings of the IFAC workshop on Automatic Control in Offshore Oil and Gas Production, Esbjerg, Denmark, Vol. 51(8), pp. 126-131, 2018

The layout has been revised.

Paper D

Control Pairings of a Deoiling Membrane Crossflow Filtration Process based on Theoretical and Experimental Results

Kasper L. Jepsen, Simon Pedersen and Zhenyu Yang

The paper has been submitted to
Journal of Process Control, pending decision for revised version.

The layout has been revised.

Paper E

Online Backwash Optimization of Membrane Filtration for Produced Water Treatment.

Kasper L. Jepsen, Mads V. Bram, Leif Hansen, Zhenyu Yang and Steven M.Ø. Lauridsen

The paper is pending approval by Total, to be submitted to *Journal of Membrane Science*.

The layout has been revised.

Paper F

Power Consumption Optimization for Multiple Parallel Centrifugal Pumps

Kasper L. Jepsen, Leif Hansen, Christian Mai and Zhenyu Yang.

The paper has been published in
Proceedings of IEEE Conference on Control Technology and Applications (CCTA),
Mauna Lani, HI, pp. 806-811, 2017

ISSN (online): 2446-1636
ISBN (online): 978-87-7210-409-6

AALBORG UNIVERSITY PRESS